A tale of three methods: estimates of primary production in the Oslofjord

Primary production in darkening coastal waters; a method comparison

Tonje Aurland Storholt

Thesis submitted for the degree of Master of Science in Marine Biology and Limnology

60 credits

Department of Bioscience

Faculty of Mathematics and Natural Sciences

UNIVERSITY OF OSLO

May 2023

2023

A tale of three methods: estimates of primary production in the Oslofjord.

Primary production in darkening coastal waters; a method comparison.

Author: Tonje Aurland Storholt

Department of Biosciences (IBV)

Faculty of Mathematics and Natural Sciences

UNIVERSITY OF OSLO (UiO)

http://www.duo.uio.no/

Print: Reprosentralen, Universitetet i Oslo

Abstract

Few studies have quantified rates of primary production in the Oslofjord, and none of those studies have compared rates from different methods. In addition, there has been an increase in terrestrial run-off to coastal areas, including the Oslofjord, resulting in a reduction of the optical clarity. This study aims to investigate how primary production is affected by the observed coastal darkening, and to compare different methods of quantifying primary production.

This study used three different methods of quantifying primary production; the vertically generalized production model (VGPM) based on chlorophyll concentration, the bio-optical method (BO-PP) based on *in situ* fluorescence and *in vivo* absorbance and lastly an incubation experiment with the stable isotope ^{13}C, as a tracer in carbon fixation (^{13}C-PP). All three methods were closely correlated, but with different scales. The results yielded a difference of an order of magnitude between the VGPM and the ^{13}C-PP estimates, with the estimates based on the BO-PP situated almost in the middle. The VGPM rates are an overestimate due to downscaling to a localized area. The low estimates from ^{13}C-PP show a possible N-limitation in the incubation bottles. The overall trend in estimates from all methods is an increase in production with an increase in optical clarity.

Acknowledgements

This thesis represents the end of an era for me, being 5 years in the making – a culmination of my bachelors and master degree at UiO. This thesis would not have been possible without the help of some great people along the way.

First I would like to direct a massive “thank you” to my supervisors Dag Hessen (UiO) and Tom Andersen (UiO), for always answering my questions. Your knowledge and guidance have been vital for this thesis to become what it is today. A special shout-out to Tom, for your patience with me regarding all things R, I appreciate everything you have taught me.
This thesis would be nothing without the water samples, so thank you to Aleksandr Berezovski for your invaluable help when retrieving the samples. Thank you to Sindre and the rest of the crew at Trygve Braarud for making the field samplings such a fun experience. Per Johan Færøvig also deserves a thank you, for all of your help with planning and prepping, and valuable insights. Berit Kaasa thank you for your help in the lab. William Hagopian thank you for your valuable insights on stable isotopes. I would also like to thank Peter Dørsch at NMBU and the Biogeochemical Stable Isotope Facility run by Dr. Brian Popp at SOEST at the University of Hawaii, for your help with analyzing samples.

Hanne, thank you for being such an amazing friend through this period, from living together on Svalbard to field sampling to countless hours of watching “Iskrigerne”. I cannot express my gratitude for our friendship enough, forged in the trials of the Arctic it will last a lifetime. Jackie, thank you for all of our great conversations and the late night chips runs at REMA, our friendship is so dear to me. Eli, thank you for being a great friend and for always making me laugh. Thank you to Silje, Hanna and Julie for contributing to making the long hours at the office so fun. Thank you to the rest of the “marine crew” for these last two years, it is an experience I will treasure forever.
Last, but not least I would like to thank my family, especially my mom and my sister. Your unwavering belief and support and your unconditional love means everything to me, and I would not be where I am without you.

Abbreviations

ATP – adenosine triphosphate

BO-PP –bio-optical method for primary production

CDOM – colored dissolved organic matter

$CDOM_{sa}$ – spectrally averaged CDOM absorbance

CO_2 – carbon dioxide

DIC – dissolved inorganic carbon

ETR – electron transport rate

GC – gas chromatography

GPP – gross primary production

LC1 – light curve 1

$NADPH_2$ – nicotinamide adenine dinucleotide hydrogen phosphate

NPP – net primary production

NPQ – non-photochemical quenching

O_2 – molecular oxygen

PAM – pulse amplitude modulated

PAR – photosynthetically active radiation

POC – particulate organic carbon

PP – primary production

PQ – photosynthetic quotient

PSI – photosystem I

PSII – photosystem II

PSU – practical salinity unit

QY – quantum yield

SST – sea surface temperature

TIC – total inorganic carbon

UiO – University of Oslo

VGPM – vertically generalized production model

VPDB – Vienna Pee Dee Belemnite

Table of contents

1 Introduction

Primary production is the basis for life and an integral part of ecosystem metabolism. Primary production refers to the production of organic matter from inorganic carbon, using energy from the sun, a process known as photosynthesis (Behrenfeld et al., 2001; Field et al., 1998; Siegel et al., 2013). In general terms photosynthesis is described as (Steemann Nielsen, 1952):

$$H_2O\ (l) + \ CO_2\ (g) + energy\ \rightarrow (CH_2O)\ (s) + \ O_2\ (g)$$

The energy refers to the photosynthetically active radiation (PAR) in the region between 400 nm and 700 nm in the solar radiation spectrum. PAR is absorbed by pigments in the chloroplasts within the cells of the photosynthetic organism. The chloroplasts, more specifically the thylakoid membrane, also contain the electron carriers, which generate a reducing power in the form of $NADPH_2$ by utilizing the absorbed energy, this is referred to as the light dependent reaction. In addition, biochemical energy in the form of ATP is generated across the same membranes. This light dependent system is divided into two subsystems: photosystem I (PSI) and photosystem II (PSII). Together $NADPH_2$, ATP and necessary enzymes create carbohydrates (CH_2O) from CO_2 and H_2O, in the Calvin cycle, with O_2 as a fortunate bi-product (Kirk, 1994). The Calvin cycle, also known as the dark reaction or light independent reaction of photosynthesis, is where CO_2 is absorbed.

Photosynthesis is not only the basis for almost all non-photosynthetic forms of life, it has shaped the planet by providing oxygen to the atmosphere, and is also essential for current climate development by removing and sequestering CO_2 from the atmosphere (Falkowski, 2012). Since more than 50% of annual human CO_2-emissions are removed from the atmosphere primarily by photosynthesis, estimates of rates of primary production are especially relevant in the context of climate change (Behrenfeld et al., 2009; P. G. Falkowski et al., 1998; Henson et al., 2018; López-Sandoval et al., 2018). Primary production is divided into gross and net production, where gross primary production (GPP) is the total production, including energy used for respiration. Net primary production (NPP) is the production when respiration is accounted for.

$$NPP = GPP - respiration$$

This distinction is important, as it is the NPP that is available for transfer in the trophic levels, thus controls the energy transfer and heterotrophic production (Falkowski, 2012; Falkowski et al., 1998). Primary production in the marine environment is about equal to land production, even though the oceans cover 70% of the Earth's surface (Field et al., 1998). While the photosynthetic organisms on land are large, vascular plants, the main contributors to the oceanic primary production are small, single celled organisms – phytoplankton (Falkowski, 2012). Algae, including phytoplankton, funnel most of the absorbed light energy to a reaction center associated with PSII, called P_{680}. The electron transport associated with light absorbance takes place in the reaction center (Kirk, 1994).

Understanding the mechanisms behind oceanic and coastal production, the carbon cycle, ecosystem effects and food-web structure have been contributors to develop methods for estimating the productivity. Staehr et al. (2012) conducted a literature review, with the goal of investigating the history of primary production estimating methods. They found that the amount of studies regarding aquatic primary production has risen drastically the last few decades, with an increasing focus on the carbon budget and effects and drivers of climate change. In addition, descriptive and comparative studies detailing changes in the production on different time scales accounts for a large part of the investigated studies (Staehr et al., 2012).

1.1 History of methodology in estimates of primary production

The history of estimating ecosystem metabolism, and as a consequence the primary production, spans almost a century (Staehr et al., 2012). While different methodologies have been developed alongside ecosystem science, most of them, in particular the early methods, have played a pivotal role in the development of aquatic ecology (Dineen, 1953; Juday, 1940). One of these pioneering methods is the measurement of O_2 in incubation bottles accredited to Gaarder & Gran (1927). They measured the primary production in the Oslofjord using the production of oxygen gas in

bottles, light and dark incubated water samples, as a proxy for primary production. Incubation bottles are divided into light and dark bottles where the light bottles provide an estimate of NPP since the phytoplankton have access to light for photosynthesis. The dark bottle on the other hand provides an estimate of the respiratory losses based on the assumption of no photosynthesis in the absence of light. GPP is the difference between these bottles. The productivity is calculated by assuming a photosynthetic quotient (PQ), which is the ratio of mol evolved O_2 to mol assimilated CO_2 (Sakamoto et al., 1984; Williams et al., 1979). However, this method contains sensitivity issues, and is mostly suitable for regions with high production (Gazeau et al., 2005; Steemann Nielsen, 1952; Williams et al., 1979).

1.2 Isotopic tracers in primary production estimates

While the literature study by Staehr et al. (2012) stated that there is no single, widely used method for quantifying primary production, the method by Steemann Nielsen (1952) has been regarded as among the more robust and the preferred choice when estimating primary production at sea (Regaudie-de-Gioux et al., 2014). This method uses the radioactive carbon isotope, ^{14}C, as a tracer in the production of organic matter, usually in incubation bottles, also known as the ^{14}C-PP method. The resulting concentration of ^{14}C in the organic matter can by measuring the emitted β-rays, the rate of radioactive disintegration, using a scintillation counter. By knowing the exact amount of ^{14}C added to the water sample, the rate of carbon assimilation can be calculated. Calculation of the rate of assimilation also requires total amount of CO_2, dissolved inorganic carbon (DIC) in the water and the ratio of (^{14}C + ^{13}C + ^{12}C) / ^{14}C in DIC (Steemann Nielsen, 1952). The method assumes that ^{14}C and ^{12}C are assimilated at the same rate, that ^{14}C is only incorporated into organic matter through photosynthesis and that no ^{14}C is lost during respiration. While these requirements are not fulfilled, they are accounted for in the study (Steemann Nielsen 1952). The rate of incorporation of carbon in photosynthesis discriminates towards heavier isotopes and an isotopic discrimination factor = 1.06 is usually applied.

The ^{14}C-PP method is simple and has high sensitivity, even in areas of low production. However, restrictions against using the radioactive isotope has limited the use of this method during recent

years (López-Sandoval et al., 2018). Slawyk et al. (1977) suggested the use of the stable carbon isotope, ^{13}C, as a tracer, also known as the ^{13}C-PP method. In the initial suggestion, it is stated that the ^{13}C-PP method was not developed to replace the ^{14}C-PP method, but rather to act as an addition in estimates of productivity, for example coupled with other stable isotope tracers such as ^{15}N (Slawyk et al., 1977). The ^{13}C-PP method has been further investigated and developed, and experiments using both the ^{14}C-PP and the ^{13}C-PP methods have yielded results indicating that the ^{13}C-PP method is a reliable and robust replacement for the ^{14}C-PP method in light of restrictions regarding the handling of radioactive material (López-Sandoval et al., 2018; Regaudie-de-Gioux et al., 2014; Slawyk et al., 1984). While the ^{14}C method is more straight forward since the β-radiation emitted by the algae can be measured directly, the ^{13}C method requires different instrumentation. Typically the carbon assimilation is measured with isotope ratio mass spectrometry (IRMS), or cavity ring-down spectrometry (CRDS), on glass fiber filters, onto which the contents of incubation bottles have been filtered. CRDS, used by López-Sandoval et al. (2019), is an easier and more robust method of measuring isotopic abundance on glass fiber filters, compared to IRMS. The ratio of ^{13}C to ^{12}C on the filters is compared to a pre-determined standard ratio, for $^{13}C/^{12}C$ this is the Vienna Pee Dee Belemnite (ratio = 0.0112372) (IAEA, 1995), and reported as $\delta^{13}C$ (‰). Calculations of the productivity require measurements of the amount of carbon on the filters, in addition to the $\delta^{13}C$, to be able to calculate the concentration of carbon on the filters, from the $\delta^{13}C$, via the ratio. These measurements can be taken simultaneously or separate (Sakamoto et al., 1984). Measurements of productivity from incubation bottles are direct measurements of volumetric production. All productivity estimates from bottle incubation experiment have the same weakness. This is known as the “bottle effect”. This is a term that refers to observable, yet unaccountable effects on growth in bottle incubation experiments (Pernthaler & Amann, 2005).

1.3 The vertically generalized production model

Compared to the abovementioned carbon based methods of quantifying primary production, the vertically generalized production model (VGPM) is a chlorophyll a based production model. VGPM is a method that uses remote sensing technology, and estimates the chlorophyll concentration based on sea surface color, and thus avoids the “bottle effect” (Behrenfeld et al., 2005; Westberry

et al., 2008). The oceanic primary production in the famous production map from Field et al. (1998) is a result of the VGPM. The theory behind the model is that production varies in a predictable manner in relation to the chlorophyll concentration (Behrenfeld & Falkowski, 1997a). The model employs a variable called P^b_{opt}, which is the chlorophyll-specific production per unit volume. This variable is based on empiric knowledge from 10 000s of measurement using the ^{14}C method. P^b_{opt} allows for the conversion of the chlorophyll concentration to NPP, which is a rate (Behrenfeld & Falkowski, 1997a). The conversion from volume specific to area specific production employs the euphotic depth and a light dependent term. The light-dependent term is necessary as the primary productivity varies in the water column, due to the exponential reduction in light intensity with depth (Behrenfeld & Falkowski, 1997b). The euphotic zone is defined as the area between the surface and to the depth where 1% of PAR surface irradiance remains, which is the area of the water column where there is sufficient light for photosynthesis (Lee et al., 2007).

1.4 Bio-optical estimates of primary production

The bio-optical approach to quantifying primary production is another method to avoid bottle incubations and omit the "bottle effect" (Kolber & Falkowski, 1993). This method is based on light measurements in the PAR region and measurements of how PAR is absorbed in the water column. The method calculates absorbance coefficients for different components in the water column, and calculates their contribution to the total light absorbance (Smith et al., 1987, 1989). The absorbance is measured from particulate matter on glass fiber filters, where the total absorbance is compared to absorbance after depigmentation (bleaching). The absorbance after pigment bleaching represents the absorbance by detritus. The difference represents the algal absorbance of light in the PAR region, and both algal and detritus absorbance are necessary for the calculation of the primary production (Tassan & Ferrari, 1995; Thrane et al., 2014).

The method is also dependent on the efficiency of PSII in regard to the utilization of absorbed quanta, known as the quantum yield (QY) of PSII (Genty et al., 1989; Smith et al., 1987, 1989). The QYs are measured using active fluorescence, either with pulse amplitude modulated fluorometry (PAM) (Schreiber, 2004) or fast repetition rate fluorometry (FRRF) (Kolber & Falkowski, 1993). The

QYs are necessary for the calculations of the rates of electron transport (ETRs). ETRs are further applicable in the calculations of the gross carbon fixation, when an appropriate value for the quantum yield of CO_2 fixation is assumed, by measuring the *in vivo* rate of light absorbance. This value is assumed to be 8 photons per CO_2 molecule. However, Kirk (1994) proved that this is a theoretical minimum and that the actual amount of photons needed is 10-12. During the last two decades this method has grown in popularity due its fast and inexpensive nature. In addition, the optical approach is quite flexible, and optical properties are easily applicable to other methods as well (Kromkamp & Forster, 2003; Thrane et al., 2014).

1.5 Primary production in the Oslofjord

The Oslofjord is an important ecosystem, and serves as a recreational area for a large fraction of the Norwegian population. This high population density has impacted the fjord substantially over the past century. It has been a basis for research for at least a century, and still is. The Oslofjord is divided into an inner and outer part, with a sill at Drøbak. The outer Oslofjord receives water from the Glomma river and its catchment, which drains most of the large forests in the eastern parts of Norway (Frigstad et al., 2020). Parallel to the increase in the concentration of CO_2 in the atmosphere and increasing temperatures, there has been an observed increased concentration of dissolved organic matter in many boreal lakes and rivers ("browning") which affects optical properties in both freshwaters and recipient coastal areas (Aksnes et al., 2009; Opdal et al., 2019).

A reduction in optical clarity could cause adverse effects on coastal ecosystems, such as a shift towards more tactile predators as jellyfish, which are not dependent on sight to hunt, and a decrease in the primary production (Urtizberea et al., 2013). A reduction in the water clarity is essentially a reduction in the euphotic zone. The irradiance decreases exponentially with depth, due to attenuation. The depth of the euphotic zone can be investigated with Secchi depth measurement, a standard method of investigating optical clarity that has been in use for over a 100 years (Dupont & Aksnes, 2013; Fleming-Lehtinen & Laamanen, 2012).

The attenuation of light in the water column is a result of a combination of different parameters, including particle absorbance, both algal and non-algal (detritus), and absorbance by water itself, especially in the high wavelength part of the spectrum. In addition, dissolved organic matter (DOM), and colored dissolved organic matter (CDOM) in particular, has physicochemical properties which absorb light in the short wavelength part of the spectrum, and colors the water column (Lee et al., 2013). Increased run-off of CDOM is likely a consequence of increased land vegetation, which reaches the fjords due to riverine input (Deininger & Frigstad, 2019; Finstad et al., 2016).

In light of climate change a there has been a growing interest and need for primary production estimates, not only for the carbon budget, but also for how production and ecosystems are affected by the ongoing changes (Falkowski, 2012). A recent study from the Oslofjord, a result from long-term monitoring, reveals a decrease in the chlorophyll a concentration as a result of decreasing nutrients (Lundsør et al., 2020). The long-term monitoring revealed a pattern of three blooms; in March, June and September, in the inner Oslofjord. This pattern is likely to extend to the outer Oslofjord (Aure et al., 2014; Paasche & Østergren, 1980). The study also revealed a shift to a later onset of the growing season (Lundsør et al., 2020). The observed shift in the onset of the growth season, could be credited to higher sea surface temperatures (SST), although increased SSTs are predicted to result in an earlier onset of the growth season, due to earlier stratification of the water column (Desmit et al., 2020). However, the stratification of the Oslofjord is controlled by salinity rather than temperature, but there was an observed shift towards lower salinities at a later date compared to earlier investigations (Lundsør et al., 2020; Staalstrøm et al., 2012). The lowered salinities are a result of freshwater input. The CDOM follows the freshwater, and due to afforestation a there is an increase in CDOM concentration per unit of freshwater (Frigstad et al., 2020). Other factors such as the survival of higher numbers of zooplankton through the warm winters could potentially contribute to a later onset of the growing season (Behrenfeld & Boss, 2014). However, a main contributor to this shift could be the observed coastal darkening in the Oslofjord, due to increased run-off, though more studies are required (Aksnes et al., 2009; Frigstad et al., 2020; Opdal et al., 2019). The coastal zones are amongst the most productive systems, and

contribute to 20% of the annual oceanic primary production. Investigations of how this productivity is affected by ongoing changes are therefore important (Ducklow et al., 2022).

1.6 Objectives and aims

The phytoplankton phenology has been extensively studied and monitored in the Oslofjord, e.g. the intensities and timing of phytoplankton blooms. On the other hand, rates of primary productivity are not as extensively studied. The study by Gaarder & Gran (1927) in relation to the launch of the O_2 method is one of few studies of productivity rates in the Oslofjord. A study conducted by Throndsen (1978) using the ^{14}C-PP method is another.

The objective of this thesis is to compare the methods mentioned above; the ^{13}C-PP method, VGPM and the bio-optical method, which has not yet been done for the Oslofjord, with the specific aim of answering which method yields the most reliable estimates of primary production in this study. The second objective is to contribute to understanding whether and how primary productivity is affected by darkening coastal waters, with the specific aim of answering whether a higher CDOM concentration yields detrimental effects on primary production.

2 Materials and methods

In relation to this thesis, three field samplings were conducted in the outer Oslofjord.
All samples were analyzed using methods necessary for three different estimates of primary production along a salinity gradient from the Glomma estuary.

2.1 Field sampling

The sampling was conducted along a coastal transect with decreasing riverine influence. This transect consists of 5 predefined monitoring stations in outer Oslofjord, visualized in Figure 1, from brackish to coastal water; L1 (Glomma), L5 (Kjøkøy), I1 (Ramsø), Ø1[1] (Leira), OF2 (Missingene). The stations represent both a salinity and an optical gradient, specifically chosen due to their relation to the Glomma estuary. The sampling was conducted aboard the University of Oslo research vessel F/F Trygve Braarud during three separate cruises: 12th of May, 2nd and 29th of June in 2022.
These dates are selected to catch the end of the spring flood and the summer bloom observed in the Oslofjord.

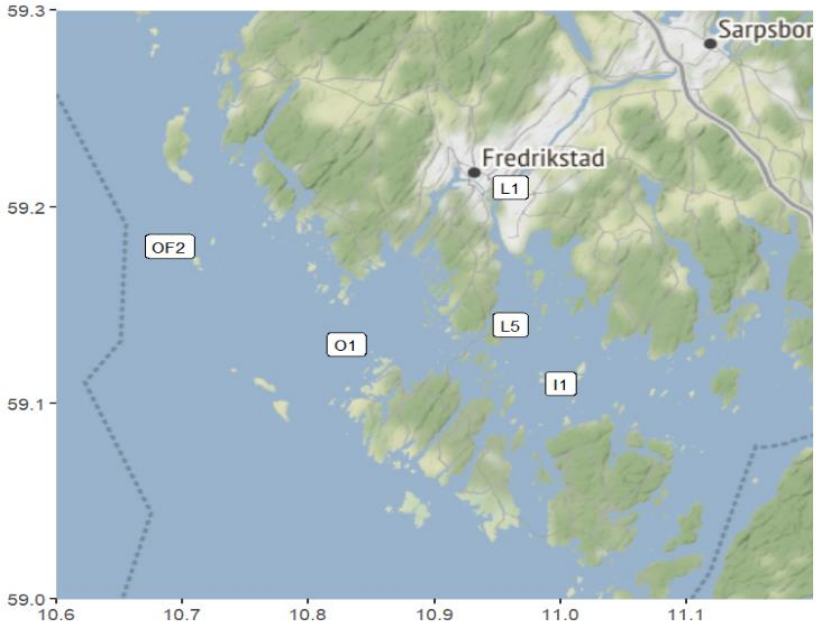

Figure 1: Map showing the different stations, from brackish (L1) to coastal (OF2) water. Map made with Stamen map in ggmap **(Kahle & Wickham, 2013)**.

[1] From here and throughout the thesis, Ø1 is referred to as O1.

2.1.1 Sampling

The on-ship CTD (Seabird S9+) was deployed at each station to gather information about the conductivity, temperature and depth. Water samples were collected using Niskin bottles, 5 L, attached to the CTD-rig. Water was collected from 3 m and 4 m depth and transferred into a 10 L canister for mixing. After thorough mixing, half the volume was transferred to a 5 L canister and stored in darkness.

Light measurements were taken with a trio of hyperspectral irradiance RAMSES sensors from TriOS (Rastede, Germany). One is an on-board reference, fastened to the ship deck. The two remaining sensors are fastened to a rig which is lowered into the surface water. These measure the downwelling and upwelling irradiance. These measurements are needed to quantify the amount of photosynthetically active radiation (PAR) available for phytoplankton in the water column. Irradiance was measured at 1 m intervals from surface (0 m) to 10 m depth, at each station. Lastly, Secchi depth measurements were conducted to investigate water clarity.

2.2 Primary production by incubation with isotopic tracers

The incubation method was inspired by a protocol by López-Sandoval et al. (2019) and required estimates of carbon uptake in light and dark bottles using the stable isotope of carbon, ^{13}C, as a tracer. This experiment is referred to as "^{13}C-PP experiment".

2.2.1 Preparing solutions

A stock solution of ^{13}C bicarbonate was prepared by weighing (AG204 Bergman, Norway) 2.18 g of 98% $NaH^{13}CO_3$ (sodium bicarbonate, molecular weight 85.00, Sigma-Aldrich) and dissolve it in 1 L of MilliQ-water. The resulting concentration was 25.6 mmol/L. In addition, a solution of 6 M HCl was prepared for removing inorganic isotope on filters.

2.2.2 Incubation

For the ^{13}C-PP experiment water was distributed into 1 L borosilicate bottles. This process was repeated thrice for every station, resulting in triplicates. 5 mL of the ^{13}C stock solution was pipetted into each bottle, yielding a concentration of 0.13 mmol/L NaH^{13}CO3 in each bottle. One bottle from each trio was covered in aluminum foil, this was the dark bottle. The trios were held together by zip ties, creating a rosette of bottles, and placed upside-down in an outdoor pool with continuous flow of surface water at the UiO field station in Drøbak. The bottles were incubated for 24 hours.

2.2.3 Filtering

Each bottle was filtered onto one Whatman GF/F 47 mm filter. The filter was then placed into a MilliPore Petrislide where 50 µL 6 M HCl was pipetted onto the filter. The hydrochloric acid facilitates dissolution of inorganic carbonates, thus removing it from the sample. After filtering the slides were packaged with aluminum foil and kept frozen at -20 °C until analysis.

2.2.4 Gas chromatography - CO_2 analysis

Total inorganic carbon (TIC) in the water samples was required for the backtracking of the amount of CO_2 available for uptake by algae. TIC was measured with helium headspace-analysis on acidified water samples using gas chromatography (GC).[2] The gas samples were prepared according to a protocol by (Åberg & Wallin, 2014). However, these samples are from the aforementioned remaining water stored in plastic bottles for approximately 5 to 6 months.

The vials were loaded into a CTC GC Autosampler coupled with an Agilent Model 7890A GC, which has a He back-flash. GC separates gases based on their velocities and the concentration was measured at the end of the separation column by a thermal conductivity detector. See Yang et al. (2015) for further details on GC methodology.

[2] Performed by Peter Dörsch at the University of Life Sciences, NMBU.

2.2.5 Isotope ratio mass spectrometry - ^{13}C stable isotope analysis

Isotope ratio mass spectrometry analysis[3] of the filters from the ^{13}C-PP experiment was conducted to measure the algal uptake of carbon during incubation. Instrumentation used was a Thermo Scientific Delta V Advantage coupled with a Costech Instruments Elemental Combustion System to perform stable isotope analysis of enriched samples on glass fiber filters. Before analysis the filters were compressed into pellets and placed on a carousel. The pellets were dropped one by one into a combustion chamber. The isotopic composition of the evolved CO_2 gas was measured by the IRMS, and reported as relative deviations from a standard material (Vienna Pee Dee Belemnite – VPDB), $\delta^{13}C$ (IAEA, 1995).

$$\delta^{13}C = 1000 * \left(\frac{(\frac{13C}{12C})_{sample}}{(\frac{13C}{12C})_{VPDB}} - 1 \right)$$

2.3 Bio-optical measurements and analysis

The bio-optical method of estimating photosynthetic rates (BO-PP) is dependent on measurements of the absorbance of different substances affecting the optical properties of the water and the suspended particles, in addition to the effectiveness of photosystem II in regard to the utilization of absorbed quanta.

2.3.1 Pulse amplitude modulated fluorometry

Pulse amplitude modulated (PAM) fluorometry was used for measuring the light dependent quantum yield (QY) of photochemistry in photosystem II. This was used as a proxy for the QY of CO_2-fixation. The measurements are conducted using a PSI AquaPen (Drásov, Czech Republic), a portable fluorometer which can be attached to a computer. The water samples need to be fresh, thus the measurements were done in the field. For these measurements, the reaction centers in the photosystem need to be dark-adapted such that they are in the open state. This was achieved

[3] Performed by the Biogeochemical Stable Isotope Facility run by Dr. Brian Popp at the School of Ocean and Earth Science and Technology at the University of Hawaii.

by keeping the water samples in the dark for the time between stations, approximately 30 minutes. The measurements were conducted using blue light excitation at 450 nm using AquaPen´s predefined light curve 1 (LC1) protocol. Blue light excitation measures all phytoplankton. The same cuvette was used for each subsample from the same location, but the cuvette was replaced when a water sample from a different location was measured.

The LC1 protocol consist of sending fully saturating light flashes, at approximately 3000 µmol quanta/m^2/s, through the water samples. First, yielding the maximum value, the flash was sent through the fully dark adapted sample. Secondly the sample underwent a series of 6 saturating flashes when the sample was subjected to rising light intensity incubation levels, each incubation is 60 seconds long. The intensity levels are 10, 20, 50, 100, 300 and 500 µmol quanta/m^2/s

2.3.2 Filtering

For the bio-optical method 250 mL of water was filtered onto a 25 mm Whatman GF/F filter using a filtration rack with a vacuum pump. Three replicates were taken for each station, resulting in a total of 45 filters. Each filter was rolled and placed into a 2 mL Eppendorf tube. The Eppendorf tubes were packaged with aluminum foil and frozen at -20 °C. The filters are necessary for determining pigment and detritus absorbance with integrating sphere spectrophotometry. The remaining water was transferred to 1 L plastic bottles and stored in a climate room at approximately 4 °C.

2.3.3 Integrating sphere spectrophotometer - filter absorbance

To determine the absorbance by pigment and detritus in the water column integrating sphere spectrophotometry was conducted using a UV-2550 spectrophotometer, with an attached ISR-2200 integrating sphere (Shimadzu, Japan). The integrating sphere spectrophotometer sends monochromatic light, in the PAR region, through the sample filter and measuring the absorbance at each wavelength, compared to the reference filter. Due to the spherical construction of the instrument, together with the white inside coating, minimal light is lost as a consequence of

scattering, although there might be a chance of backscattering. However, this can be accounted for during data-processing.

The analysis was performed on the aforementioned 25 mm GF/F filters, including two extra filters to serve as a baseline and a reference. The sample filters were thawed on a microscope slide and 200 µL of MilliQ water were pipetted onto each filter to ensure a moist filter. The filters were then covered with a second microscope slide. The first sample was placed in the sample slot of the integrating sphere, after running a reference and a baseline. The reference filter was kept in the reference slot for the duration of the analysis. After the first filter was analyzed, using the *UVProbe Ver. 2.21* program, 200 µL of sodium hypochlorite solution ("Klorin", < 5% NaClO) was pipetted onto the filter. The filter was left to bleach for approximately 1 minute before a second analysis was conducted. Bleaching removes pigment, and the resulting absorbance corresponds to detritus absorbance.

2.3.4 UV-vis spectrophotometry – CDOM absorbance

To determine the CDOM absorbance in the water samples, they were subjected to UV-vis spectrophotometry. The water was filtered through 25 mm GF/C filters to remove particles. The SHIMADZU UV-2550 spectrophotometer sends light between 400 nm and 750 nm through 50 mm quartz cuvettes, one with MilliQ water, which acts as a reference, and one with the filtered sample water. The computer program *UVProbe Ver. 2.21* computes the absorbance as a function of wavelength[4].

2.4 Calculations

Three different methods of calculating rates of primary production were used for this thesis; the vertically generalized production model, the bio-optical method and the ^{13}C-PP method. The VGPM and ^{13}C-PP yields NPP, while BO-PP yields GPP.

[4] The analysis was conducted by Hanne Halkjelsvik Børseth for the master thesis "Organic matter and iron from the deep forest to the outer Oslofjord", on water samples obtained during the same cruises as for this thesis.

2.4.1 VGPM calculations

Equation for vertically generalized production model, first described by Behrenfeld & Falkowski (1997a):

$$\boldsymbol{VGPM} = [\boldsymbol{chlorophyll\ a}] * \boldsymbol{P^b_{opt}} * \boldsymbol{daylength} * \boldsymbol{z_{eu}} * \boldsymbol{f}(\boldsymbol{PAR}) \qquad (1)$$

Chlorophyll a concentration (mg/m^3) was obtained from the peak within the 660-680 nm region in the pigment absorbance spectra from integrating sphere spectrophotometry, $a_{IS}(\lambda)$, using the specific absorbance at 670 nm, $a^*_{ph}(670)$ from Mitchell & Kiefer (1988); Figure 7. In summary:

$$[chlorophyll\ a] = \frac{a_{IS}(670)}{a^*_{ph}(670)} = \frac{a_{IS}(670)}{0.011}$$

The chlorophyll-specific production per unit volume, P^b_{opt}, was calculated using the polynomial model from Behrenfeld & Falkowski (1997a), with sea surface temperatures obtained from the CTD.

Day length was obtained using a function created in RStudio, which accounts for the declination angle of the sun and latitude to compute day length in hours, based on Brock (1981).

The euphotic depth, z_{eu}, was found using light data from TriOS measurements standardized relative to sea surface irradiance, and was the depth where 1% of surface irradiance remains. The light dependent component in the equation is given by:

$$f(PAR) = 0.66125 * \frac{E_0}{E_0 + 4.1},$$

as described in Behrenfeld & Falkowski (1997b).

Surface PAR irradiance, E_0, was downloaded from the STRÅNG database, and converted from W/m^2 to mol quanta /m^2/day.

$$E_0 = \frac{(60 * 60 * \sum_{t1}^{t2} irr(PAR))}{1000000} * 4.57^{5}$$

2.4.2 ^{13}C-PP calculations

Calculations of rates of primary production using stable isotopes were based on equation 1 from López-Sandoval et al. (2019):

$$^{13}\text{C-PP} = \frac{\left(\frac{\delta^{13}C_{POC-light} - \delta^{13}C_{POC-dark}}{\delta^{13}C_{DIC-labeled} - \delta^{13}C_{DIC-natural}}\right) * POC}{t}$$

Particulate organic carbon (POC) is the amount of carbon retained on the filters (µmol/L). The incubation time is referred to as "t" = 1 day. $\delta\,^{13}C_{POC\text{-}light}$ is the δ^{13}C value in the POC retained on the filters after filtering the water from the light incubated bottles, while $\delta\,^{13}C_{POC\text{-}dark}$ refers to corresponding δ^{13}C value in the dark incubated bottles. $\delta^{13}C_{DIC\text{-}natural}$ refers to the natural δ^{13}C value, before the enrichment. $\delta^{13}C_{DIC\text{-}labeled}$ refers to the added inorganic carbon to the water samples, the stock solution. This was calculated by taking the enrichment of DIC into account (López-Sandoval et al., 2019):

$$\delta^{13}C_{DIC-labeled} = \left[\frac{\left(\frac{\mu M^{13}C_{DIC-natural} + \mu M^{13}C_{DIC-stock}}{\mu M^{12}C_{DIC-natural} + \mu M^{12}C_{DIC-stock}}\right)}{(\frac{13C}{12C})_{VPDB}} - 1\right] * 1000$$

The natural δ^{13}C in DIC in sea water from Table 1 in Rau et al. (1996) was used to calculate the $\mu M^{13}C_{DIC\text{-}natural}$ and $\mu M^{12}C_{DIC\text{-}natural}$, the concentrations of ^{13}C and ^{12}C in DIC before enrichment. $\mu M^{13}C_{DIC\text{-}stock}$ was calculated by: $\mu M^{13}C_{DIC\text{-}stock}$ = [DIC] * [% Atom ^{13}C /100]. Where the DIC concentration (µmol/L) is obtained from the GC, and the% Atom ^{13}C is the percentage of ^{13}C in the

[5] From Thimijan & Heins (1983)

stock $NaH^{13}CO_3$, which is indicated on the commercial label. $\mu M^{12}C_{DIC\text{-}stock}$ was calculated by: $\mu M^{12}C_{DIC\text{-}stock}$ = [DIC] * [100 -% Atom ^{13}C /100] (López-Sandoval et al., 2019).

The incubation yielded production per volume, areal primary production was calculated using a similar approach as VGPM, described in section 2.4.1, when integrating from volume to area:

$$\boldsymbol{PP_{13_C}} = (\boldsymbol{^{13}C_{PP} * 12}) * \boldsymbol{z_{eu}} * \boldsymbol{f(PAR)} \qquad (2)$$

The factor 12 is the conversion from µmol/L (from POC) to mg/m^3.

2.4.3 BO-PP calculations

Equation for areal primary production using the bio-optical method:

$$\boldsymbol{BO_{PP}} = \boldsymbol{0.08 * \Delta E_a * QY * 12000} \quad (3)$$

The factor 0.08 is the number of CO_2 molecules fixed per absorbed quantum. As demonstrated by Kirk (1994) an appropriate value is 12 photons, yielding 1 CO_2 molecule / 12 quanta = 0.08. ΔE_a is the pigment absorbance and light dependent (mol of quanta /area / time) component in the equation and requires measurements from integrating sphere spectrophotometry and UV-vis spectrophotometry, in addition to surface irradiance. The factor 12000 is the conversion from mol of quanta to mg C.

To correct for backscatter in the spectrophotometer the absorbance at 750 nm was subtracted from the absorbance in the PAR spectrum. Pigment absorbance was computed by subtracting the absorbance of the bleached filter from the absorbance of the non-bleached filter. The pigment and detritus absorbance coefficients per meter, $\varepsilon_a(\lambda)$ and $\varepsilon_d(\lambda)$, were computed by multiplying the absorbance with the natural logarithm of 10 and then divide everything with the path length of the water column: volume filtered/ area of filter (V/A). In summary:

$$\varepsilon_a(\lambda) = \ln(10) * \frac{\left(Abs_f(\lambda) - Abs_f(750)\right) - \left(Abs_{fb}(\lambda) - Abs_{fb}(750)\right)}{\frac{V}{A}}$$

$$\varepsilon_d(\lambda) = \ln(10) * \frac{\left(Abs_{fb}(\lambda) - Abs_{fb}(750)\right)}{\frac{V}{A}}$$

The CDOM absorbance coefficient , $\varepsilon_c(\lambda)$, was calculated in the same manner. However, the path length was the length of the quartz cuvette.

$$\varepsilon_c(\lambda) = \ln(10) * \frac{\left(Abs_{dom}(\lambda) - Abs_{dom}(750)\right)}{0.05}$$

The specific water absorbance coefficient, ε_w, was collected from Morel & Prieur (1977). The absorbance coefficients were spectrally averaged by computing the average absorbance over the PAR region, 400 - 700 nm.

$$\overline{\varepsilon_a} = \frac{\sum \varepsilon_{a_i} \Delta \lambda_i}{\sum \Delta \lambda_i (nm)}$$

$$\overline{\varepsilon_d} = \frac{\sum \varepsilon_{d_i} \Delta \lambda_i}{\sum \Delta \lambda_i (nm)}$$

$$\overline{\varepsilon_c} = \frac{\sum \varepsilon_{c_i} \Delta \lambda_i}{\sum \Delta \lambda_i (nm)}$$

$$\overline{\varepsilon_w} = \frac{\sum \varepsilon_{w_i} \Delta \lambda_i}{\sum \Delta \lambda_i (nm)}$$

$$\varepsilon_{tot} = \overline{\varepsilon_a} + \overline{\varepsilon_d} + \overline{\varepsilon_c} + \overline{\varepsilon_w}$$

The surface irradiance was integrating to the depth of the pycnocline using Beer-Lamberts law of monochromatic light moving through a liquid.

$$E_{pyc} = E_0^{-\varepsilon_{tot} * z_{pyc}}$$

The irradiance left at the pycnocline was used in calculating delta E.

$$\Delta E = E_0 - E_{pyc}$$

ΔE_a describes how much of the irradiance is absorbed by pigments per square meter in the water column from surface to pycnocline.

$$\Delta E_a = \frac{\bar{\varepsilon_a}}{\varepsilon_{tot}} * \Delta E$$

2.5 Statistical analysis

All statistical analyses for this thesis were conducted in R version 4.2.2 and all figures were made using the package ggplot2 (Wickham, 2016). The linear models were made with the base R function lm(). Light data from TriOS measurements were modeled with hierarchical linear models (the lmer()-function from the lme4()-package). The map was made using the ggmap-package and Stamen maps (Kahle & Wickham, 2013). CTD data was analyzed with the "oce"- and "ocedata"-packages. PAR-data for each incubation date, at the coordinates corresponding to the UiO field station in Drøbak, were downloaded from the "STRÅNG"-database (https://strang.smhi.se/) and processed in RStudio.

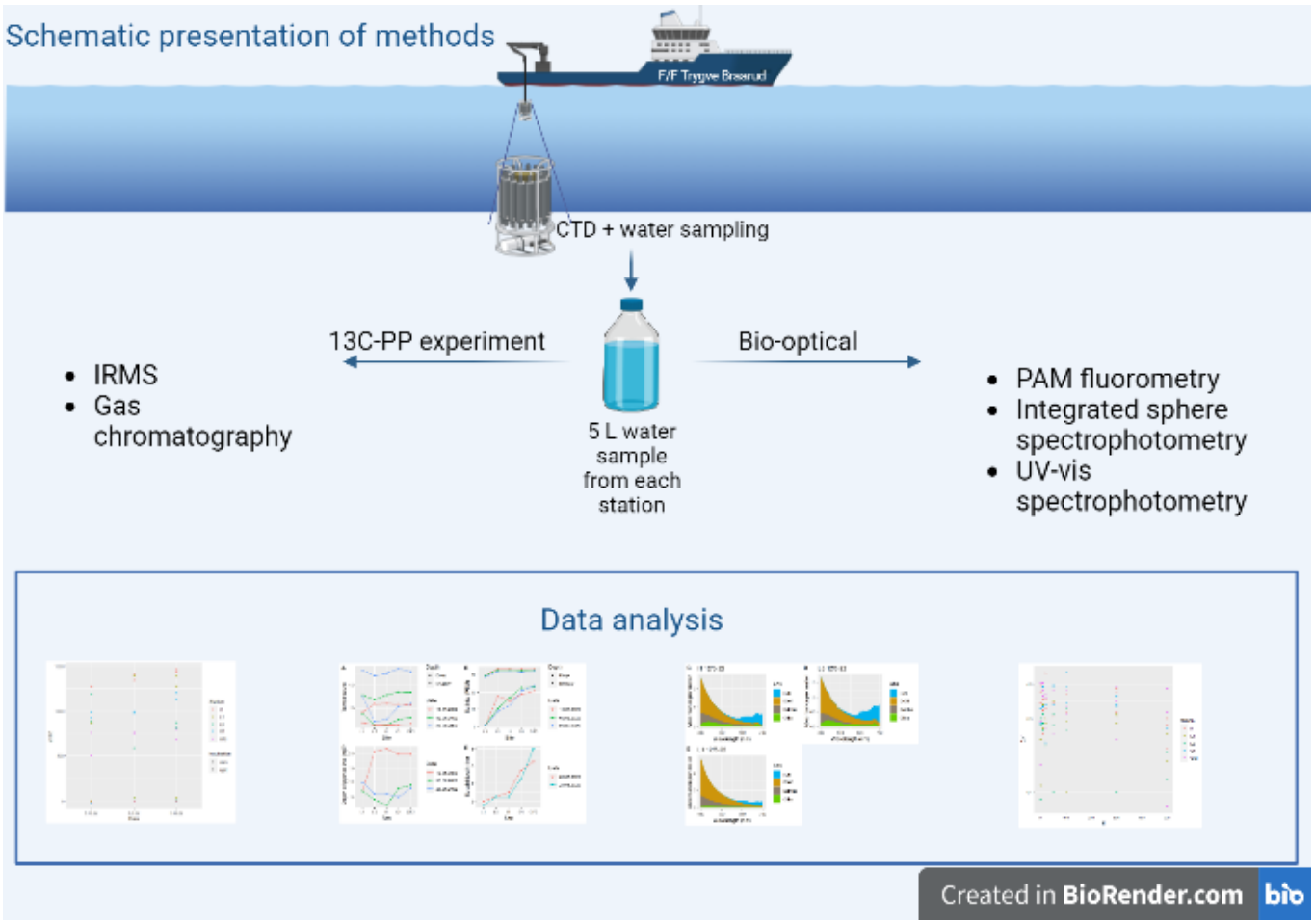

Figure 2: Schematic presentation of methods, created in BioRender.com

3 Results

The results are divided into 5 sections. The first is the section describing the physicochemical and optical properties of the water column at each station for each cruise date. The three following sections will present results from the VGPM, ^{13}C-PP experiment and the BO-PP method of quantifying primary production, respectively. The last section will compare the methods.

3.1 Physicochemical and optical properties of the water column

The physicochemical and optical properties of the water column were investigated using CTD-data and Secchi depth data. The temperature and salinity data shown in Figure 3 are from a subset of CTD-data in the same depth interval as the water samples, 3-4 m. An example of the full CTD-profile for station OF2, 12th of May 2022 can be found in Figure 15 in the appendix. As shown in Figure 3A the temperature is quite consistent across stations for each date, with increasing temperatures from the first to the last cruise date. The upper water layer holds a temperature around 10°C at the 12th of May, between 12-13 °C at the 2nd of June and around 17-18 °C at the 29th of June. Figure 3B show an increasing salinity from the innermost to the outermost station, with the highest salinities at station OF2 ranging between 20 and 25 PSU. L1 had the lowest salinities, all at approximately 1 PSU.

The pycnocline is defined as the largest relative density change per unit depth, the Brunt-Väisälä frequency squared (N^2) maximum, in the CTD-profiles. The depth of the pycnocline remained relatively stable at station L1, between 7 m and 10 m, across dates, while the other stations show a large variability in the depth of the pycnocline, especially between the first and the second cruise. On the 12th of May the pycnocline is stable at around 20 m depth for all stations, except L1. The dates in June show a shallower pycnocline, compared to the cruise in May. The largest variability in the pycnocline is found at station I1, which has the maximum depth at approximately 22 m and minimum depth at 2.5 m. The optical properties are visualized with Secchi depths in Figure 3D, showing a similar trend as the salinity, with increasing transparency from the innermost to the

outermost station. Maximum water transparency, or Secchi depth, is recorded at the 29th of June at 8 m at OF2. Minimum water transparency is recorded at L1 at 29th of June at 1 m.

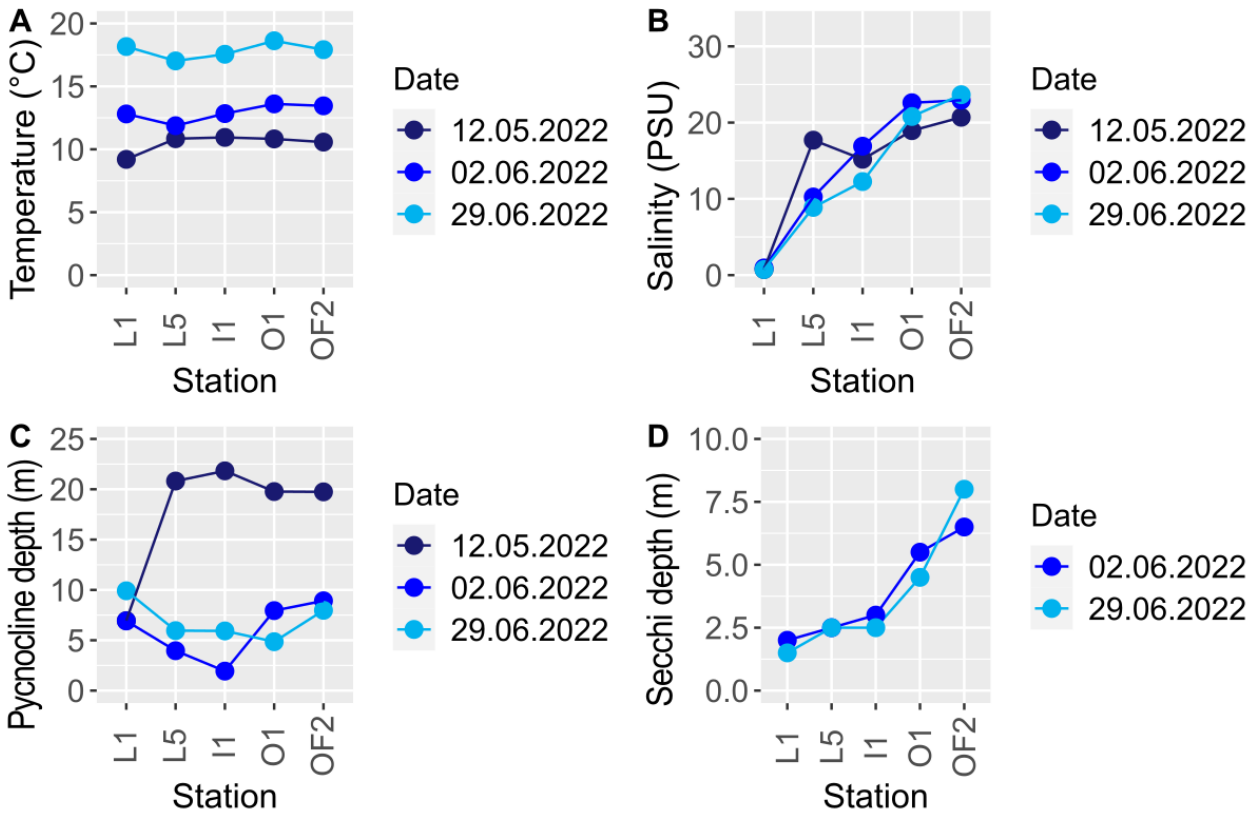

Figure 3: The stations in the Oslofjord transect described by different parameters; **A** = Temperature (°C), **B** = Salinity (PSU), **C**= Depth of pycnocline (m), **D** = Secchi depth (m). 12th of May is missing due to equipment failure during this cruise.

Further investigations of the optical properties were made with irradiance measurements from TriOS-data. The attenuation coefficient for each wavelength at each station was found using the hierarchical model, as the coefficient is the negative slope of log-transformed irradiance against depth, grouped by wavelength. The overall patterns of attenuation for all stations show a peak around 450 nm and a decrease towards 550 nm, and then an increase in attenuation for wavelengths higher than 550 nm, as visualized in Figure 4. Station L1 has the highest attenuation coefficient across wavelength, between 0.5 m^{-1} and 2.5 m^{-1}. High noise at wavelengths with

highest attenuation is due to sensitivity limitations with the spectrometer. The lowest overall attenuation coefficient is at OF2, between 0.2 m^{-1} and 0.75 m^{-1}.

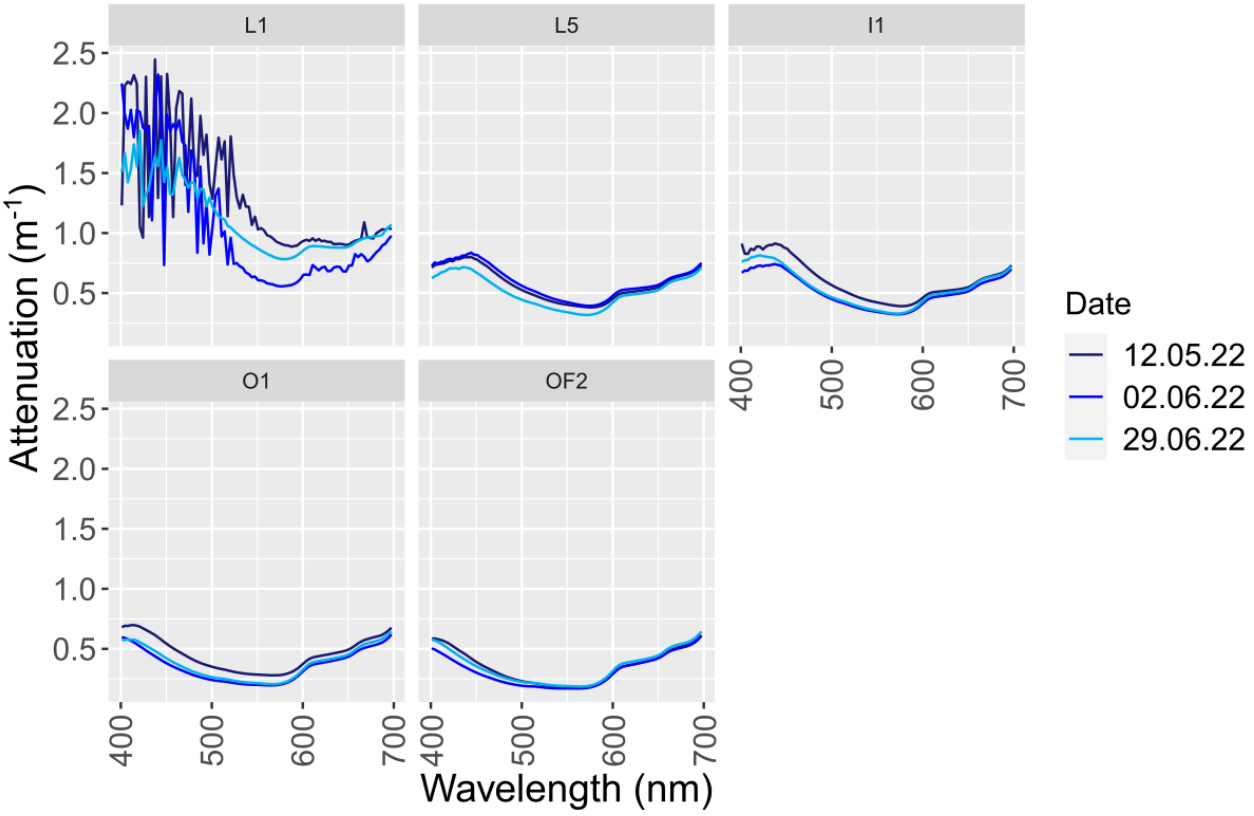

Figure 4: The attenuation coefficient (m^{-1}) at each wavelength (nm) in PAR region at each station. High noise at wavelengths with highest attenuation is due to sensitivity limitations with the spectrometer.

The attenuation coefficients were used to predict the endmembers of the attenuation coefficient minimum and the wavelength at the minimum with salinity as the predictor variable in a linear model, shown in Figure 5. The salinity range from the CTD-data was used to define endmembers, where freshwater = 0 PSU and saline water = 33 PSU. The attenuation coefficient and the wavelength minimums show the same trend of high values in fresh water compared to saline water. The attenuation coefficient endmember is between 0.6 m^{-1} and 0.7 m^{-1} in freshwater and between -0.2 m^{-1} and 0.07 m^{-1} in saline water. For the wavelength minimum the endmember is between 578 nm and 587 nm in freshwater and between 552 nm and 564 nm in saline water. In

addition, measurements of DIC, from GC, were used to predict concentrations of dissolved inorganic carbon in fresh and saline water. The DIC concentrations show a trend of low concentration in freshwater and higher concentration in saline water. The endmember for the predicted concentration of DIC is between 352 µmol/L and 566 µmol/L in freshwater and between 1932 µmol/L and 2199 µmol/L in saline water. This corresponds to DIC concentrations between 4 mg/L and 7 mg/L in freshwater and between 23 mg/L and 26 mg/L in saline water. All predictions are presented with 95% confidence intervals, Figure 5.

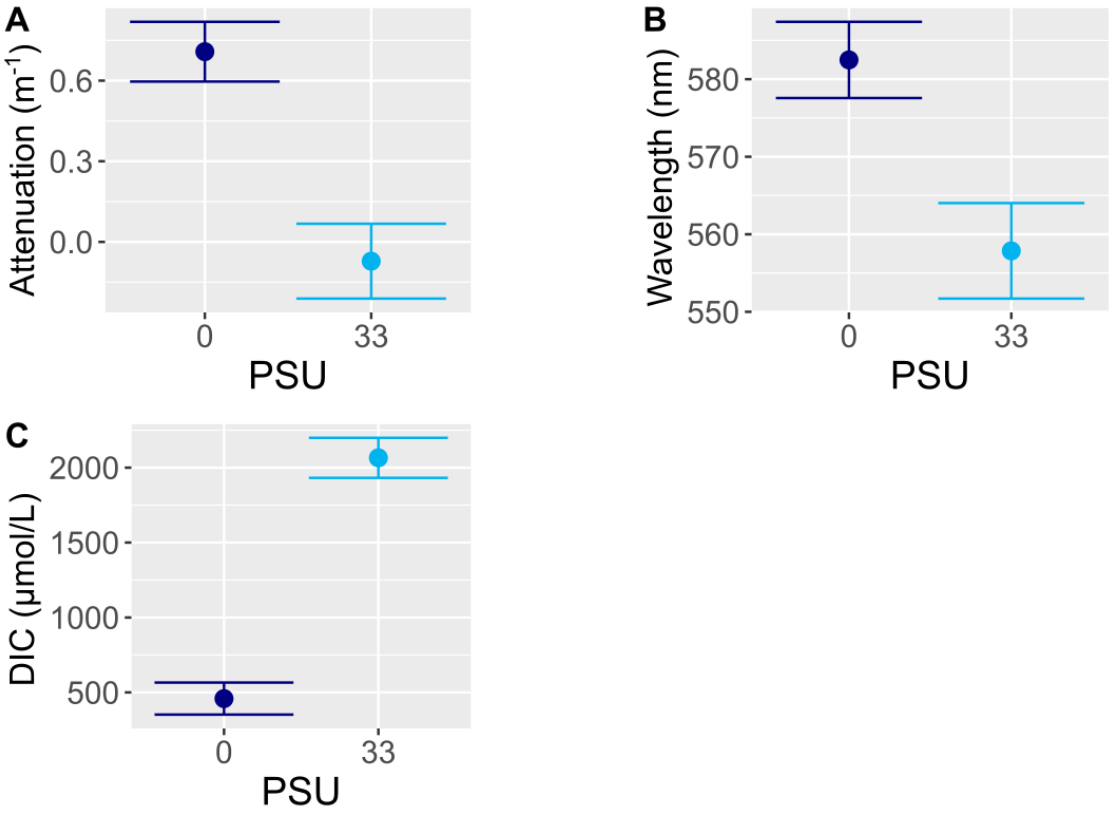

Figure 5: Predicted endmembers, in a 95% confidence interval, for minimum attenuation (m^{-1}), wavelength at minimum (nm) and DIC (µmol /L) in fresh (PSU = 0) and saline (PSU= 33) water.

Lastly, the surface irradiance measurements, E_0, are visualized in Figure 16, Figure 17 and Figure 18 in the appendix. Figure 16 shows the time course of PAR the irradiance for the first incubation experiment, from 12th of May to the 13th of May, where t_1 is the start of the incubation and t_2 is the end. Using the E_0- equation, the integral of this curve yields 30 mol /m^2/d. This is the lowest

recorded amount of photons, as the incoming flux during the second incubation yields 52 mol/m^2/d and the third yields 64 mol/m^2/d.

3.2 Primary production estimated by VGPM

Estimates of primary productivity based on VGPM were calculated based equation 1. The estimates show a trend of increasing productivity with increasing salinity, as seen in Figure 6, with a range from around 500 mg/m^2/d to around 5500 mg/m^2/d.

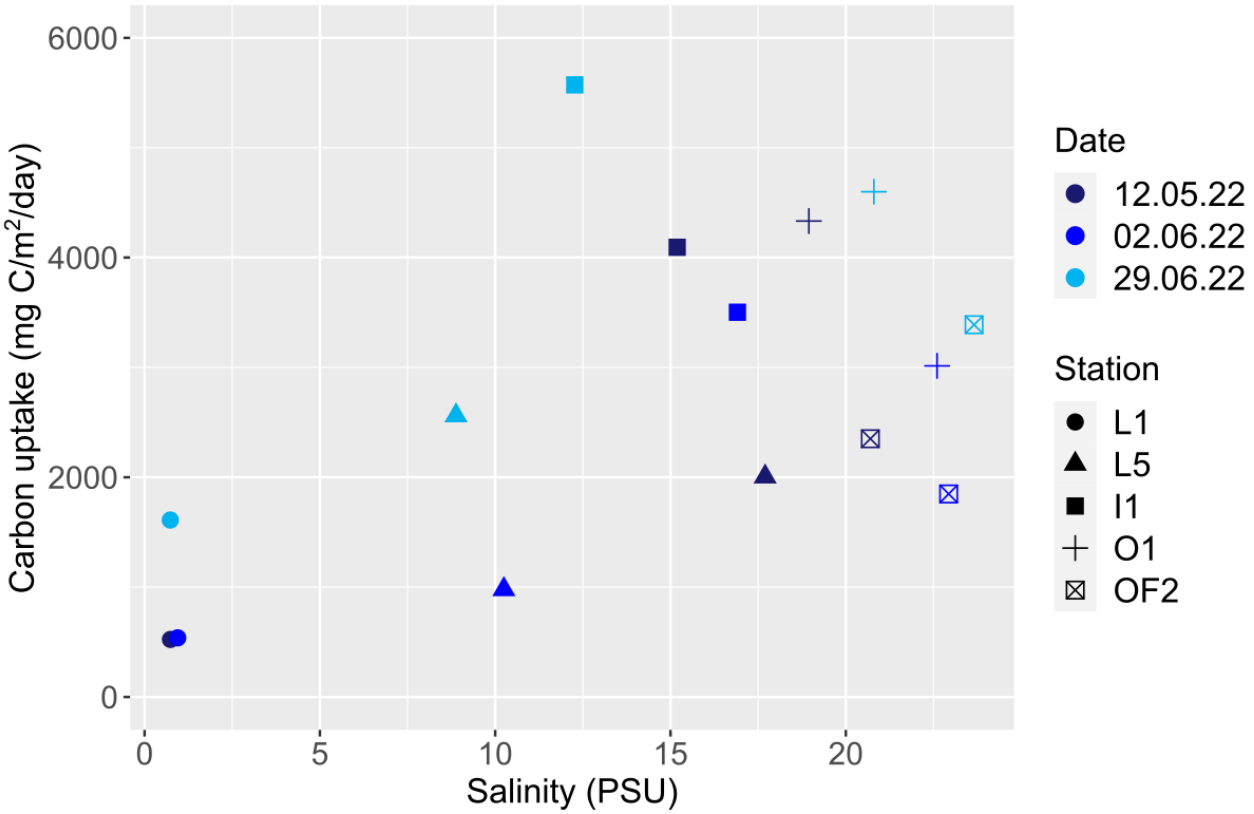

Figure 6: VGPM rates of net carbon uptake (mg C/m^2/d) from equation 3 against salinity (PSU) across stations (symbols) and dates (color).

3.3 Primary production estimated from ^{13}C incubations

Equation 2 was used to calculate primary production based on δ^{13}C measurements from IRMS. The rates of primary production show an increase in production with an increase in salinity, Figure 7.

The production ranges between 20 mg/m^2/d and 350 mg/m^2/d, an order of magnitude lower than the VGPM estimates. The highest production is seen at station I1, at the 29th of June, when salinity = 12.5 PSU.

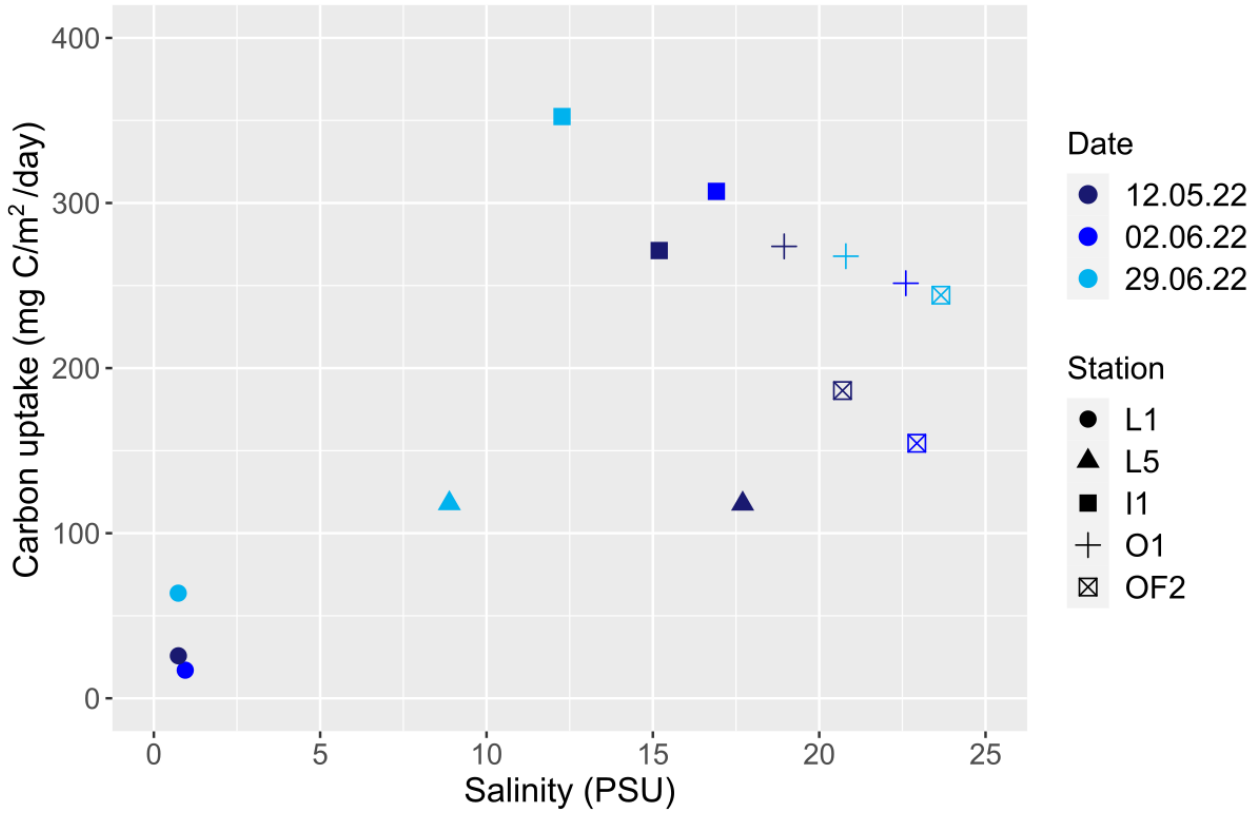

Figure 7: Net carbon uptake (mg/m^2/d) from ^{13}C-PP experiment, using equation 2, with salinity (PSU) as predictor variable.

3.4 Primary production estimated with the bio-optical method

The calculated absorbance coefficients were used to visualize the contribution of each component, i.e.: water, CDOM, non-algal particles (detritus) and algae (photosynthetic pigment) to the absorbance of light per meter in the water column in the PAR region. The absorbance coefficients for each parameter are stacked on top of each other in a cumulative plot, for each wavelength as shown in Figure 8.

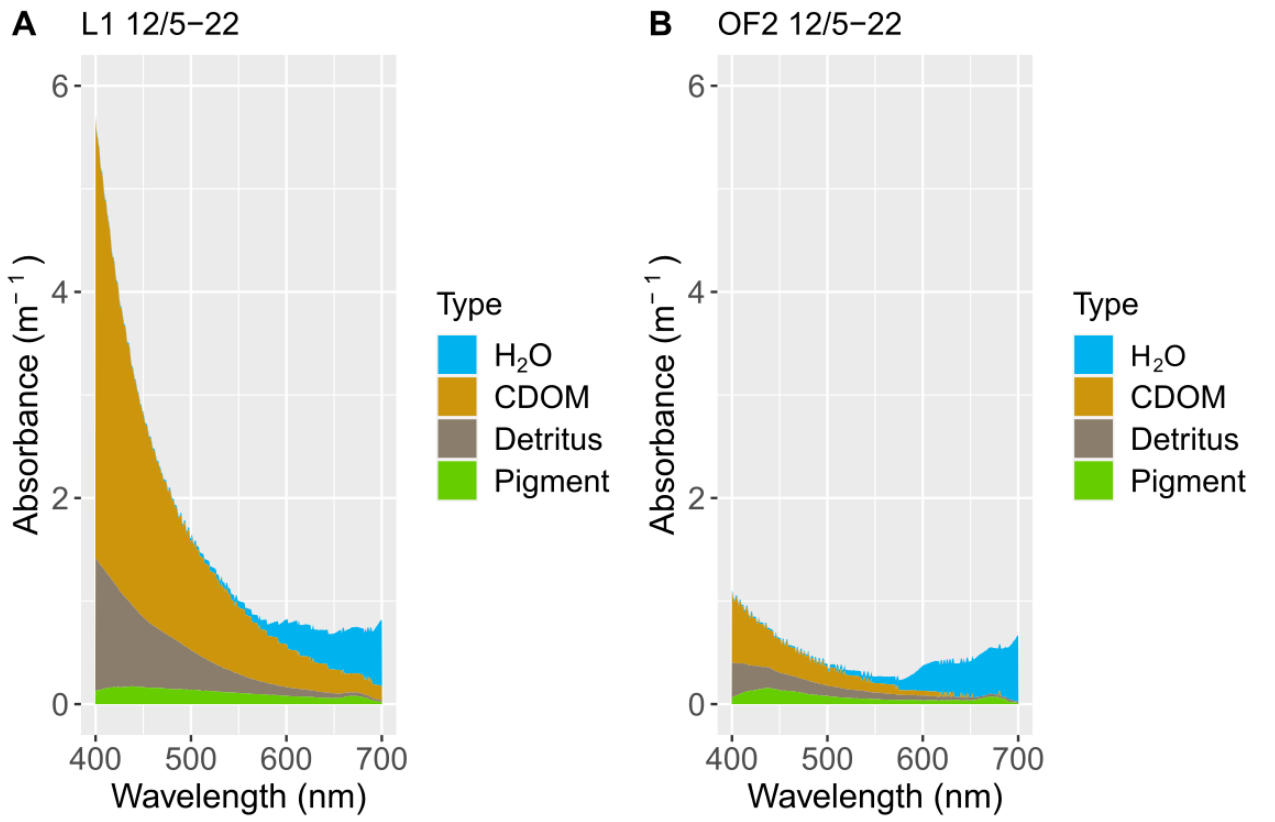

Figure 8: Cumulative absorbance spectra for water, colored dissolved organic matter, detritus and photosynthetic pigment. The pigment absorbance is represented by the green area at the bottom, while the grey-brown area on top of pigment represents detritus absorbance. CDOM absorbance is shown in the brown-orange area, while water is represented with the blue area. **A** = Station OF2 at the 12th of May 2022, **B** = Station L1 at the 12th of May 2022.

As visualized in Figure 8, the cumulative absorbance peaks towards the short wavelength end of the PAR-spectrum, at 400 nm. On the 12th of May CDOM is the main contributor to the absorbance at all stations, especially in the 400-550 nm range. Above 550 nm the main contributor gradually shifts towards water itself. Figure 8 displays the extremes, the lowest and the highest cumulative absorbance. All stations show characteristic peaks in pigment absorbance at approximately 440 nm and 675 nm. These patterns are observable in the cumulative absorbance spectra for all stations and dates (see appendix: Figure 19, Figure 20, Figure 21, Figure 22 and Figure 23).

To explore differences in the absorbance across stations and dates, the spectrally averaged contributions of each component were calculated in regard to the total absorbance. Station L1 generally has the highest total absorbance and CDOM as the largest contributor across all dates. However, station L5 at 29th of June, has the highest single peak at approximately 1.80 m^{-1}. Station OF2 has the lowest total absorbance across all dates, with the minimum at 0.5 m^{-1} at 12th of May. In addition, as shown in Figure 9, station OF2 has the lowest contribution of pigment absorbance across stations and dates.

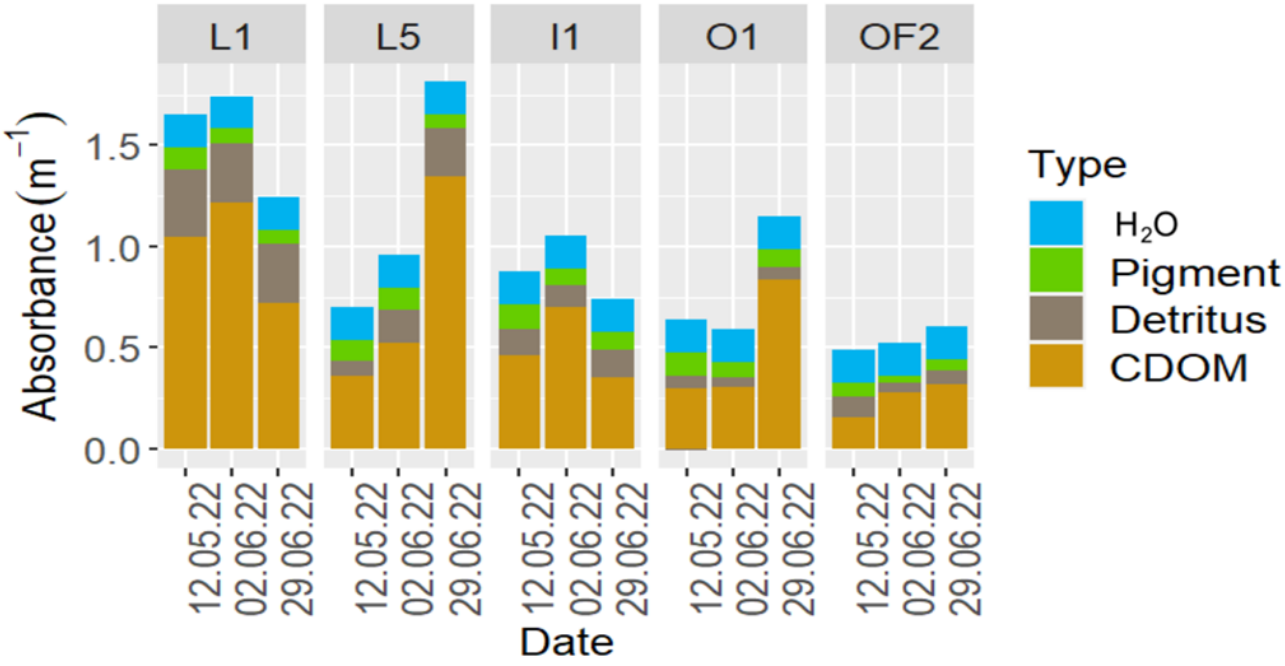

Figure 9: Total absorbance (m^{-1}) for spectrally averaged absorbance for water (H_2O), photosynthetic pigment, detritus and colored dissolved organic matter at each station and date. The CDOM absorbance is represented by the orange area at the bottom, while the grey-brown area represents detritus absorbance. Pigment absorbance is represented by the green area and the blue area represents the water absorbance

The total absorbance and chlorophyll a absorbance coefficients are used in the calculations of rates of carbon uptake ($mg/m^2/d$) using equation 3. The rates are calculated using the mean quantum yield across the incubation intensities for each station and date. The quantum yields

from PAM fluorometry are visualized in Figure 24, Figure 25 and Figure 26 in the appendix, on a log-scale. When plotted with salinity as the predictor variable, the bio-optical rates of carbon uptake show an increase in productivity with an increase in salinity, and a consistency at different salinities except for 10-15 PSU, as visualized in Figure 10. The overall linear trend shows an increase in productivity from 500 mg/m^2/d at the lowest salinity to 2.2 g/m^2/d at the highest salinity. However, the maximum value and the outlier show a productivity of approximately 2.7 g/m^2/d for station I1 on the 29th of June.

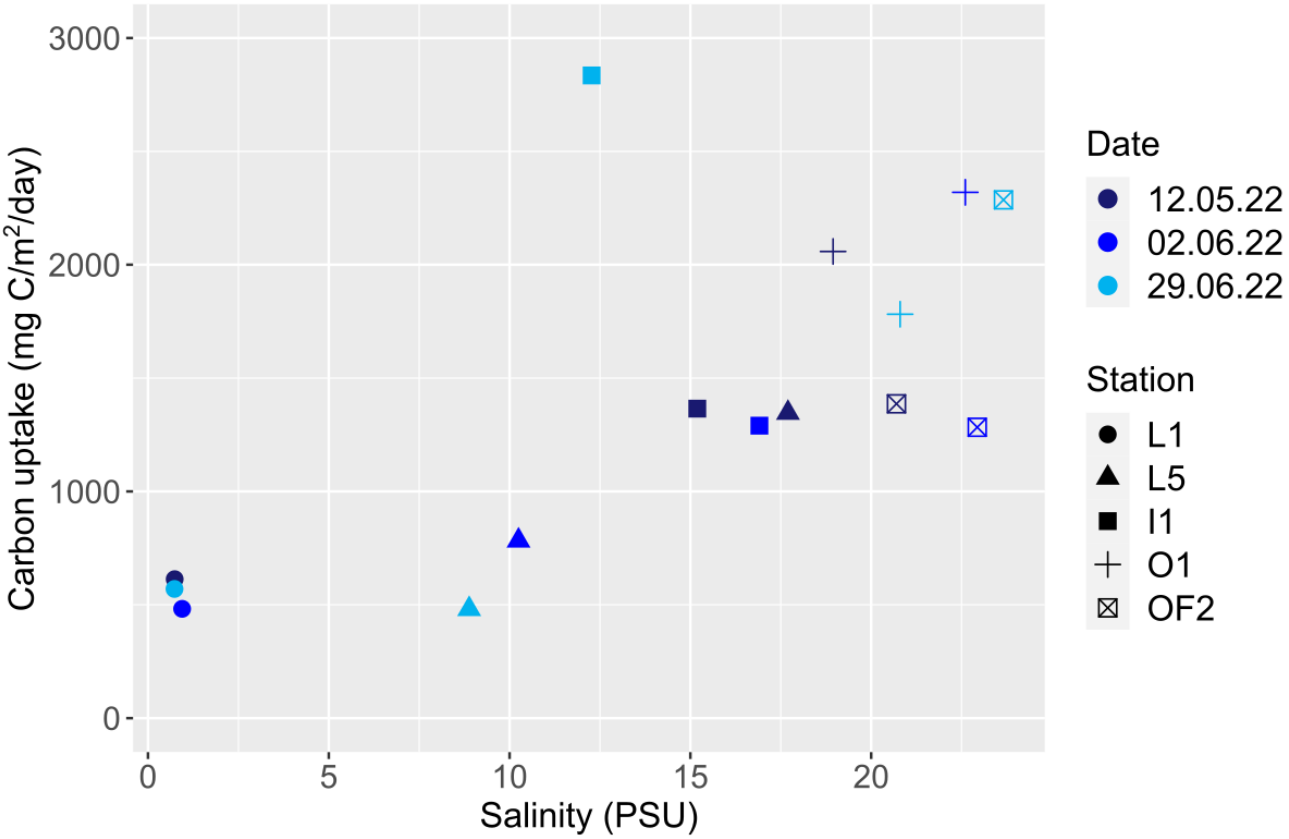

Figure 10: Bio-optical rates of gross carbon uptake (mg C/m^2/d/) from equation 1 with salinity (PSU) as predictor variable

3.5 Method comparison

To compare differences between the different methods of quantifying primary production, and their relationships with salinity and the spectrally averaged CDOM absorbance ($CDOM_{sa}$) , a

scatterplot was made. The plot shows a negative correlation between $CDOM_{sa}$ absorbance and salinity. This negative relationship is also observable between $CDOM_{sa}$ and the BO-PP and more loosely between $CDOM_{sa}$ and ^{13}C-PP. The relationship between $CDOM_{sa}$ and VGPM show a similar negative trend, but with large variability and lower correlation. All productivity estimates show a positive correlation with increasing salinity, though with high variability. The productivity estimates displays positive correlation when compared to each other, with strong correlation seen between the estimates from the ^{13}C-PP experiment and the VGPM, though with an order of magnitude difference in estimates.

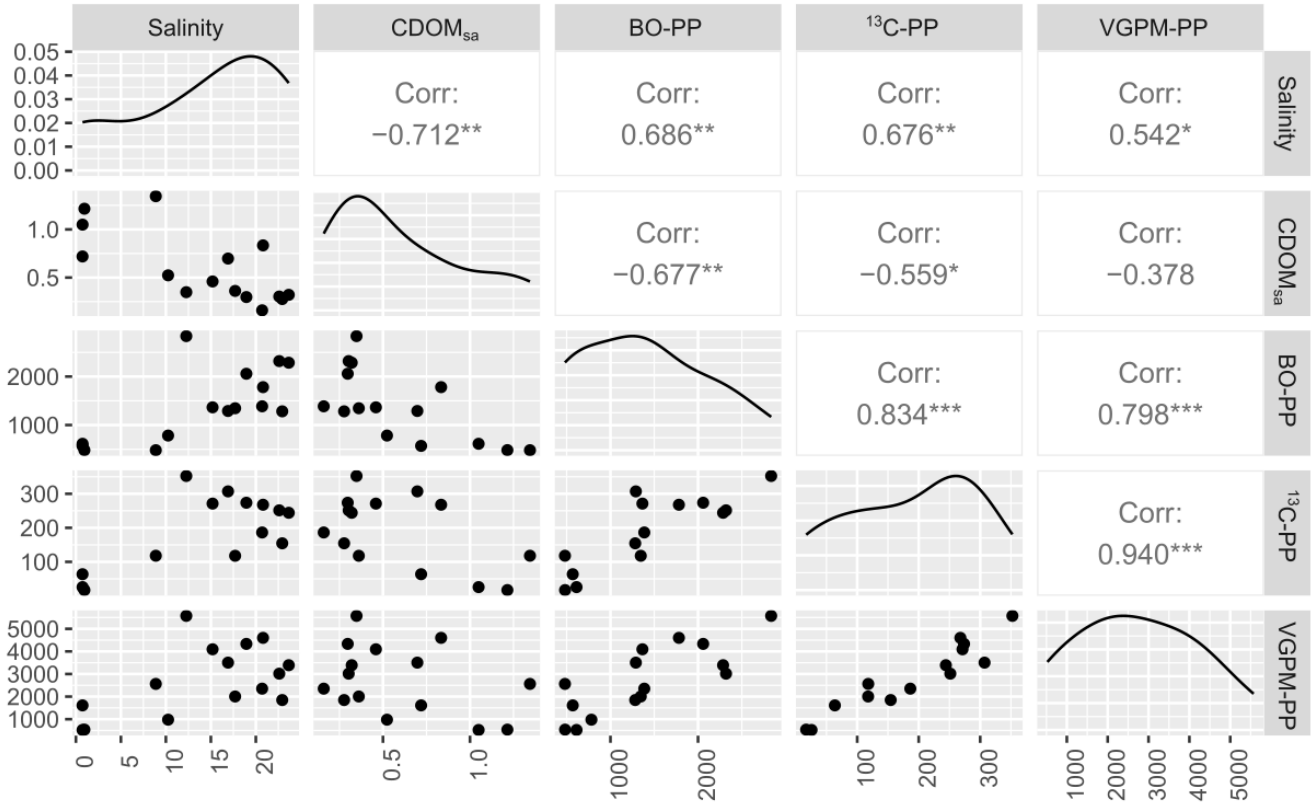

Figure 11: Scatterplot for salinity (PSU), spectrally averaged CDOM absorbance ($CDOM_{sa}$) (m^{-1}), BO-PP (mg C/m^2/d), ^{13}C-PP (mg C/m^2/d) and VGPM-PP (mg C/m^2/d). The diagonal represents the variable distribution. The salinity in the lower left corner display correct values, the upper left yields incorrect values[6].

[6] This is a known bug for GGally::ggpairs. https://stackoverflow.com/questions/69377548/ggally-ggpairs-plot-y-axis-of-the-first-variable-is-labelled-with-wrong-values

The negative correlation between $CDOM_{sa}$ and salinity is further investigated by fitting a linear model with salinity as a predictor variable for the response in $CDOM_{sa}$ absorbance, as visualized in Figure 12. This reveals a slope = -0.035, with standard error (SE) = 0.004 (-0.035 ± 0.004).

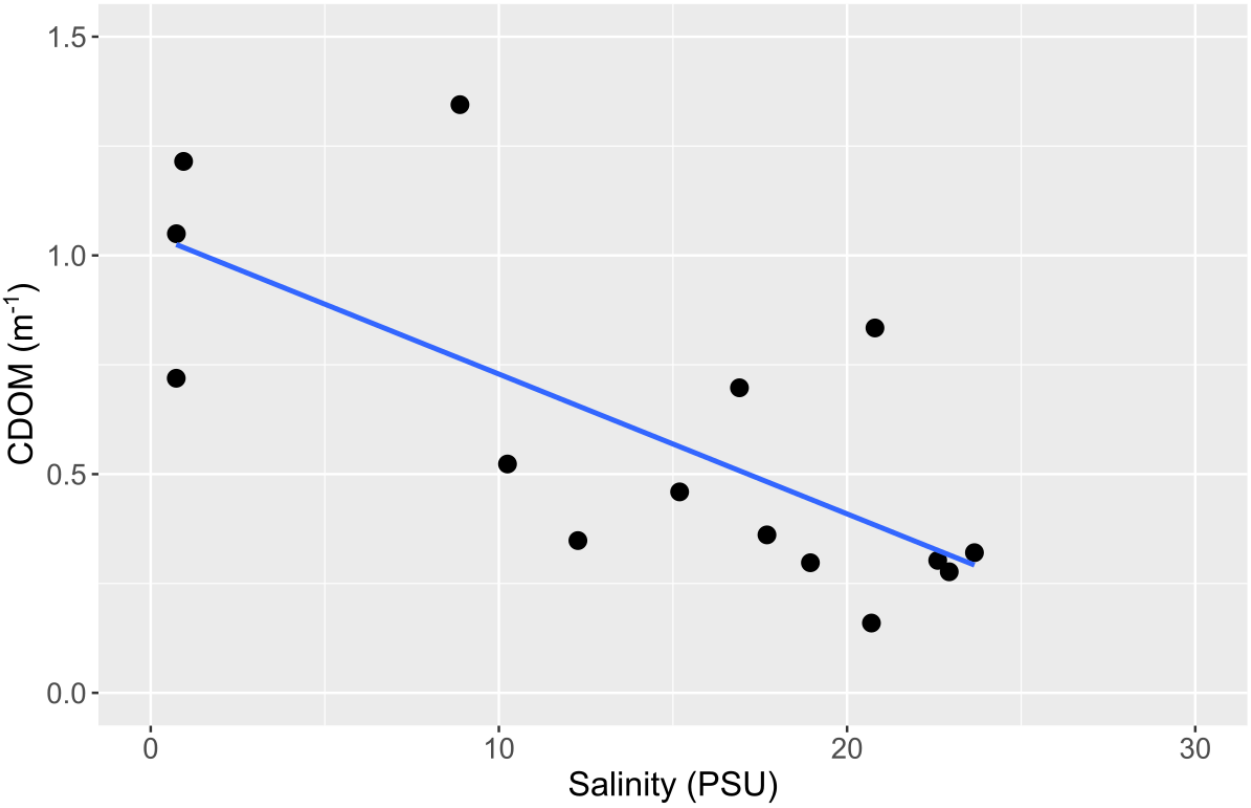

Figure 12: The $CDOM_{sa}$ absorbance (m^{-1}) with salinity (PSU) as a predictor variable. Fitted with regression line; slope = -0.035 ± 0.004.

To assess the relationship between the chlorophyll concentration and the primary production, volumetric primary production was calculated (µg/L/d) based on the production in the incubation bottles. The production ranges from 11 µg/L/d to 65 µg/L/d, while the chlorophyll concentration has a range between 4 µg/L and approximately 12 µg/L. Chlorophyll a concentration is used as a predictor variable for volumetric production, to look at the change in production in relation to change in chlorophyll. This is described with the slope of the fitted regression line in Figure 13A,

slope = 4 ± 1. The volumetric primary production displays a positive correlation with chlorophyll concentration, but with variation along the line.

Investigation of how the carbon uptake per mg chlorophyll a against temperature fit with the P_{opt}^{b}, was conducted by plotting the chlorophyll specific production with temperature as a predictor variable, with the polynomic P_{opt}^{b} from Behrenfeld and Falkowski (1997a) as an overlay. The unimodal shape with decrease > 20 °C follows from the model prediction by Behrenfeld and Falkowski (1997a). The chlorophyll specific production show increase with temperature, yet with quite some scatter, ranging from 2 mg C/mg chlorophyll to 8 mg C/mg chlorophyll, within the temperature interval from 10-20 °C, Figure 13B.

In addition, salinity was used as a predictor variable to investigate changes in chlorophyll specific primary production in relation to changes in salinity. This relationship is illustrated in Figure 13C. The calculated chlorophyll specific primary production is represented by dots. The data is fitted with a regression line, slope = 0.16 ± 0.05.

To assess whether the observed increase in production with increasing salinity, is rather a result of the decreased $CDOM_{sa}$ absorbance along the salinity gradient, chlorophyll specific primary production was plotted against $CDOM_{sa}$ absorbance. The data is fitted with a regression line with slope = -2 ± 1. This is illustrated in Figure 13D, which shows a slight decrease in chlorophyll specific primary production with an increase in $CDOM_{sa}$ absorbance.

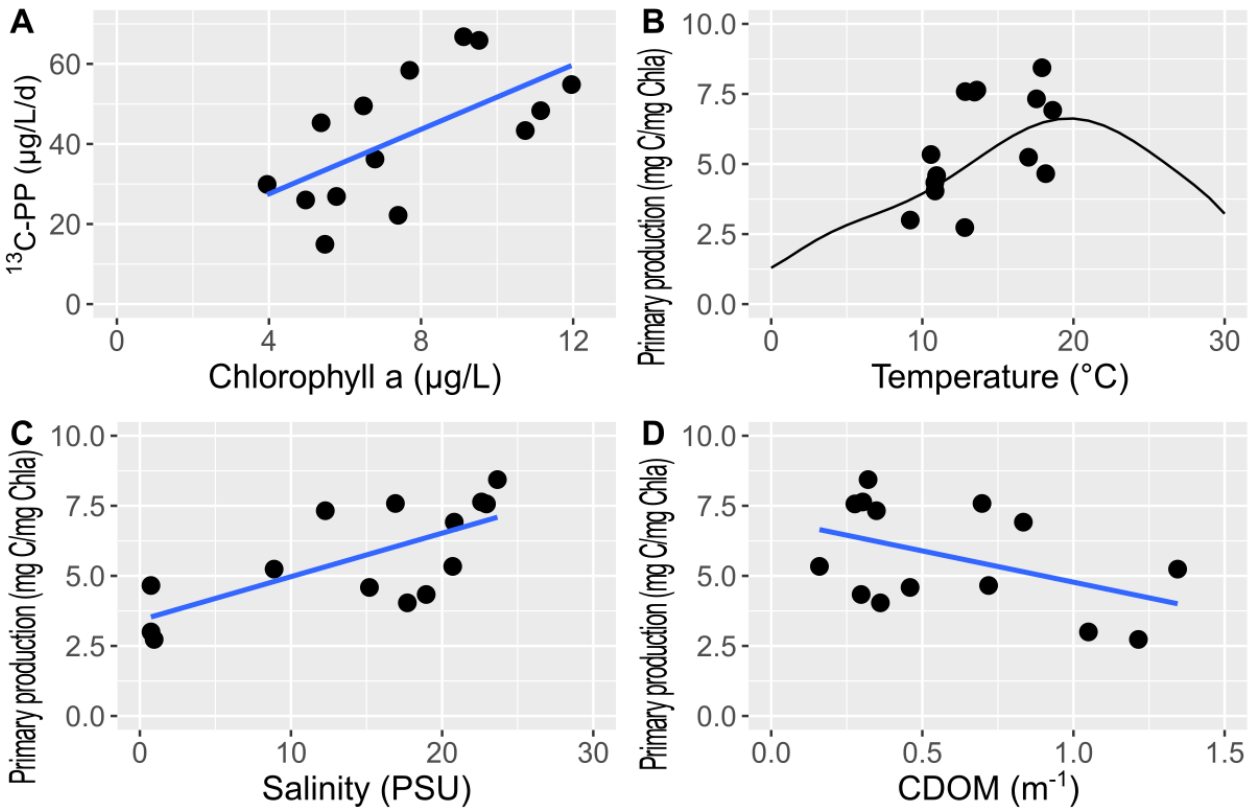

Figure 13: Figures visualizing the relationships between primary production, chlorophyll a, temperature, salinity and $CDOM_{sa}$ absorbance. **A** = Volumetric primary production (µg/L/d) against the concentration of chlorophyll a (µg/L); fitted with regression line, slope = 4 ± 1, **B** = chlorophyll specific primary production (mg C/ mg chla) against temperature °C, with P^{b}_{opt} as an overlay. **C** =chlorophyll specific primary production (mg C/ mg chla) with salinity as predictor variable; fitted with regression line, slope = 0.16 ± 0.05. **D** = chlorophyll specific primary production (mg C/ mg chla) with $CDOM_{sa}$ absorbance (m^{-1}) as predictor variable; fitted with regression line, slope = -2 ± 1

4 Discussion

All primary production estimates in the Oslofjord transect display an overall similar trend of increasing production with higher salinities, and a negative relationship with CDOM absorbance. The overall trend of increasing production with increasing salinity is more likely to be an increase in production due to the decrease of CDOM absorbance, rather than a response to the salinities *per se*. This is supported by the negative correlation between all estimates and CDOM absorbance, and the correlation between higher salinities, less freshwater input from Glomma, and lower CDOM absorbance.

4.1 Optical properties of the Oslofjord

The physicochemical and optical analysis from the Oslofjord reveal a clear salinity gradient from the innermost towards the outermost station in the field transect, with a similar trend observed in the optical clarity measured with Secchi depth. This is further supported by the predicted endmembers for the fresh and saline water. The predicted attenuation minimum is higher in the fresh water compared to the saline water, meaning that the attenuation generally is higher in the innermost part of the Glomma estuary, compared to the outer stations. The visualizations of the attenuation across wavelength display a similar relationship between stations, with a high attenuation coefficient at the innermost station. The high variability (the “noise”) in the attenuation for station L1 might be a result of the dark water and sensitivity limitations of the sensor. Figure 8 and Figure 9 reveal that CDOM accounts for most of the absorbance in the water column, especially in the shorter wavelength of the PAR region. In general, the highest CDOM absorbance is found at the Glomma station, L1, with the greatest influence of terrestrial run-off, even though the highest absorbance is found at L5 for the last cruise date. However, there is no apparent reason as to why this station has one single high extreme for CDOM absorbance, while the L1 station is relatively low for the same date. It could be a consequence of localized weather increasing the run-off at this particular location, or more likely a measurement error.

The wavelength minimum is also higher in fresh water, resulting in a color difference between fresh and saline water, with darker or browner water at lower salinity. As the endmembers are predicted by use of a linear model over a salinity range from 0 to 33 PSU, it could be argued that these results apply to other coastal areas with substantial riverine influence. This is supported by Urtizberea et al. (2013), who measured a CDOM attenuation between 0.03 m^{-1} in clear oceanic water and 0.2 m^{-1} in coastal areas. These measurements align with the predictions in Figure 5. However the predictions are for total attenuation, not solely CDOM attenuation, and thus are higher. Several studies have observed a trend of darkening waters in relation to increased run-off due to afforestation and an intensifying hydrological cycle as a consequence of increasing global temperatures, especially in eastern parts of Norway (de Wit et al., 2016; Finstad et al., 2016; Frigstad et al., 2020; Opdal et al., 2023). A negative relationship was found between $CDOM_{sa}$ absorbance and salinity, with a linear correlation, confirming that the selected transect is indeed a gradient of increasing optical clarity when the riverine influence decreases, with the implications this has for primary production. Though not extensively investigated for marine environments (Frigstad et al., 2020), the darkening, or browning, of lakes due to increased run-off has been shown to have detrimental effects on primary production (Thrane et al., 2014). However, the darkening of coastal waters has affected the timing of the spring bloom, resulting in a later onset of the growing season (Opdal et al., 2019, 2023)

Compared to the optical properties the opposite relationship is seen with the predicted endmember for the DIC concentration, Figure 5. The DIC concentration is higher in saline water, which is to be expected. The predicted concentrations of DIC are in agreement with concentrations previously measured for sea water (Liu et al., 2013).

4.2 Estimates of primary production and their influencers

As mentioned above, all estimates display the same overall trend with increasing production with decreasing $CDOM_{sa}$. However, there is a large variability between the estimates. The estimates of primary production have different conceptual basis, yielding differences in which parameters are being used for the depth integration and conversion to area specific production. The BO-PP uses *in*

situ fluorescence measurements and *in vivo* absorbance spectra combined with irradiance integration to the depth of the pycnocline to estimate areal production. The VGPM is a remote sensing chlorophyll based method of quantifying rates, while the ^{13}C-PP is based on carbon fixation. The two last methods have a similar approach in estimating areal production based on the euphotic depth and a light dependent component. The VGPM also employs P^{b}_{opt} and day length as variables.

The VGPM

The chlorophyll content of phytoplankton biomass is dependent on different environmental factors, such as the light intensity or the temperature, and even the phytoplankton community composition (Behrenfeld et al., 2005; Desmit et al., 2020). Due to these variations, chlorophyll is a poor proxy for estimating carbon biomass, which the VGPM is based upon. While the VGPM does include temperature and light as parameters in the calculation, equation 1, the plasticity of chlorophyll a is a source of uncertainty in all chlorophyll based estimates of primary production (Behrenfeld et al., 2009; Siegel et al., 2013). Figure 13A visualizes the relationship between the estimated chlorophyll a concentration and the direct measurements of carbon fixation, revealing a positive correlation, suggestion that the chlorophyll as a proxy for primary production is a fair assumption for this study.

Another constraint with the VGPM, in this context, is that the model is based on remote sensing technology, designed to integrate a large number of spatial-temporal observations to estimate global production, as seen in Field et al. (1998). This global perspective reveals a problem with the parameterization down to a localized area, yielding less sensitive estimates and underperforms compared to local field studies (Behrenfeld et al., 2009).

The ^{13}C-PP method

On the other hand, there is a high correlation, 0.9, between the ^{13}C-PP estimates and the VGPM estimates of primary production. This linear relationship could be explained by the similar approach in determining the areal primary productions for these two estimates, both are

dependent on the euphotic depth and surface irradiance. The ^{13}C-PP estimates are generally lower than both of the other methods, in fact there is an order of magnitude difference between VGPM estimates and ^{13}C-PP estimates. The ^{13}C-PP has however been shown to match well with estimates based on radioisotope uptake (^{14}C-PP), even in areas of low production (López-Sandoval et al., 2018).

As the ^{13}C-PP method has been shown to be a replacement for the ^{14}C-PP method, with a 1:1 relationship between estimates (López-Sandoval et al., 2018), it is a fair assumption that the drawbacks of the ^{14}C-PP method are transferrable to the ^{13}C-PP methods, as they are based on the same principles and mostly the same procedure. The bottle incubations using the O_2 method is a well-known method of measuring NPP in the light bottles and respiration in the dark bottle, yielding GPP. However, in ^{14}C-PP bottle incubations there is a large uncertainty in whether it is the GPP or the NPP that is measured in the light bottles (Peterson, 1980). Most likely it is a mixture. Another factor which contributes to the uncertainty of what is measured in the bottles is the length of the incubation period. However, incubation lasting 24 hours, as was done for this study, is generally believed to yield a measure of net photosynthesis (Laws et al., 2000). There are also constraints with the dark bottle as it is no direct measurement for the respiration losses. This study follows the same principles as in López-Sandoval et al. (2019) where the light bottle is a measure of NPP and the dark bottle is a measure of the natural abundance of ^{13}C in organic matter.

Some of the estimated low production could be a result of the “bottle effect”, where you observe effects on growth that are not a result of the planned experiment. This effect is a known constraint on bottle incubation methods, ^{13}C-PP included. Photoinhibition is a widespread observed effect of bottle incubations in static surface water, especially in high intensity irradiance situations (Gilbert et al., 2000; Peterson, 1980; Steemann Nielsen, 1962). Compared to light limitations, photoinhibition is a poorly understood mechanism. Light limitation is a stoichiometric mechanism between the absorbed quanta and absorbed CO_2, while photoinhibition is a more complex time-dependent mechanism. The energy from the light absorbance excites the chlorophyll, putting it in a high energy state. This high energy can dissipate as heat, a process known as non-photochemical

quenching (NPQ). NPQ is a photoprotective mechanism which protects the phytoplankton from oxidative stress (Kromkamp et al., 2008; Müller et al., 2001). High intensity irradiance situations could also lead to photorespiration, the opposite mechanism of photosynthesis (Peterson, 1980). As the bottles in this experiment where incubated at surface level in an outdoor pool, with natural lighting, it is plausible that the phytoplankton underwent significant irradiance stress, leading to photoinhibition resulting in detrimental effects on the growth.

Temperature is another factor which affects the primary production. Behrenfeld & Falkowski (1997a) introduced the P^b_{opt} as a model to visualize how production is temperature-dependent. According to them production increases until the sea surface temperatures reaches 20 °C, when there is a shift towards a decrease in production. As visualized in Figure 13B, the estimated chlorophyll specific production follows the model below 20 °C, though with large variation. However, these temperature-dependent production estimates are based on the SST from CTD-data, not the actual temperatures in the pool where the bottles were incubated. This is because the temperature-data was corrupted and unusable. As the irradiance was high during the incubations, especially the last two dates, it is entirely possible that the temperature within the pool or even within the bottles surpassed the SST, even with continuous flow of surface water, pushing the production over the temperature limit, resulting in lower production. However, both the highest irradiance and the highest temperatures where recorded during the last incubation period. If there were any detrimental effects of irradiance and temperature during this incubation, the resulting estimates should have been lower than the estimates from the previous incubations, though they are generally higher for the last date, Figure 7.

Other factors that may limit production in the bottles are grazing, CO_2 deficiency and nutrient limitation. This method is the only one out of the three that can be influenced by these important ecological and ecosystem processes, contributing an insight into dynamics which remains undisclosed in the other two methods.

For the Oslofjord there has been an observed shift towards a later onset of the growing season,

which could be attributed to the observed reduction in optical clarity (Aksnes et al., 2009; Lundsør et al., 2020; Opdal et al., 2019). After the initial phytoplankton bloom the upper water column is deprived of nutrients, resulting in a limitation for growth. The spring bloom in the Oslofjord is primarily inhibited by phosphorus limitation in the stratified layer, but long term monitoring have revealed a persistent nitrogen limitation in the stratified layer, and the chlorophyll content in phytoplankton remains low even after increased concentration of phosphorus (Lundsør et al., 2020). Additionally a study by Andersen et al. (1991) revealed that the microalgae in the Oslofjord have a larger capacity for internal storage of phosphorus, compared to nitrogen. However there was no observed limitation of algal growth due to nutrient limitation in this experiment. In the Oslofjord there is a pattern of a second bloom after the spring flood, where the freshwater bring new nutrients to the water column (Lundsør et al., 2020). This flood is observable in Figure 7, when there is a considerable shift in the salinity the second innermost station from the first to the second cruise date, suggesting that the flood took place somewhere in between these dates. The renewal of nutrients associated with spring flood is not correlated with the spring bloom, but it could sustain growth through the summer and potentially the autumn bloom (Frigstad et al., 2020). The VGPM and ^{13}C-PP estimates a higher production for the last date across stations, which could be a result of input of new nutrients and stratification of the water column after the flood. This pattern is however not noticeable in the BO-PP. All the methods yield different results as to when the stations are most productive, which is likely a result of which parameters the methods use and the importance of the parameters in the model. There is no clear relationship except the optical gradient.

The BO-PP

As opposed to the ^{13}C-PP method, the BO-PP method omits constraints associated with bottle incubations, and is both fast and cheap in comparison (Kolber & Falkowski, 1993). On the other hand the bio-optical estimates are influenced by different factors, one of them being uncertainties in the absorbance measurements the calculations are based upon. Due to scattering within the spectrophotometer, the algal absorbance could be artificially amplified and thus create an overestimation of the algal contribution to the total absorbance (Kirk, 1994). However, part of the

possible scattering, e.g. backscattering, was accounted for during calculation of the absorbance coefficients.

Another factor which influences the BO-PP estimates is the use of fluorescence measurements as a proxy for production. PAM fluorometry yields QYs for photosystem II, as a measurement of the utilization of absorbed quanta. The QYs for all stations generally do not exceed 0.5, meaning that less than 50% of the absorbed quanta where used in photochemical work, the maximum theoretical photosynthetic efficiency is measured to 0.8 (Torres et al., 2021). The remaining energy is emitted as fluorescence or dissipated as heat (NPQ). This low efficiency could be a result of the samples not being fully dark-acclimated. However, low QYs are shown to be correlated with nutrient limitation, more specifically nitrogen stress (Kolber et al., 1988, 1990). This is supported by the observed nitrogen limitation in the Oslofjord (Lundsør et al., 2020). The low QYs enhance the credibility of nutrient limitations in the incubation bottles.

The calculations of the rates of electron transport are another source of uncertainty with this method. The use of QYs from PSII to calculate ETRs has a higher correlation with the production of O_2, rather than the fixation of CO_2 (Lawrenz et al., 2013). The CO_2-fixation is assumed to be proportional to the ETR, which leads to an overestimation of primary production. However, this proportionality is supported for phytoplankton, adding to the credibility of these estimates (Gilbert et al., 2000; Kromkamp et al., 2008). On the other hand, ETRs vary with environmental factors and the taxonomic composition of phytoplankton communities, similar to the chlorophyll concentration and show a higher variability compared to carbon fixation (Lawrenz et al., 2013).

The factor for the ratio of mol fixed CO_2 / mol photons is chosen as 0.08 in this study, due to physiological limitations in the photosynthetic process, yielding a conservative estimate as the theoretical minimum is 0.125 (1 mol fixed CO_2/8 mol photons) (Kirk, 1994). However, this might be an upper limit to the carbon fixation in natural conditions, resulting in overestimates of primary production. Babin et al. (1996) found the maximum quantum yield for carbon fixation to average

between 0.03 and 0.05 mol C/ mol photons in eutrophic waters and at approximately 0.005 mol C/mol photons in the upper layer of oligotrophic (nutrient depleted) waters.

4.3 The plausibility of the estimates

Kromkamp et al. (2008) found a remarkable linear relationship, on the log-scale, between the bio-optical and ^{14}C-PP methods, with the bio-optical estimates systematically higher than the ^{14}C-PP estimates. Using PAM fluorometry the bio-optical estimates were 1.6 times higher than the ^{14}C-PP estimates for the same stations. A similar relationship is observed in this study, with a positive correlation of 0.8 between BO-PP and ^{13}C-PP, Figure 11. The BO-PP estimates are higher than ^{13}C-PP, but this is to be expected as the former yields estimates of GPP, while the latter yields estimates of NPP. Following this, the rates from Throndsen (1978) should be lower than the BO-PP estimates in this thesis, as Throndsen used ^{14}C-PP, but remarkably they are almost identical. Throndsen estimated a production around 2.5 mg C/ m^2/d, while the estimates from the BO-PP range between 0.7 mg C/m^2/d and 2.7 mg C/m^2/d. It is not prudent to draw conclusions as to why, because all PP-estimates are a snapshot of production in the specific area at that specific time. However, at the time of Throndsen´s investigation, the Oslofjord, especially its inner part, was eutrophic due to sewage from the city of Oslo, which increases the primary production (Braarud, 1969). As mentioned above drastic measures were taken to reduce the nutrient input in the fjord. Alongside this reduction of nutrients there has been an observed reduction in the chlorophyll concentration (Lundsør et al., 2020), which could suggest that the productivity of the Oslofjord has decreased in the last 30 years. Lundsør et al. (2020) also revealed that the concentrations of chlorophyll a do not exceed 12 µg/L, a persistent low concentration since 1990, after a peak in 1980, when the chlorophyll concentration reached 20 µg/L. A coupling between de-eutrophication and reduction in chlorophyll a is not exclusive to the Oslofjord, and the reduction in chlorophyll is also linked to higher SSTs (Desmit et al., 2020).

In this study, the chlorophyll a concentration used in VGPM and chlorophyll specific production was calculated from the *in vivo* absorbance peak at 670 nm using the specific absorbance of chlorophyll a at 670 nm from Mitchell & Kiefer (1988). The resulting concentrations are consistent

with the reported concentrations from Lundsør et al. (2020), which are a result of long-term monitoring and the method of measuring chlorophyll a with *in vivo* absorbance at 665 nm. The agreement between these measurements adds to the comparability between these studies.

An interesting observation is that the VGPM yields higher production estimates than the BO-PP, as the former is a measure of NPP and the latter is a measure of GPP. Respectively these methods have a high correlation with the direct measurements of C-fixation, the ^{13}C-PP. The correlation between these methods is slightly lower in comparison, but still high. The VGPM estimates are an order of magnitude higher than ^{13}C-PP, and more than double the estimated GPP from the BO-PP, further supporting the overestimation by downscaling to localized areas. This overestimation was also observed by Hill & Zimmerman (2010), when the estimates revealed an order of magnitude error, after retrieving the wrong chlorophyll concentration. The chlorophyll concentration multiplied with the euphotic depth is the single most important parameter in determining production using VGPM, followed by P^b_{opt} (Behrenfeld & Falkowski, 1997b). Because of their high influence on the estimates, uncertainties in these parameters have large consequences. Carr et al. (2006) observed overestimation by the P^b_{opt} when the SSTs where between 10 and 20 °C. On the other hand, the chlorophyll specific primary production is in the same order of magnitude as P^b_{opt} in this study. In addition, CDOM absorption in the water column has proven a vital part of ecosystem modeling and remote sensing estimates, though it is not a part of the VGPM version used here (Siegel et al., 2013; Urtizberea et al., 2013).

4.4 The final show-down

Few studies aim to compare rates of primary production from different methods, and fewer aim to test which method is most suitable to answer specific scientific questions (Staehr et al., 2012). This thesis aims to fulfill the first, if not the second. While the same overall pattern is visible in all estimates, the differences in the calculated rates are quite large. The rates from the ^{13}C-PP method are, as the replacement for ^{14}C-PP, regarded as the standard to which everything is compared, due to the direct measurements of C-fixation. The ^{13}C-PP are the lowest estimates, and both the rates from BO-PP and VGPM are overestimates compared to these rates. However, for the BO-PP, this is

an expected and acceptable overestimate as it is a measure of the GPP, compared to the assumed NPP estimates from the ^{13}C-PP method. The VGPM has a history of overestimation and should only be used as approximations (Carr et al., 2006; Hill & Zimmerman, 2010).

The ^{14}C-PP method has been the preferred method of quantifying primary production, due to its highly sensitive measurements and the simplicity of the method (Regaudie-de-Gioux et al., 2014). In addition, this method yields a direct measurement of C-fixation. The calculated rates have been used in remote sensing calibrations of algorithms retrieving the oceanic primary production, and are the empirical basis on which the P^b_{opt} is built on (Behrenfeld and Falkowski, 1997a). The ^{13}C-PP method is a replacement in light of restrictions using the radioisotope. However, the time-consuming and expensive methodology, in addition to the localized spatial-temporal coverage are important drawbacks to keep in mind.

The bio-optical method could increase the spatial-temporal coverage of PP-estimates due to the fast and cheap methodology, in both marine and limnic environments (Kromkamp & Forster, 2003; Lawrenz et al., 2013). In addition to avoiding the effects of bottle incubations and the extrapolating from bottles to *in situ*, the bio-optical method is certain in that it measures gross primary production (Peterson, 1980; Wilhelm et al., 2004). However, the main uncertainty with this method is in the assumptions regarding the ETRs. As chlorophyll, ETRs are highly variable with environmental factors and the taxonomic composition and display a larger variability in the estimates compared to C-fixation measurements (Lawrenz, 2013).

The largest spatial-temporal coverage of PP-estimates is found with using the VGPM, which is suited for a global perspective. This method incorporates temperature and light intensity which are important factors in the variability of chlorophyll a concentration in phytoplankton biomass (Behrenfeld et al., 2005; Desmit et al., 2020). In addition, this method requires no fieldwork as it is based on remote sensing, which lessens the time-consumption. However, the variability in chlorophyll as a proxy for carbon fixation biomass and in the P^b_{opt}, are unneglectable factors.

In summary all methods have their pros and cons in regards to precision and logistics; expenses and time. An important aspect of choosing a method is the spatial-temporal scale of the region investigated, in addition to which specific scientific question you want an answer to. For this study, due to its localized nature, the ^{13}C-PP method and BO-PP method yields the most plausible estimates of primary production.

Kromkamp et al. (2008) found that the turbidity in the water column is the controlling factor for the observed variability in the photosynthetic parameters, which can be deduced from the positive relationship between the optical gradient and primary production estimates in this study, when the increase in salinity is a proxy for the increase in water clarity. Both the link between increasing SSTs and turbidity with decreasing chlorophyll are interesting in a climate change perspective, as an increase in both is an expected consequence of climate warming (Cadée & Hegeman, 2002; de Wit et al., 2016). For the Oslofjord there has been an observed shift towards a later onset of the growing season, which could be attributed to the observed reduction in optical clarity (Aksnes et al., 2009; Lundsør et al., 2020; Opdal et al., 2019). For this study the increasing production with decreasing CDOM indicates that increasing run-off will further influence primary production, by contributing to a decrease in the rates of carbon fixation.

4.5 Future prospects

The production estimates in this study are all a snapshot of the primary production at the specific location at the specific time. To make inferences in a climate change perspective and about the long-term effects of increased run-off it would be interesting to have several cruises throughout the year, for several years, to observe whether the observed trend in the production is just variation or a result of a changing climate. It would also be interesting to investigate other fjords, with a varying amount of terrestrial run-off to get an overview and a greater basis for comparative studies.

An interesting aspect would be the inclusion of nutrient measurements, for further investigations of the observed pattern and assess whether there is a trade-off between additional nutrients and increased CDOM attenuation related to the spring flood, when it comes to primary production.

It would have been interesting to have ^{14}C-PP estimates for the same samples to investigate correlation between the ^{14}C and ^{13}C, which could support the low estimates from the ^{13}C-PP method, but unfortunately there is no facility for running this kind of radioisotope experiments at the institute.

5 Conclusion

The transect sampled for this study has a clear optical gradient, with a negative correlation between $CDOM_{sa}$ absorbance and salinity. This relationship is reflected in the increase of primary production estimates with increasing salinity, when the salinity is a proxy for decreasing $CDOM_{sa}$ absorbance, thus increasing water clarity. This overall trend is observed in the estimates for all three methods. However, there is a large discrepancy between the estimates, due to different parameterization and uncertainties within each model. Rates of primary production are difficult quantify and no analytical methods are based solely on first principles (Behrenfeld & Falkowski, 1997b). The VGPM yields estimates an order of magnitude higher than the ^{13}C-PP method, with the BO-PP method yielding estimates in between. The BO-PP and the ^{13}C-PP methods are the most suitable for localized studies, such as this, due to overestimations by the VGPM as a result of the downscaling to a localized spatial area.

As terrestrial run-off is predicted to increase due to intensification of the hydrological cycle and afforestation, it is imperative to understand how the coastal primary production is affected by the resulting darkening of the water column (Finstad et al., 2016; Frigstad et al., 2020; Opdal et al., 2023). This study shows that a higher $CDOM_{sa}$ absorbance has a negative effect on primary production.

References

Aksnes, D., Dupont, N., Staby, A., Fiksen, Ø., Kaartvedt, S., & Aure, J. (2009). Coastal water darkening and implications for mesopelagic regime shifts in Norwegian fjords. *Marine Ecology Progress Series*, *387*, 39–49. https://doi.org/10.3354/meps08120

Andersen, T., Schartau, A. K. L., & Paasche, E. (1991). Quantifying external and internal nitrogen and phosphorus pools, as well as nitrogen and phosphorus supplied through remineralization, in coastal marine plankton by means of a dilution technique. *Marine Ecology Progress Series*, *69*(1/2), 67–80.

Aure, J., Danielssen, D. S., & Naustvoll, L.-J. (2014). Miljøundersøkelser i norske fjorder: Ytre Oslofjord 1937-2011. *38 s.* https://imr.brage.unit.no/imr-xmlui/handle/11250/280455

Babin, M., Morel, A., Claustre, H., Bricaud, A., Kolber, Z., & Falkowski, P. G. (1996). Nitrogen- and irradiance-dependent variations of the maximum quantum yield of carbon fixation in eutrophic, mesotrophic and oligotrophic marine systems. *Deep Sea Research Part I: Oceanographic Research Papers*, *43*(8), 1241–1272. https://doi.org/10.1016/0967-0637(96)00058-1

Behrenfeld, M. J., & Boss, E. S. (2014). Resurrecting the Ecological Underpinnings of Ocean Plankton Blooms. *Annual Review of Marine Science*, *6*(1), 167–194. https://doi.org/10.1146/annurev-marine-052913-021325

Behrenfeld, M. J., Boss, E., Siegel, D. A., & Shea, D. M. (2005). Carbon-based ocean productivity and phytoplankton physiology from space. *Global Biogeochemical Cycles*, *19*(1). https://doi.org/10.1029/2004GB002299

Behrenfeld, M. J., & Falkowski, P. G. (1997a). Photosynthetic rates derived from satellite-based chlorophyll concentration. *Limnology and Oceanography*, *42*(1), 1–20. https://doi.org/10.4319/lo.1997.42.1.0001

Behrenfeld, M. J., & Falkowski, P. G. (1997b). A consumer's guide to phytoplankton primary productivity models. *Limnology and Oceanography*, *42*(7), 1479–1491. https://doi.org/10.4319/lo.1997.42.7.1479

Behrenfeld, M. J., Randerson, J. T., McClain, C. R., Feldman, G. C., Los, S. O., Tucker, C. J., Falkowski, P. G., Field, C. B., Frouin, R., Esaias, W. E., Kolber, D. D., & Pollack, N. H. (2001). Biospheric Primary Production During an ENSO Transition. *Science*, *291*(5513), 2594–2597. https://doi.org/10.1126/science.1055071

Behrenfeld, M. J., Westberry, T. K., Boss, E. S., O'Malley, R. T., Siegel, D. A., Wiggert, J. D., Franz, B. A., McClain, C. R., Feldman, G. C., Doney, S. C., Moore, J. K., Dall'Olmo, G., Milligan, A. J., Lima, I., & Mahowald, N. (2009). Satellite-detected fluorescence reveals global physiology of ocean phytoplankton. *Biogeosciences*, *6*(5), 779–794. https://doi.org/10.5194/bg-6-779-2009

Brock, T. D. (1981). Calculating solar radiation for ecological studies. *Ecological Modelling*, *14*(1), 1–19. https://doi.org/10.1016/0304-3800(81)90011-9

Braarud, T. (1969). Pollution effect upon the phytoplankton of the Oslofjord. I *23 s.* [Working paper]. ICES. https://imr.brage.unit.no/imr-xmlui/handle/11250/101524

Cadée, G. C., & Hegeman, J. (2002). Phytoplankton in the Marsdiep at the end of the 20th century; 30 years monitoring biomass, primary production, and Phaeocystis blooms. *Journal of Sea Research*, *48*(2), 97–110. https://doi.org/10.1016/S1385-1101(02)00161-2

Carr, M.-E., Friedrichs, M. A. M., Schmeltz, M., Noguchi Aita, M., Antoine, D., Arrigo, K. R., Asanuma, I., Aumont, O., Barber, R., Behrenfeld, M. J., Bidigare, R., Buitenhuis, E. T., Campbell, J., Ciotti, A., Dierssen, H., Dowell, M., Dunne, J., Esaias, W., Gentili, B.,Gregg, W., Groom, S., Hoepffner, N., Ishizaka, J., Kameda, T., Le Quéré, C., Lohrenz, S., Marra, J., Mélin, F., Moore, K., Morel, A., Redd, T. E., Ryan, J., Scardi, M., Smyth, T., Turpie, K., Tilstone, G., Waters, K., & Yamanaka, Y. (2006). A comparison of global estimates of marine primary production from ocean color. *Deep Sea Research Part II: Topical Studies in Oceanography*, *53*(5–7), 741–770. https://doi.org/10.1016/j.dsr2.2006.01.028

de Wit, H. A., Valinia, S., Weyhenmeyer, G. A., Futter, M. N., Kortelainen, P., Austnes, K., Hessen, D. O., Räike, A., Laudon, H., & Vuorenmaa, J. (2016). Current Browning of Surface Waters Will Be Further Promoted by Wetter Climate. *Environmental Science & Technology Letters*, *3*(12), 430–435. https://doi.org/10.1021/acs.estlett.6b00396

Deininger, A., & Frigstad, H. (2019). Reevaluating the Role of Organic Matter Sources for Coastal Eutrophication, Oligotrophication, and Ecosystem Health. *Frontiers in Marine Science*, *6*. https://www.frontiersin.org/articles/10.3389/fmars.2019.00210

Desmit, X., Nohe, A., Borges, A. V., Prins, T., De Cauwer, K., Lagring, R., Van der Zande, D., & Sabbe, K. (2020). Changes in chlorophyll concentration and phenology in the North Sea in relation to de-eutrophication and sea surface warming. *Limnology and Oceanography*, *65*(4), 828–847. https://doi.org/10.1002/lno.11351

Dineen, C. F. (1953). An Ecological Study of a Minnesota Pond. *The American Midland Naturalist*, *50*(2), 349–376. https://doi.org/10.2307/2422094

Ducklow, H., Cimino, M., Dunton, K. H., Fraser, W. R., Hopcroft, R. R., Ji, R., Miller, A. J., Ohman, M. D., & Sosik, H. M. (2022). Marine Pelagic Ecosystem Responses to Climate Variability and Change. *BioScience*, *72*(9), 827–850. https://doi.org/10.1093/biosci/biac050

Dupont, N., & Aksnes, D. L. (2013). Centennial changes in water clarity of the Baltic Sea and the North Sea. *Estuarine, Coastal and Shelf Science*, *131*, 282–289. https://doi.org/10.1016/j.ecss.2013.08.010

Falkowski, P. G. (2012). Ocean Science: The power of plankton. *Nature*, *483*(7387), Artikkel 7387. https://doi.org/10.1038/483S17a

Falkowski, P. G., Barber, R. T., & Smetacek, V. (1998). Biogeochemical Controls and Feedbacks on Ocean Primary Production. *Science*, *281*(5374), 200–206. https://doi.org/10.1126/science.281.5374.200

Field, C. B., Behrenfeld, M. J., Randerson, J. T., & Falkowski, P. G. (1998). Primary Production of the Biosphere: Integrating Terrestrial and Oceanic Components. *Science*, *281*(5374), 237–240. https://doi.org/10.1126/science.281.5374.237

Finstad, A. G., Andersen, T., Larsen, S., Tominaga, K., Blumentrath, S., de Wit, H. A., Tømmervik, H., & Hessen, D. O. (2016). From greening to browning: Catchment vegetation development and reduced S-deposition promote organic carbon load on decadal time scales in Nordic lakes. *Scientific Reports*, *6*(1), Artikkel 1. https://doi.org/10.1038/srep31944

Fleming-Lehtinen, V., & Laamanen, M. (2012). Long-term changes in Secchi depth and the role of phytoplankton in explaining light attenuation in the Baltic Sea. *Estuarine, Coastal and Shelf Science*, *102–103*, 1–10. https://doi.org/10.1016/j.ecss.2012.02.015

Frigstad, H., Kaste, Ø., Deininger, A., Kvalsund, K., Christensen, G., Bellerby, R. G. J., Sørensen, K., Norli, M., & King, A. L. (2020). Influence of Riverine Input on Norwegian Coastal Systems. *Frontiers in Marine Science*, *7*. https://www.frontiersin.org/articles/10.3389/fmars.2020.00332

Gazeau, F., Borges, A. V., Barrón, C., Duarte, C. M., Iversen, N., Middelburg, J. J., Delille, B., Pizay, M.-D., Frankignoulle, M., & Gattuso, J.-P. (2005). Net ecosystem metabolism in a micro-tidal estuary (Randers Fjord, Denmark): Evaluation of methods. *Marine Ecology Progress Series*, *301*, 23–41. https://doi.org/10.3354/meps301023

Genty, B., Briantais, J.-M., & Baker, N. R. (1989). The relationship between the quantum yield of photosynthetic electron transport and quenching of chlorophyll fluorescence. *Biochimica et Biophysica Acta (BBA) - General Subjects*, *990*(1), 87–92. https://doi.org/10.1016/S0304-4165(89)80016-9

Gilbert, M., Domin, A., Becker, A., & Wilhelm, C. (2000). Estimation of primary productivity by chlorophyll a in vivo fluorescence in freshwater phytoplankton. *Photosynthetica*, *38*(1), 111–126. https://doi.org/10.1023/A:1026708327185

Gaarder, T., & Gran, H. H. (1927). Investigations of the production of plankton in the Oslo Fjord. *Rapp. et Proc. Verb., Cons. Internat. Explor. Mer*, *42*, 1–48.

Henson, S. A., Cole, H. S., Hopkins, J., Martin, A. P., & Yool, A. (2018). Detection of climate change-driven trends in phytoplankton phenology. *Global Change Biology*, *24*(1), e101–e111. https://doi.org/10.1111/gcb.13886

Hill, V. J., & Zimmerman, R. C. (2010). Estimates of primary production by remote sensing in the Arctic Ocean: Assessment of accuracy with passive and active sensors. *Deep Sea Research*

Part I: Oceanographic Research Papers, *57*(10), 1243–1254. https://doi.org/10.1016/j.dsr.2010.06.011

IAEA. (1995). *Reference and intercomparison materials for stable isotopes of light elements*. IAEA, Vienna.

Juday, C. (1940). The Annual Energy Budget of an Inland Lake. *Ecology*, *21*(4), 438–450. https://doi.org/10.2307/1930283

Kahle, D., & Wickham, H. (2013). ggmap: Spatial Visualization with ggplot2. *The R Journal*, *5*(1), 144–161.

Kirk, J. T. O. (1994). *Light and Photosynthesis in Aquatic Ecosystems*. Cambridge University Press.

Kolber, Z., & Falkowski, P. G. (1993). Use of active fluorescence to estimate phytoplankton photosynthesis in situ. *Limnology and Oceanography*, *38*(8), 1646–1665. https://doi.org/10.4319/lo.1993.38.8.1646

Kolber, Z., Wyman, K. V., & Falkowski, P. G. (1990). Natural variability in photosynthetic energy conversion efficiency: A field study in the Gulf of Maine. *Limnology and Oceanography*, *35*(1), 72–79. https://doi.org/10.4319/lo.1990.35.1.0072

Kolber, Z., Zehr, J., & Falkowski, P. G. (1988). Effects of Growth Irradiance and Nitrogen Limitation on Photosynthetic Energy Conversion in Photosystem II. *Plant Physiology*, *88*(3), 923–929.

Kromkamp, J. C., Dijkman, N. A., Peene, J., Simis, S. G. H., & Gons, H. J. (2008). Estimating phytoplankton primary production in Lake IJsselmeer (The Netherlands) using variable fluorescence (PAM-FRRF) and C-uptake techniques. *European Journal of Phycology*, *43*(4), 327–344. https://doi.org/10.1080/09670260802080895

Kromkamp, J. C., & Forster, R. M. (2003). The use of variable fluorescence measurements in aquatic ecosystems: Differences between multiple and single turnover measuring protocols and suggested terminology. *European Journal of Phycology*, *38*(2), 103–112. https://doi.org/10.1080/0967026031000094094

Lawrenz, E., Silsbe, G., Capuzzo, E., Ylöstalo, P., Forster, R. M., Simis, S. G. H., Prášil, O., Kromkamp, J. C., Hickman, A. E., Moore, C. M., Forget, M.-H., Geider, R. J., & Suggett, D. J. (2013). Predicting the Electron Requirement for Carbon Fixation in Seas and Oceans. *PLOS ONE*, *8*(3), e58137. https://doi.org/10.1371/journal.pone.0058137

Laws, E. A., Landry, M. R., Barber, R. T., Campbell, L., Dickson, M.-L., & Marra, J. (2000). Carbon cycling in primary production bottle incubations: Inferences from grazing experiments and photosynthetic studies using 14C and 18O in the Arabian Sea. *Deep Sea Research Part II: Topical Studies in Oceanography*, *47*(7–8), 1339–1352. https://doi.org/10.1016/S0967-0645(99)00146-0

Lee, Z., Hu, C., Shang, S., Du, K., Lewis, M., Arnone, R., & Brewin, R. (2013). Penetration of UV-visible solar radiation in the global oceans: Insights from ocean color remote sensing. *Journal of Geophysical Research: Oceans*, *118*(9), 4241–4255. https://doi.org/10.1002/jgrc.20308

Lee, Z., Weidemann, A., Kindle, J., Arnone, R., Carder, K. L., & Davis, C. (2007). Euphotic zone depth: Its derivation and implication to ocean-color remote sensing. *Journal of Geophysical Research: Oceans*, *112*(C3). https://doi.org/10.1029/2006JC003802

Liu, X., Byrne, R. H., Adornato, L., Yates, K. K., Kaltenbacher, E., Ding, X., & Yang, B. (2013). In Situ Spectrophotometric Measurement of Dissolved Inorganic Carbon in Seawater.

Environmental Science & Technology, *47*(19), 11106–11114. https://doi.org/10.1021/es4014807

López-Sandoval, D. C., Delgado-Huertas, A., & Agustí, S. (2018). The 13C method as a robust alternative to 14C-based measurements of primary productivity in the Mediterranean Sea. *Journal of Plankton Research*, *40*(5), 544–554. https://doi.org/10.1093/plankt/fby031

López-Sandoval, D. C., Delgado-Huertas, A., Carrillo-de-Albornoz, P., Duarte, C. M., & Agustí, S. (2019). Use of cavity ring-down spectrometry to quantify 13C-primary productivity in oligotrophic waters. *Limnology and Oceanography: Methods*, *17*(2), 137–144. https://doi.org/10.1002/lom3.10305

Lundsør, E., Stige, L. C., Sørensen, K., & Edvardsen, B. (2020). Long-term coastal monitoring data show nutrient-driven reduction in chlorophyll. *Journal of Sea Research*, *164*, 101925. https://doi.org/10.1016/j.seares.2020.101925

Mitchell, B. G., & Kiefer, D. A. (1988). Chlorophyll a specific absorption and fluorescence excitation spectra for light-limited phytoplankton. *Deep-Sea Research. Part A. Oceanographic Research Papers*, *35*(5), 639–663. https://doi.org/10.1016/0198-0149(88)90024-6

Morel, A., & Prieur, L. (1977). Analysis of variations in ocean color1. *Limnology and Oceanography*, *22*(4), 709–722. https://doi.org/10.4319/lo.1977.22.4.0709

Müller, P., Li, X.-P., & Niyogi, K. K. (2001). Non-Photochemical Quenching. A Response to Excess Light Energy1. *Plant Physiology*, *125*(4), 1558–1566. https://doi.org/10.1104/pp.125.4.1558

Opdal, A. F., Andersen, T., Hessen, D. O., Lindemann, C., & Aksnes, D. L. (2023). Tracking freshwater browning and coastal water darkening from boreal forests to the Arctic Ocean.

Limnology and Oceanography Letters, *n/a*(n/a). Advanced online publication. https://doi.org/10.1002/lol2.10320

Opdal, A. F., Lindemann, C., & Aksnes, D. L. (2019). Centennial decline in North Sea water clarity causes strong delay in phytoplankton bloom timing. *Global Change Biology*, *25*(11), 3946–3953. https://doi.org/10.1111/gcb.14810

Pernthaler, J., & Amann, R. (2005). Fate of Heterotrophic Microbes in Pelagic Habitats: Focus on Populations. *Microbiology and Molecular Biology Reviews*, *69*(3), 440–461. https://doi.org/10.1128/MMBR.69.3.440-461.2005

Peterson, B. J. (1980). Aquatic Primary Productivity and the 14C-CO2 Method: A History of the Productivity Problem. *Annual Review of Ecology and Systematics*, *11*(1), 359–385. https://doi.org/10.1146/annurev.es.11.110180.002043

Paasche, E., & Østergren, I. (1980). The annual cycle of plankton diatom growth and silica production in the inner Oslofjord1. *Limnology and Oceanography*, *25*(3), 481–494. https://doi.org/10.4319/lo.1980.25.3.0481

Rau, G., Riebesell, U., & Wolf-Gladrow, D. (1996). A model of photosynthetic 13C fractionation by marine phytoplankton based on diffusive molecular CO2 uptake. *Marine Ecology Progress Series*, *133*, 275–285. https://doi.org/10.3354/meps133275

Regaudie-de-Gioux, A., Lasternas, S., Agustí, S., & Duarte, C. M. (2014). Comparing marine primary production estimates through different methods and development of conversion equations. *Frontiers in Marine Science*, *1*. https://www.frontiersin.org/articles/10.3389/fmars.2014.00019

Sakamoto, M., Tilzer, M. M., Gächter, R., Rai, H., Collos, Y., Tschumi, P., Berner, P., Zbaren, J., Dokulil, M., Bossard, P., Uehlinger, U., & Nusch, E. A. (1984). Joint field experiments for comparisons of measuring methods of photosynthetic production *. *Journal of Plankton Research*, *6*(2), 365–383. https://doi.org/10.1093/plankt/6.2.365

Schreiber, U. (2004). Pulse-Amplitude-Modulation (PAM) Fluorometry and Saturation Pulse Method: An Overview. I G. C. Papageorgiou & Govindjee (Red.), *Chlorophyll a Fluorescence: A Signature of Photosynthesis* (s. 279–319). Springer Netherlands. https://doi.org/10.1007/978-1-4020-3218-9_11

Siegel, D. A., Behrenfeld, M. J., Maritorena, S., McClain, C. R., Antoine, D., Bailey, S. W., Bontempi, P. S., Boss, E. S., Dierssen, H. M., Doney, S. C., Eplee, R. E., Evans, R. H., Feldman, G. C., Fields, E., Franz, B. A., Kuring, N. A., Mengelt, C., Nelson, N. B., Patt, F. S., Robinson, W. D., Sarmiento, J. L., Swan, C. M., Werdell, P. J., Westberry, T. K., Wilding, J. G., & Yoder, J. A. (2013). Regional to global assessments of phytoplankton dynamics from the SeaWiFS mission. *Remote Sensing of Environment*, *135*, 77–91. https://doi.org/10.1016/j.rse.2013.03.025

Slawyk, G., Collos, Y., & Auclair, J.-C. (1977). The use of the 13C and 15N isotopes for the simultaneous measurement of carbon and nitrogen turnover rates in marine phytoplankton1. *Limnology and Oceanography*, *22*(5), 925–932. https://doi.org/10.4319/lo.1977.22.5.0925

Slawyk, G., Minas, M., Collos, Y., Legendre, L., & Roy, S. (1984). Comparison of radioactive and stable isotope tracer techniques for measuring photosynthesis: 13C and 14 C uptake by

marine phytoplankton *. *Journal of Plankton Research*, *6*(2), 249–257. https://doi.org/10.1093/plankt/6.2.249

Smith, R. C., Bidigare, R. R., Prézelin, B. B., Baker, K. S., & Brooks, J. M. (1987). Optical characterization of primary productivity across a coastal front. *Marine Biology*, *96*(4), 575–591. https://doi.org/10.1007/BF00397976

Smith, R. C., Prezelin, B. B., Bidigare, R. R., & K. S., B. (1989). Bio-optical modeling of photosynthetic production in coastal waters. *Limnology and Oceanography*, *34*(8), 1524–1544. https://doi.org/10.4319/lo.1989.34.8.1524

Staehr, P. A., Testa, J. M., Kemp, W. M., Cole, J. J., Sand-Jensen, K., & Smith, S. V. (2012). The metabolism of aquatic ecosystems: History, applications, and future challenges. *Aquatic Sciences*, *74*(1), 15–29. https://doi.org/10.1007/s00027-011-0199-2

Steemann Nielsen, E. (1952). The Use of Radio-active Carbon (C14) for Measuring Organic Production in the Sea. *ICES Journal of Marine Science*, *18*(2), 117–140. https://doi.org/10.1093/icesjms/18.2.117

Steemann Nielsen, E. (1962). Inactivation of the Photochemical Mechanism in Photosynthesis as a Means to Protect the Cells Against Too High Light intensities. *Physiologia Plantarum*, *15*(1), 161–171. https://doi.org/10.1111/j.1399-3054.1962.tb07996.x

Staalstrøm, A., Aas, E., & Liljebladh, B. (2012). Propagation and dissipation of internal tides in the Oslofjord. *Ocean Science*, *8*(4), 525–543. https://doi.org/10.5194/os-8-525-2012

Tassan, S., & Ferrari, G. M. (1995). An alternative approach to absorption measurements of aquatic particles retained on filters. *Limnology and Oceanography*, *40*(8), 1358–1368. https://doi.org/10.4319/lo.1995.40.8.1358

Thimijan, R., & Heins, R. (1983). Photometric, Radiometric, and Quantum Light Units of Measure: A Review of Procedures for Interconversion. *Hortic Sci*, *18*, 818–822. https://doi.org/10.21273/HORTSCI.18.6.818

Thrane, J.-E., Hessen, D. O., & Andersen, T. (2014). The Absorption of Light in Lakes: Negative Impact of Dissolved Organic Carbon on Primary Productivity. *Ecosystems*, *17*(6), 1040–1052. https://doi.org/10.1007/s10021-014-9776-2

Throndsen, J. (1978). Productivity and abundance of ultra-and nanoplankton in Oslofjorden. *Sarsia*, *63*, 273–284.

Torres, R., Romero, J. M., & Lagorio, M. G. (2021). Effects of sub-optimal illumination in plants. Comprehensive chlorophyll fluorescence analysis. *Journal of Photochemistry and Photobiology B: Biology*, *218*, 112182. https://doi.org/10.1016/j.jphotobiol.2021.112182

Urtizberea, A., Dupont, N., Rosland, R., & Aksnes, D. L. (2013). Sensitivity of euphotic zone properties to CDOM variations in marine ecosystem models. *Ecological Modelling*, *256*, 16–22. https://doi.org/10.1016/j.ecolmodel.2013.02.010

Westberry, T., Behrenfeld, M. J., Siegel, D. A., & Boss, E. (2008). Carbon-based primary productivity modeling with vertically resolved photoacclimation. *Global Biogeochemical Cycles*, *22*(2). https://doi.org/10.1029/2007GB003078

Wickham, H. (2016). Data Analysis. I H. Wickham (Red.), *Ggplot2: Elegant Graphics for Data Analysis* (s. 189–201). Springer International Publishing. https://doi.org/10.1007/978-3-319-24277-4_9

Wilhelm, C., Becker, A., Toepel, J., Vieler, A., & Rautenberger, R. (2004). Photophysiology and primary production of phytoplankton in freshwater. *Physiologia Plantarum*, *120*(3), 347–357. https://doi.org/10.1111/j.0031-9317.2004.00267.x

Williams, P. J. le B., Raine, R. C. T., & Bryan, J. R. (1979). Agreement between the C-14 and oxygen methods of measuring phytoplankton production: Reassessment of the photosynthetic quotient. *Oceanologica Acta*, *2*(4), 411–416.

Yang, H., Andersen, T., Dörsch, P., Tominaga, K., Thrane, J.-E., & Hessen, D. O. (2015). Greenhouse gas metabolism in Nordic boreal lakes. *Biogeochemistry*, *126*(1), 211–225. https://doi.org/10.1007/s10533-015-0154-8

Åberg, J., & Wallin, B. (2014). Evaluating a fast headspace method for measuring DIC and subsequent calculation of pCO2 in freshwater systems. *Inland Waters*, *4*(2), 157–166. https://doi.org/10.5268/IW-4.2.694

Appendix A – supplementary table and figures

Coordinates

Table 1: Coordinates of the Oslofjord transect and the UiO fieldstation in Drøbak

Station	Latitude	Longitude
OF2, Missingene	59.18	10.69
Ø1, Leira	59.13	10.83
I1, Ramsø	59.11	11.00
L5, Kjøkøy	59.14	10.96
L1, Glomma	59.21	10.96
Drøbak	59.66	10.63

Water absorbance coefficent, ε_w, from Morel & Prieur (1977)

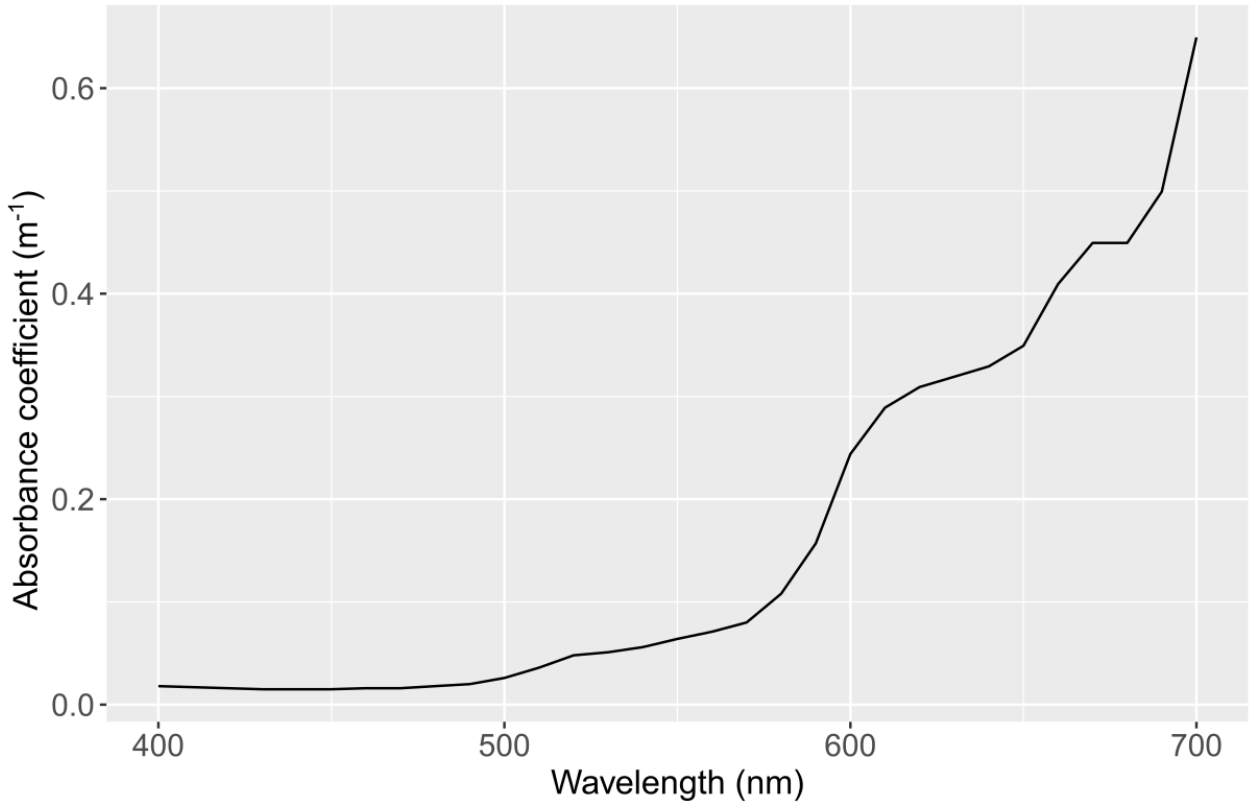

Figure 14: The absorbance coefficient (m^{-1}) in chemically and optically pure water, in the PAR region, from Morel & Prieur (1977)

Example of CTD profile, from OF2 12th May 2022

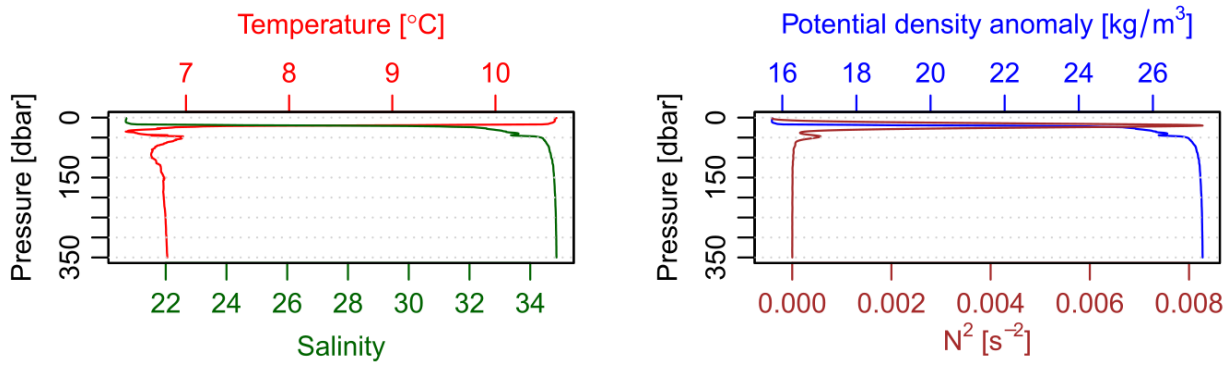

Figure 15: Example of a full CTD profile, showing salinity (PSU), temperature (°C), the potential density anomaly (kg/m^3) and the Brunt-Väisälä frequency (N^2[s^{-2}]) at OF2 12th May 2022.

Time course of surface solar irradiance, in the PAR region

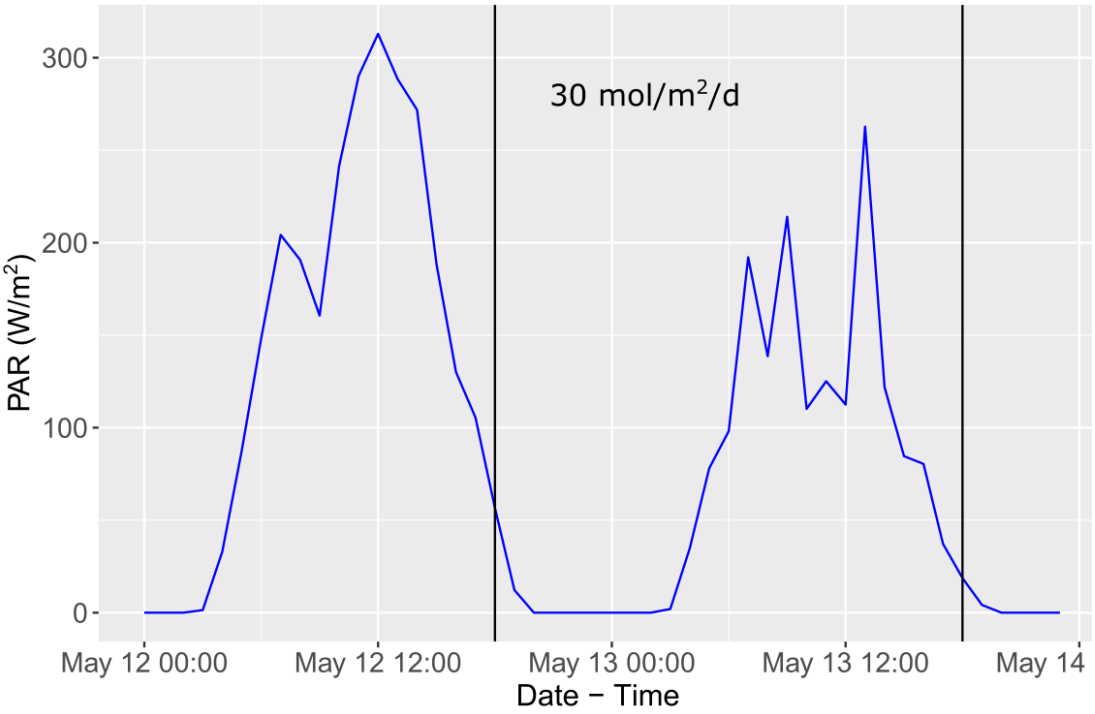

Figure 16: The surface solar irradiance time course in the PAR region (W/m^2) for incubation 1, 12th – 13th May 2022, from the STRÅNG database for the coordinates at the Drøbak field station. The vertical lines represent t_1 and t_2, start and end of incubation, used in calculation of the photon flux = 30 mol/m^2/d

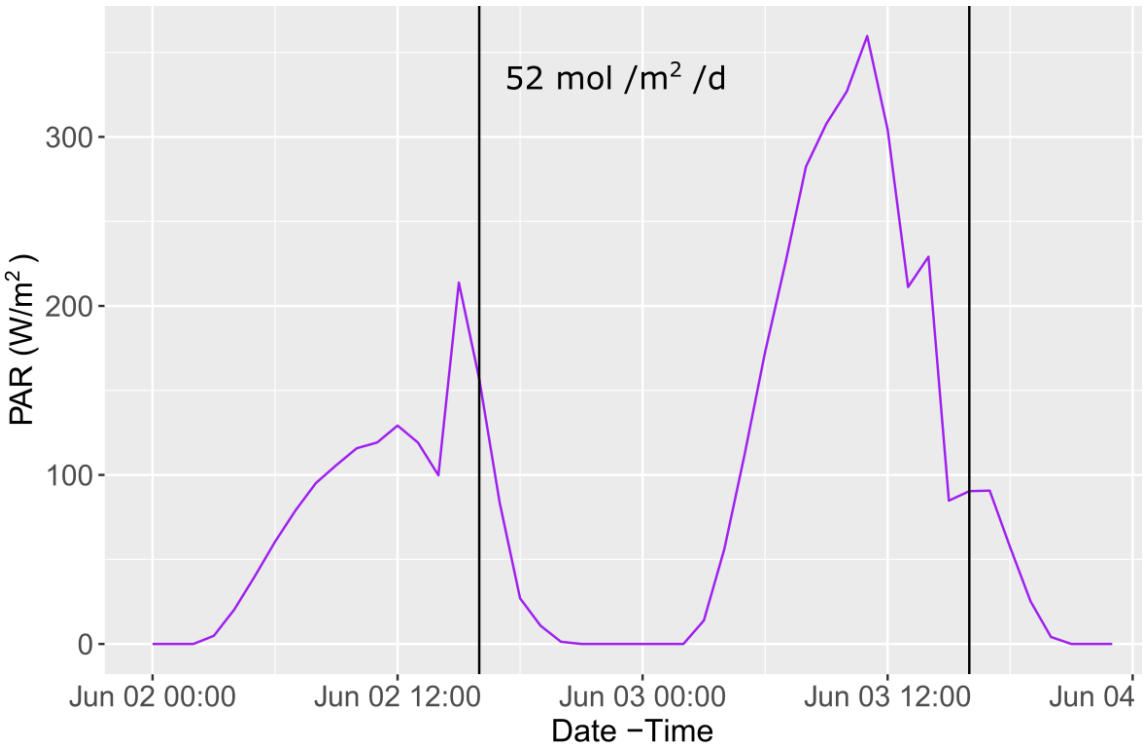

Figure 17: The surface solar irradiance time course in the PAR region (W/m^2) for incubation 2, 2nd – 3rd June 2022, from the STRÅNG database for the coordinates at the Drøbak field station. The vertical lines represent t_1 and t_2, start and end of incubation, used in calculation the photon flux = 52 $mol/m^2/d$

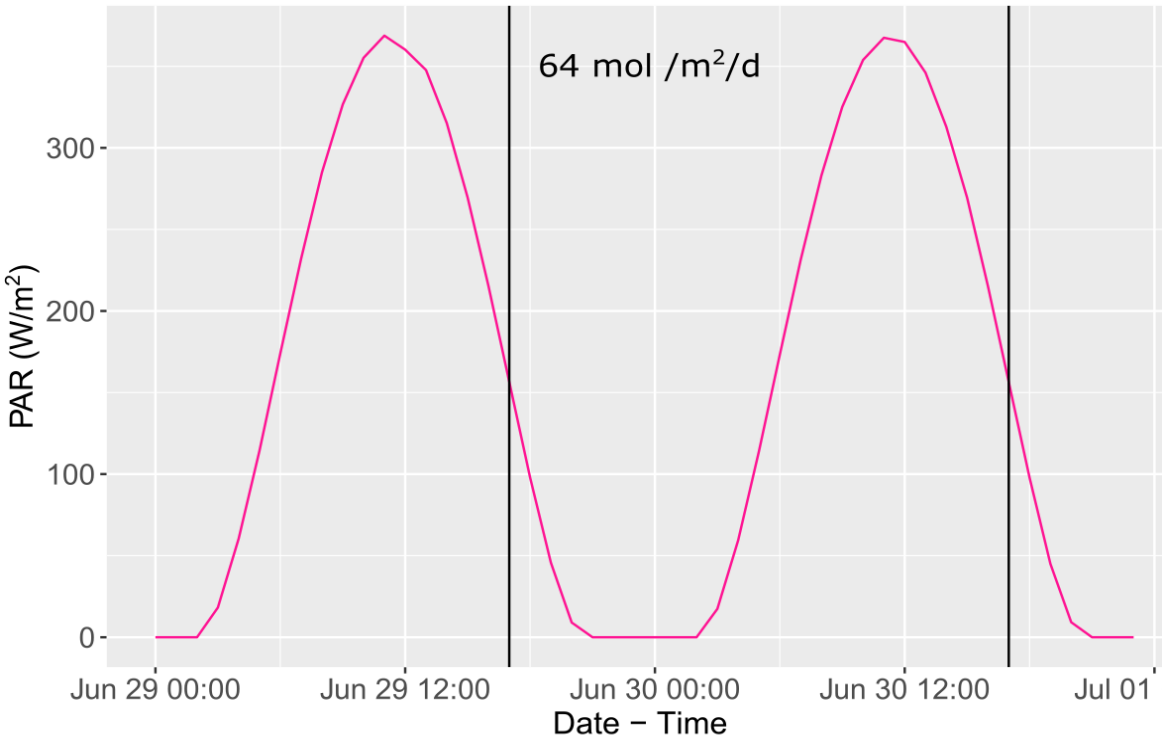

Figure 18: The surface solar irradiance time course in the PAR region (W/m^2) for incubation 3, 29th – 30th June 2022, from the STRÅNG database for the coordinates at the Drøbak field station. The vertical lines represent t_1 and t_2, start and end of incubation, used in calculation the photon flux = 64 $mol/m^2/d$

Cumulative absorbance spectra for all stations and dates

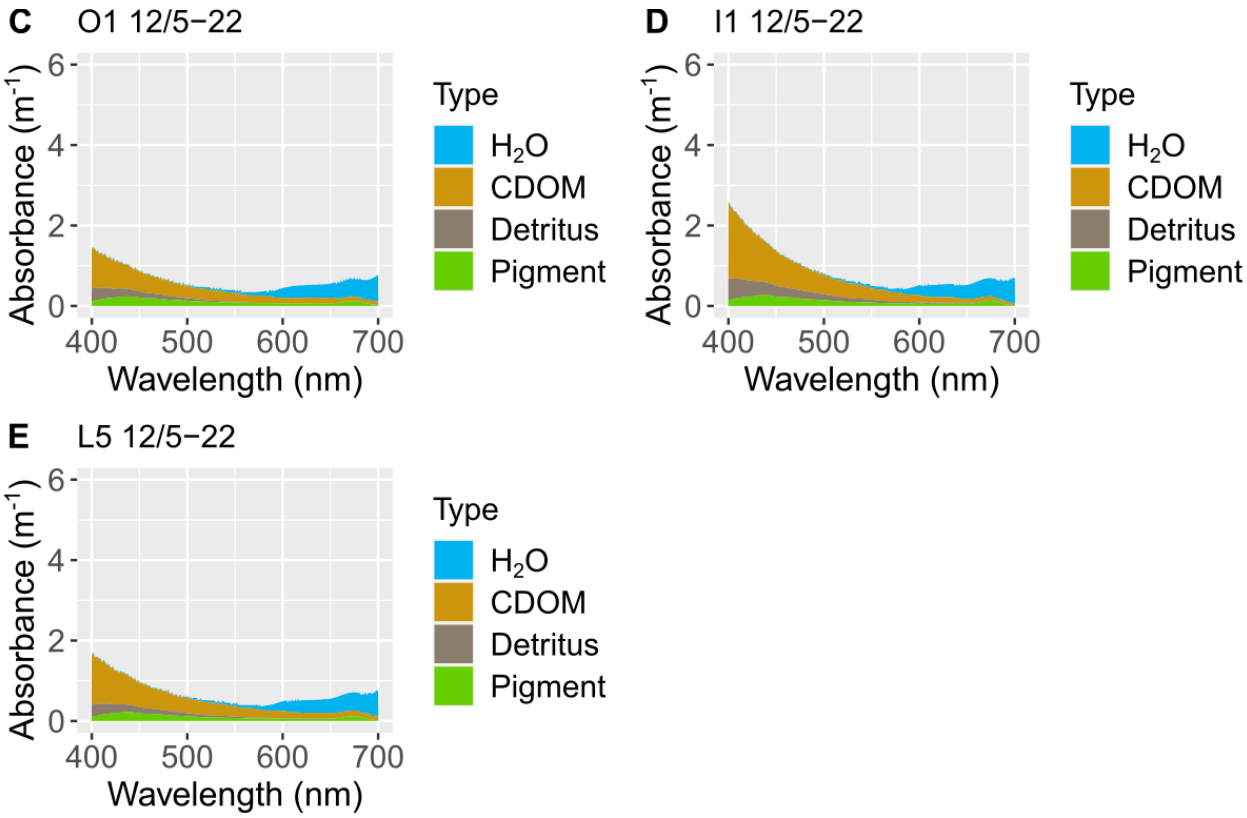

Figure 19: Cumulative absorbance spectra for water, colored dissolved organic matter, detritus and photosynthetic pigment. **C** = Station O1 at the 12th of May in 2022, **D** = Station I1 at the 12th of May 2022, **E** = Station L5 at the 12th of May in 2022

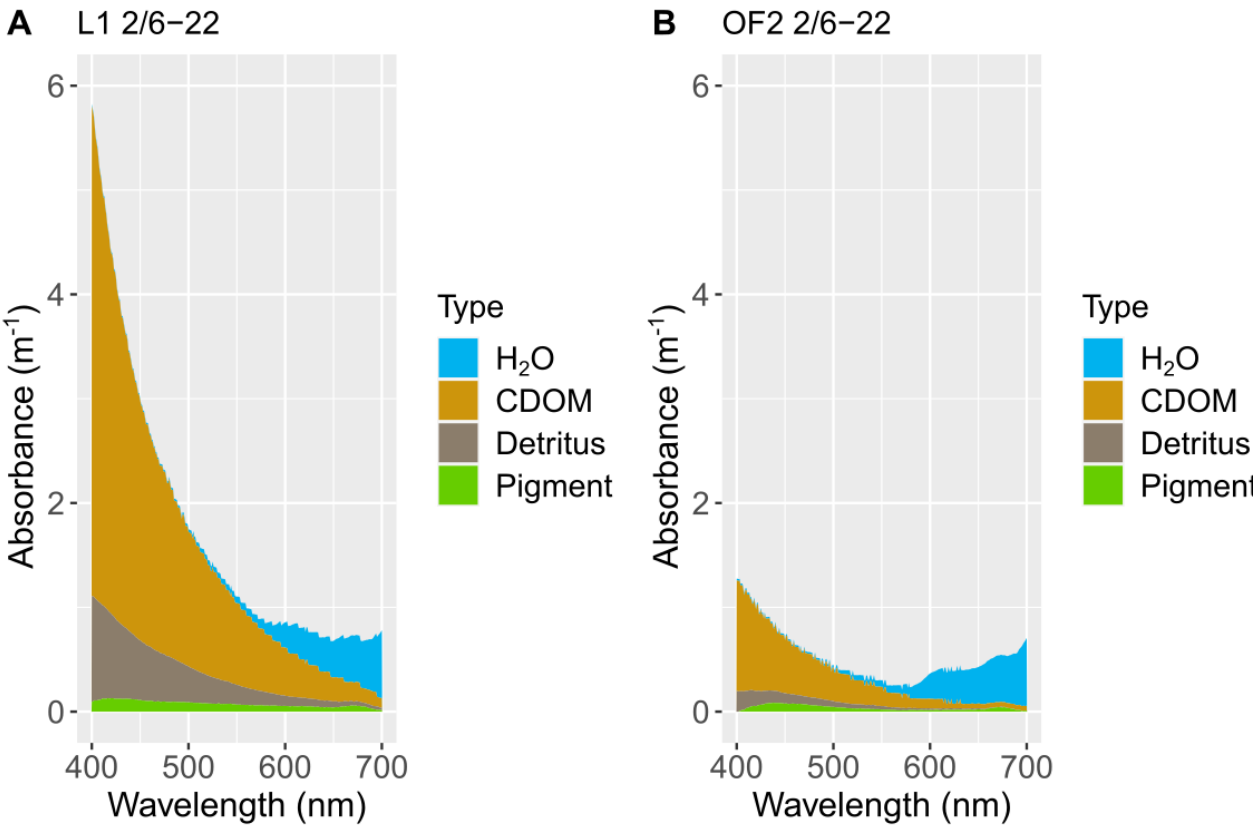

Figure 20: Cumulative absorbance spectra for water, colored dissolved organic matter, detritus and photosynthetic pigment. **A** = Station L1 at the 2nd of June in 2022, **B** = Station OF2 at the 2nd of June 2022.

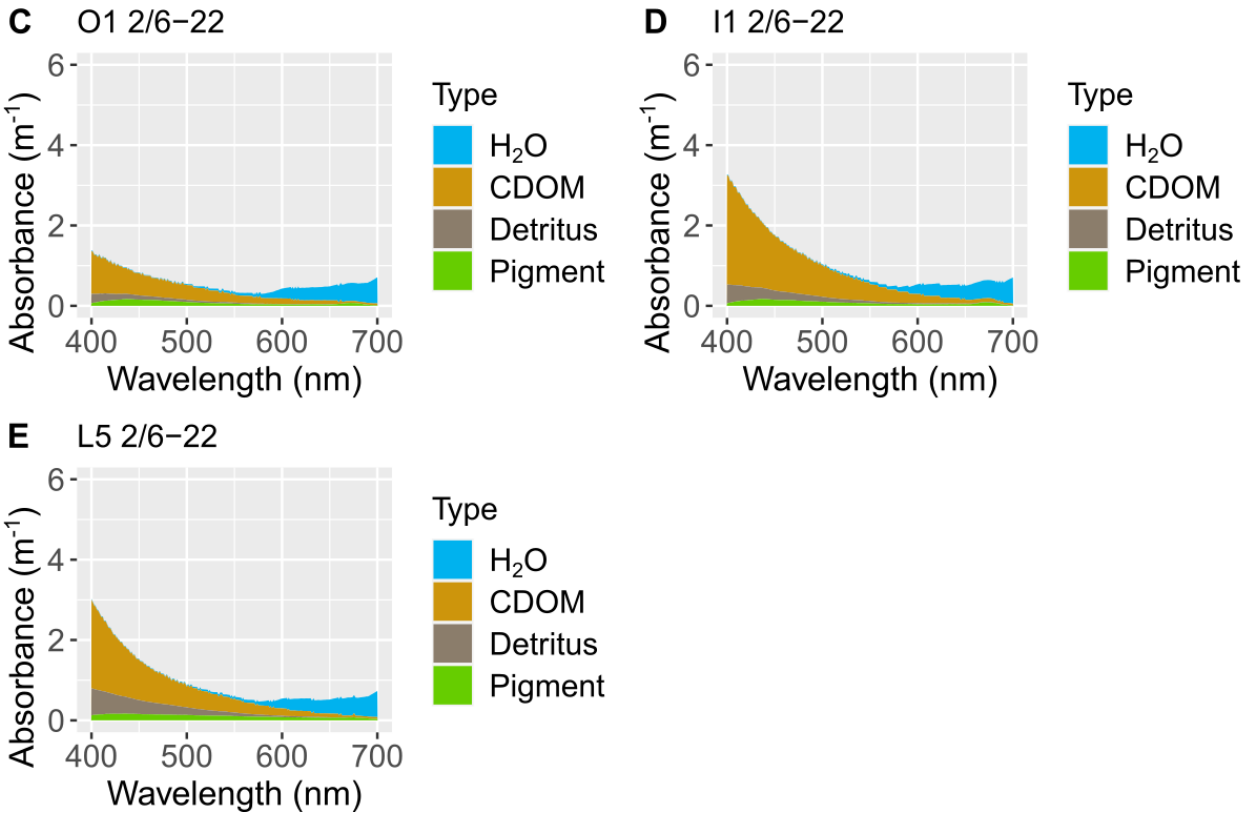

Figure 21: Cumulative absorbance spectra for water, colored dissolved organic matter, detritus and photosynthetic pigment. **C** = Station O1 at the 2nd of June in 2022, **D** = Station I1 at the 2nd of June 2022, **E** = Station L5 at the 2nd of June in 2022

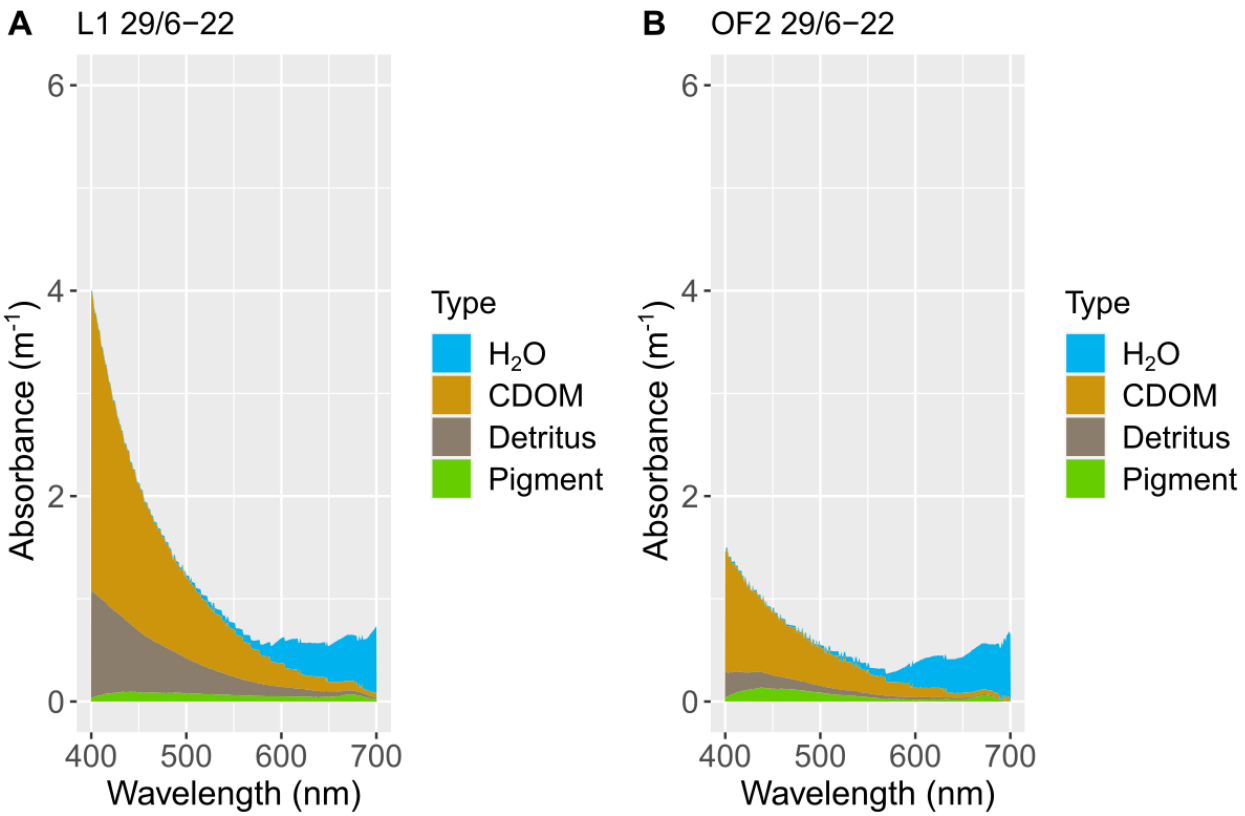

Figure 22: Cumulative absorbance spectra for water, colored dissolved organic matter, detritus and photosynthetic pigment. **A** = Station OF2 at the 29th of June in 2022, **B** = Station L1 at the 29th of June 2022.

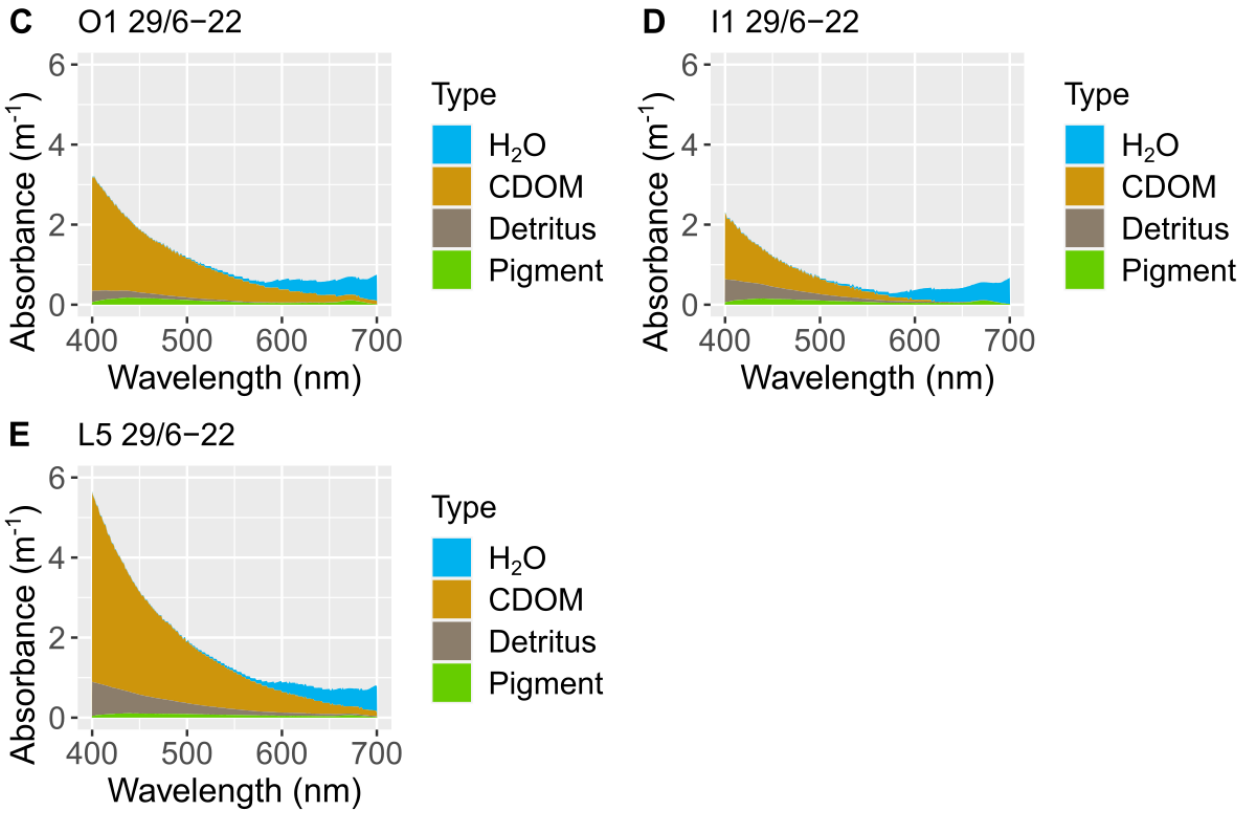

Figure 23: Cumulative absorbance spectra for water, colored dissolved organic matter, detritus and photosynthetic pigment. **C** = Station O1 at the 29th of June in 2022, **D** = Station I1 at the 29th of June 2022, **E** = Station L5 at the 29th of June in 2022

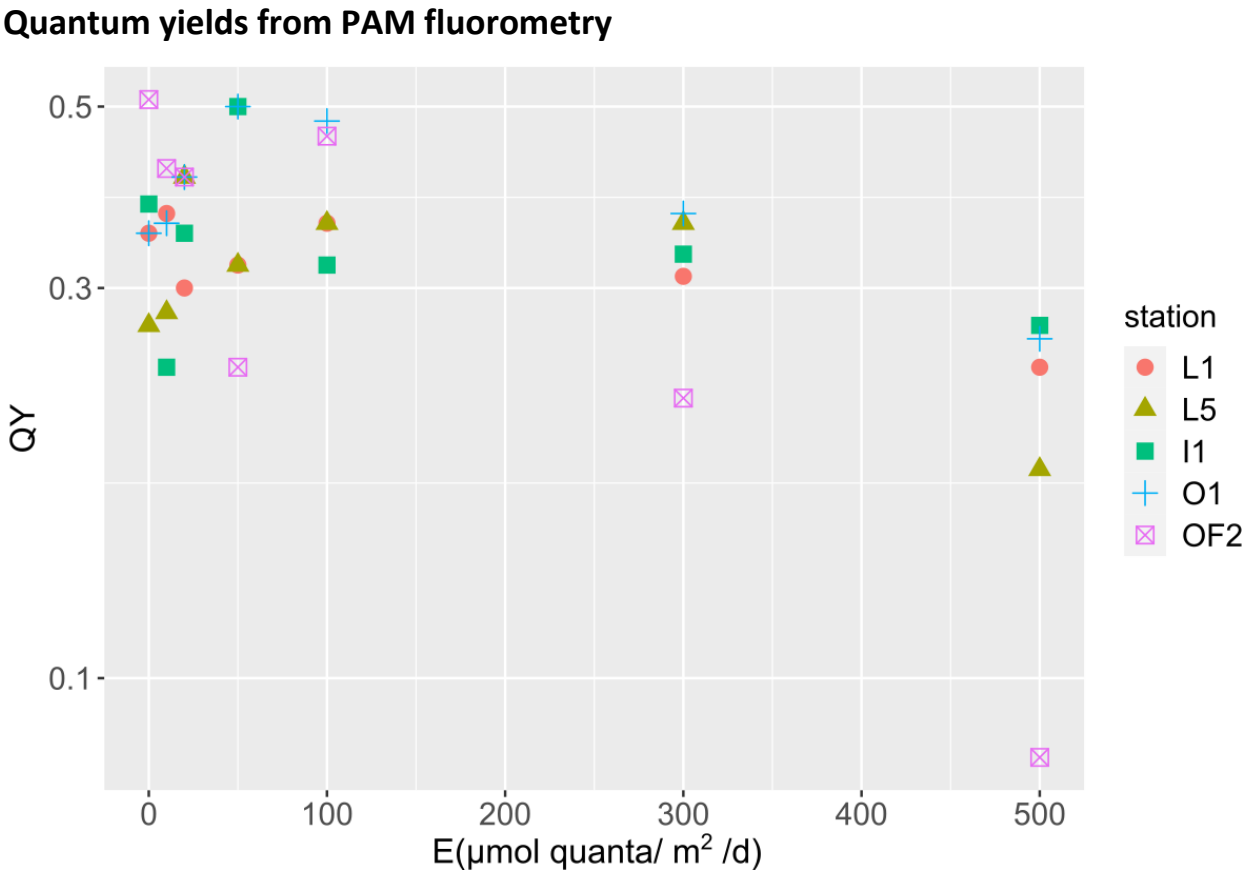

Figure 24: Measured QY, on log-scale, at different incubation intensities (µmol quanta/m^2/s). PAM fluorometry from the 12th of May 2022, across stations.

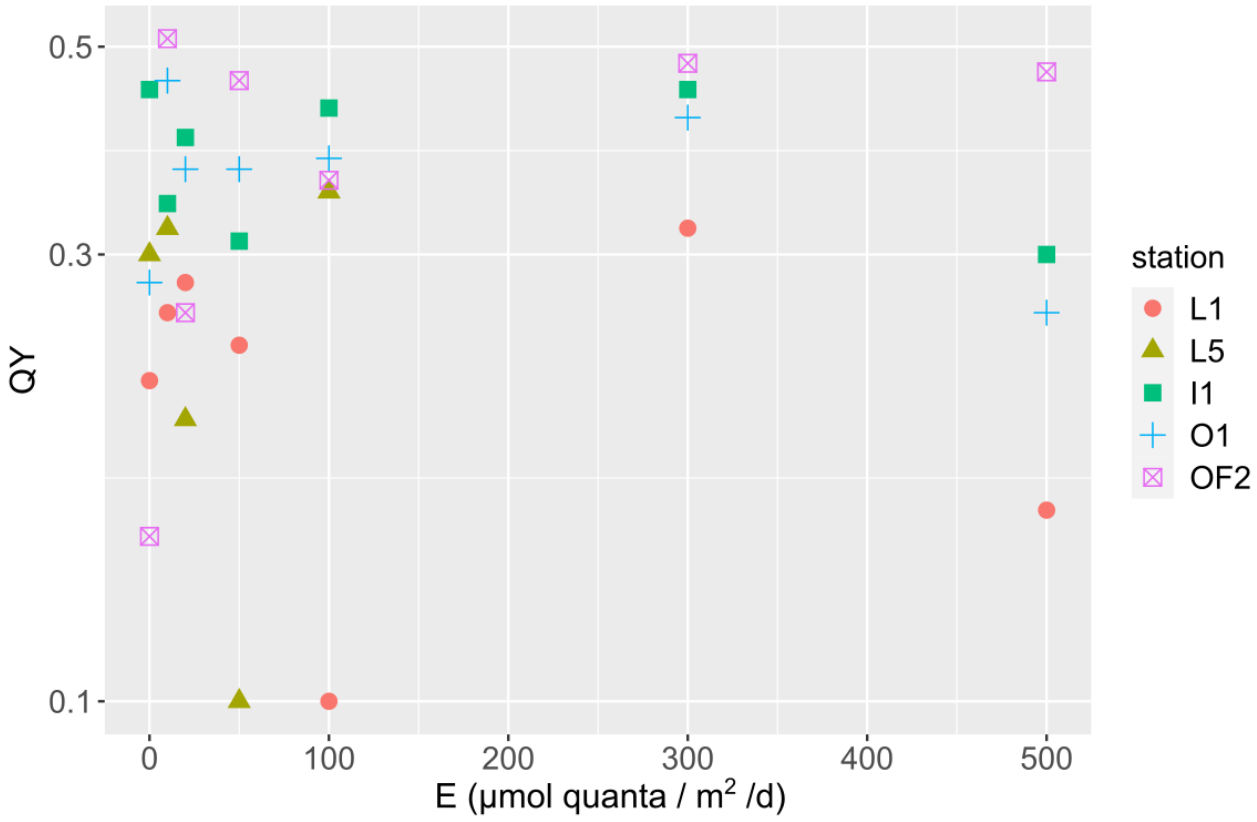

Figure 25: Measured QY, on log-scale, at different incubation intensities (µmol quanta/m^2/s). PAM fluorometry from the 2nd of June 2022, across stations.

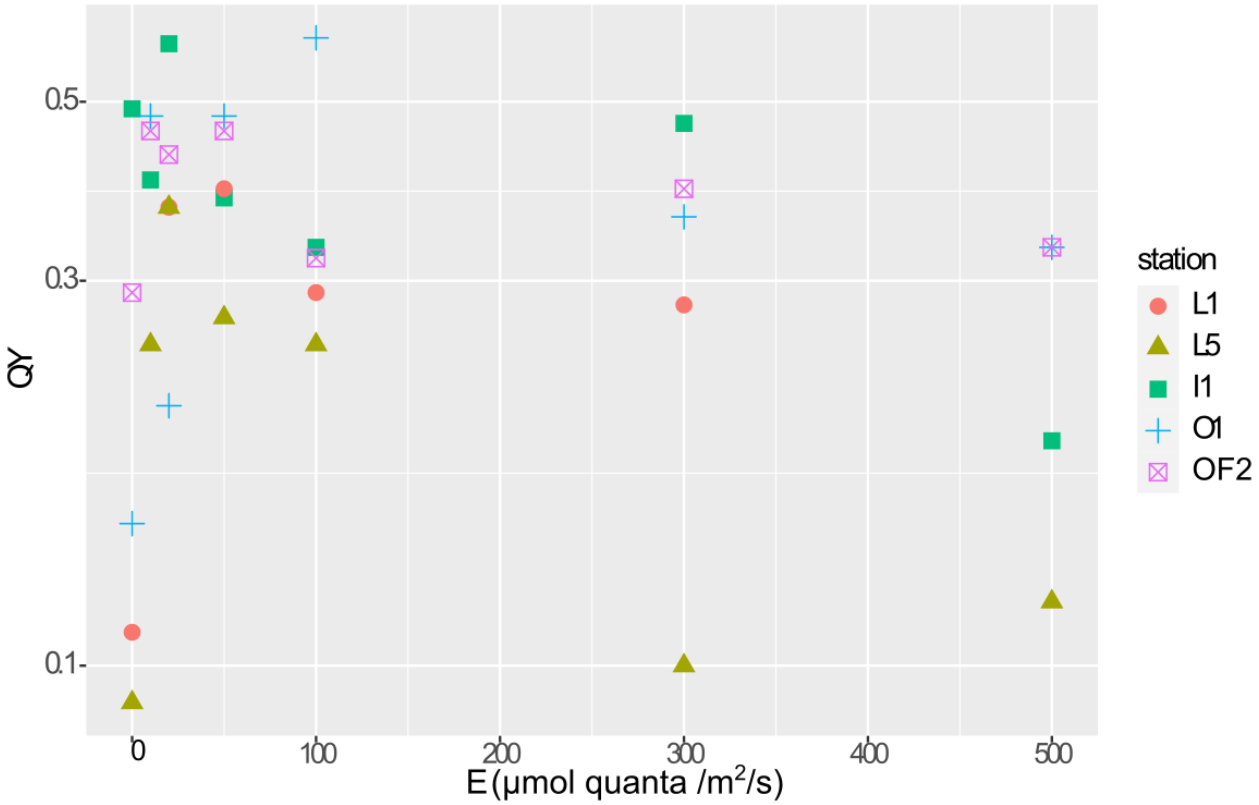

Figure 26: Measured QY, on log-scale, at different incubation intensities (µmol quanta/m^2/s). PAM fluorometry from the 29th of June, across stations.

Appendix B – selected scripts

```
library(ggplot2)
library(cowplot)
library(tidyverse)
library(readxl)
library(dplyr)
library(forcats)

my_colour_palette <- c("midnightblue", "blue", "deepskyblue2")
My_theme = theme(
 legend.text = element_text(size = 13),
 legend.title = element_text(size = 13),
 axis.text.x = element_text(size = 13, angle=90),
 axis.text.y = element_text(size = 13),
 axis.title.x = element_text(size = 14),
 axis.title.y = element_text(size = 14))
```

CTD data

```
library(oce)
library(ocedata)
```

Example for cruise 1 (repeated for all cruises)

```
#L1
C1_L1 <- read.ctd("L1_12052022.cnv")
C1_L1_smooth <- ctdDecimate(C1_L1)
plot(C1_L1_smooth)
```

```
plotProfile(C1_L1_smooth, "salinity")
plot(C1_L1_smooth, which = 2, type = "l") #smoothed data
swN2(C1_L1_smooth)
which.max(swN2(C1_L1_smooth))
C1_L1_smooth_df <- as.data.frame(C1_L1_smooth@data)
C1_L1_smooth_df$depth[which.max(swN2(C1_L1_smooth))] #6.952108 pycnocline
plot(C1_L1, which=3) # T-S diagram

#L5
C1_L5 <- read.ctd("L5_12052022.cnv")
C1_L5_smooth <- ctdDecimate(C1_L5)
plot(C1_L5_smooth)
plotProfile(C1_L5_smooth, "salinity")
plot(C1_L5_smooth, which = 2, type = "l") #smoothed data
swN2(C1_L5_smooth)
which.max(swN2(C1_L5_smooth))
C1_L5_smooth_df <- as.data.frame(C1_L5_smooth@data)
C1_L5_smooth_df$depth[which.max(swN2(C1_L5_smooth))] #20.81527


#I1
C1_I1 <- read.ctd("I1_12052022.cnv")
C1_I1_smooth <- ctdDecimate(C1_I1)
plot(C1_I1_smooth)
plotProfile(C1_I1_smooth, "salinity")
plot(C1_I1_smooth, which = 2, type = "l") #smoothed data
swN2(C1_I1_smooth)
which.max(swN2(C1_I1_smooth))
C1_I1_smooth_df <- as.data.frame(C1_I1_smooth@data)
```

```
C1_I1_smooth_df$depth[which.max(swN2(C1_I1_smooth))] #21.82703

#Ø1
C1_O1 <- read.ctd("O1_12052022.cnv") #Ø1
C1_O1_smooth <- ctdDecimate(C1_O1)
plot(C1_O1_smooth) #får 3 plot
plotProfile(C1_O1_smooth, "salinity")
plot(C1_O1_smooth, which = 2, type = "l") #smoothed data
swN2(C1_O1_smooth)
which.max(swN2(C1_O1_smooth))
C1_O1_smooth_df <- as.data.frame(C1_O1_smooth@data)
C1_O1_smooth_df$depth[which.max(swN2(C1_O1_smooth))] #19.77046

#OF2
C1_OF2 <- read.ctd("OF2_12052022.cnv")
C1_OF2_smooth <- ctdDecimate(C1_OF2)
plot(C1_OF2_smooth)

plotProfile(C1_OF2_smooth, "salinity")
plot(C1_OF2_smooth, which = 2, type = "l") #smoothed data
swN2(C1_OF2_smooth)

which.max(swN2(C1_OF2_smooth))

C1_OF2_smooth_df <- as.data.frame(C1_OF2_smooth@data)
C1_OF2_smooth_df$depth[which.max(swN2(C1_OF2_smooth))] #19.74144
```

```
C1_L1_df=C1_L1@data%>%
 as_data_frame()
C1_L1_df$Date = "12.05.2022"
C1_L1_df$Site = "L1"
C1_L1_df$Pycnocline = C1_L1_smooth_df$depth[which.max(swN2(C1_L1_smooth))]

C1_L5_df=C1_L5@data%>%
 as_data_frame()
C1_L5_df$Date = "12.05.2022"
C1_L5_df$Site = "L5"
C1_L5_df$Pycnocline = C1_L5_smooth_df$depth[which.max(swN2(C1_L5_smooth))]

C1_I1_df=C1_I1@data%>%
 as_data_frame()
C1_I1_df$Date = "12.05.2022"
C1_I1_df$Site = "I1"
C1_I1_df$Pycnocline = C1_I1_smooth_df$depth[which.max(swN2(C1_I1_smooth))]

C1_O1_df=C1_O1@data%>%
 as_data_frame()
C1_O1_df$Date = "12.05.2022"
C1_O1_df$Site = "O1"
C1_O1_df$Pycnocline = C1_O1_smooth_df$depth[which.max(swN2(C1_O1_smooth))]

C1_OF2_df = C1_OF2@data%>%
 as_data_frame()
C1_OF2_df$Date = "12.05.2022"
C1_OF2_df$Site = "OF2"
C1_OF2_df$Pycnocline = C1_OF2_smooth_df$depth[which.max(swN2(C1_OF2_smooth))]
```

```
C1_L1_deep = subset(C1_L1_df, depth == "16.982")
C1_L1_deep$Info = "Deep, 12.05.2022"
C1_L1_deep$Depth ="Deep"
C1_L1_shallow = subset(C1_L1_df, depth == "3.536")
C1_L1_shallow$Info = "Shallow, 12.05.2022"
C1_L1_shallow$Depth ="Shallow"

C1_L5_deep = subset(C1_L5_df, depth == "41.338")
C1_L5_deep$Info = "Deep, 12.05.2022"
C1_L5_deep$Depth ="Deep"
C1_L5_shallow = subset(C1_L5_df, depth == "3.471")
C1_L5_shallow$Info = "Shallow, 12.05.2022"
C1_L5_shallow$Depth ="Shallow"

C1_I1_deep = subset(C1_I1_df, depth == "39.935")
C1_I1_deep$Info = "Deep, 12.05.2022"
C1_I1_deep$Depth ="Deep"
C1_I1_shallow = subset(C1_I1_df, depth == "3.506")
C1_I1_shallow$Info = "Shallow, 12.05.2022"
C1_I1_shallow$Depth ="Shallow"

C1_O1_deep = subset(C1_O1_df, depth == "41.311")
C1_O1_deep$Info = "Deep, 12.05.2022"
C1_O1_deep$Depth ="Deep"
C1_O1_shallow = subset(C1_O1_df, depth == "3.505")
C1_O1_shallow$Info = "Shallow, 12.05.2022"
C1_O1_shallow$Depth ="Shallow"
```

```
C1_OF2_deep = subset(C1_OF2_df, depth == "40.518")
C1_OF2_deep$Info = "Deep, 12.05.2022"
C1_OF2_deep$Depth ="Deep"
C1_OF2_shallow = subset(C1_OF2_df, depth == "3.491")
C1_OF2_shallow$Info = "Shallow, 12.05.2022"
C1_OF2_shallow$Depth ="Shallow"

C1_df = rbind(C1_L1_deep,C1_L1_shallow,
C1_L5_deep,C1_L5_shallow,C1_I1_deep,C1_I1_shallow,C1_O1_deep, C1_O1_shallow,
C1_OF2_deep, C1_OF2_shallow)
```

Creating RDS with CTD data for all stations and dates

```
Cruise = rbind(C1_df,C2_df, C3_df)
saveRDS(Cruise, "ctd.rds")

ctd <- readRDS("ctd.rds")

ctd_shallow <- subset(ctd, Depth == "Shallow")
```

Secchi-depth

```
secchi = read_excel("Secchi.xlsx")
secchi$Date = as.factor(secchi$Date)
s1 = subset(secchi, Date =="2022-06-02")
s1$Date = "02.06.2022"
s2 = subset(secchi, Date =="2022-06-29")
s2$Date = "29.06.2022"
secchi = rbind(s1,s2)
```

```
#Temperature at each station and date
p1= ggplot(ctd_shallow, aes(x = fct_inorder(Site),y=temperature, color = fct_inorder(Date)))+
 geom_point(size = 3)+
 geom_line(aes(group=Info))+
 xlab("Station")+
 ylab("Temperature ( C) ")+
 labs(colour = "Date") +
 ylim(0, 20) +
 scale_color_manual(values = my_colour_palette)+
 My_theme

#Salinity at each station and date
p2=ggplot(ctd_shallow, aes(x = fct_inorder(Site), y=salinity, color = fct_inorder(Date) ))+
 geom_point(size = 3)+
 geom_line(aes(group=Info))+
 xlab("Station")+
 ylab("Salinity (PSU)")+
 labs(colour = "Date") +
 ylim(0, 33) +
 scale_color_manual(values= my_colour_palette)+
 My_theme

#Pycnocline at each station and date
p3 = ggplot(ctd_shallow, aes(x = fct_inorder(Site), y= Pycnocline, color = fct_inorder(Date)))+
 geom_point(size = 3)+
 geom_line(aes(group=Info))+
 xlab("Station")+
```

```
 ylab("Pycnocline depth (m)")+
 labs(colour = "Date") +
 ylim(0, 25) +
 scale_color_manual(values = my_colour_palette) +
 My_theme

#Secchi-depth at each station and date
p4 = ggplot(secchi, aes(x = fct_inorder(Site), y= Secchi_depth, color = fct_inorder(Date)))+
 geom_line(aes(group = Date))+
 geom_point(size = 3)+
 xlab("Station")+
 ylab("Secchi depth (m)")+
 labs(colour = "Date") +
 ylim(0, 10) +
 scale_color_manual(values = c("blue", "deepskyblue2")) +
 My_theme


plot_grid(p1, p2, p3, p4, labels = c('A', 'B', 'C','D'), label_size = 13)
ggsave(filename = "CTD.pdf", width = 7.29, height = 4.75)
```

TriOS-data

Example for station OF2, cruise 1

```
station1.1 <- "OF2-1"
OF2.1 <- dir(station1.1) # List file names
```

```
# We only use "Spectrum" files from sensor "501A". This sensor faces upward and also measures
depth. Need sensor "8175" for normalizing to surface

OF2.1 <- OF2.1[grep("Spectrum", OF2.1)]
OF2.down.1 <- OF2.1[grep("501A", OF2.1)]
OF2.air.1 <- OF2.1[grep("8175", OF2.1)]

s1.down.1 <- NULL
for (i in 1:length(OF2.down.1)) {
 # First read file as a vector of strings
 file.path <- paste(station1.1, OF2.down.1[i], sep="/")
 raw.file <- read.table(file.path, sep="\t", as.is=TRUE)$V1

 # Find "Pressure =" line to extract pressure
 p.line <- raw.file[grep("Pressure", raw.file)]
 pressure <- as.numeric(strsplit(p.line, "=")[[1]][2])

 # Find start of spectrum section and read 254 lines from there
 spec.start <- which(raw.file == "[END] of [Attributes]") + 3

 # Read the file again but only the spectrum this time
 spectrum <- read.table(file.path, skip=spec.start, nrows=254)

 # Merge spectrum with sensor and time information
 s1.down.i.1 <- data.frame(
  id = i,
  depth = 10.06 * pressure,
  wl = spectrum$V1,
  pwr = spectrum$V2)
```

```
 # Append to spectrum data frame
 s1.down.1 <- rbind(s1.down.1, s1.down.i.1)
}


s1.air.1 <- NULL
for (i in 1:length(OF2.air.1)) {
 # First read file as a vector of strings
 file.path <- paste(station1.1, OF2.air.1[i], sep="/")
 raw.file <- read.table(file.path, sep="\t", as.is=TRUE)$V1


 # Find start of spectrum section and read 254 lines from there
 spec.start <- which(raw.file == "[END] of [Attributes]") + 3

 # Read the file again but only the spectrum this time
 spectrum <- read.table(file.path, skip=spec.start, nrows=254)

 # Merge spectrum with sensor and time information
 s1.air.i.1 <- data.frame(
  id = i,
  wl = spectrum$V1,
  pwr = spectrum$V2)

 # Append to spectrum data frame
 s1.air.1 <- rbind(s1.air.1, s1.air.i.1)
}
```

```
s1.down.1 <- subset(s1.down.1, wl < 700) # Remove > 700 nm
s1.down.1 <- subset(s1.down.1, wl > 400) #remove < 400 nm
s1.down.1 <- subset(s1.down.1, depth > 0) # Remove above surface



s1.air.1 <- subset(s1.air.1, wl < 700)
s1.air.1 <- subset(s1.air.1, wl > 400)



s1.down.1$pwr.rel <- s1.down.1$pwr / s1.air.1$pwr #normalize to surface
s1.down.1$Station <- "OF2"
s1.down.1$Date <- "12.05.22"

field_1 <- rbind(s1.down.1, s2.down.1, s3.down.1, s4.down.1, s5.down.1) #all stations from cruise
1

trios <- rbind(field_1, field_2, field_3) #all cruise dates
saveRDS(trios, "trios.rds")



trios <- readRDS("trios.rds")
ctd <- readRDS("ctd.rds")
ctd_shallow <- subset(ctd, Depth == "Shallow")



trios_pos <- subset(trios, pwr > 0)
trios_pos$dsw <- with(trios_pos, factor(paste(Date, Station, wl)))
```

```
summary(m <- lmer(log(pwr.rel) ~ depth + (depth | dsw), data=trios_pos))

plot(log(trios_pos$pwr.rel), predict(m)) # Good fit :)
abline(c(0, 1), lty=2)

dsw <- rownames(ranef(m)$dsw) #date, station, wavelength
att <- -(fixef(m)[2] + ranef(m)$dsw[, 2]) # Negative slope is attenuation coefficient as function of
wavelength

date <- factor(sapply(strsplit(dsw, " "), function(x) { x[1] }))
station <- factor(sapply(strsplit(dsw, " "), function(x) { x[2] }))
wl <- as.numeric(sapply(strsplit(dsw, " "), function(x) { x[3] }))

df_t<- data.frame(Date=as.Date(date, format="%d.%m.%y"), Site=station, wl, att)


ctd_shallow$Date <- as.Date(ctd_shallow$Date, format="%d.%m.%Y")

dfc <- merge(df_t, ctd_shallow)


#Plotting the attenuation coefficient over wavelength for each station and date
df_t %>%
 mutate(date = fct_relevel(date, "12.05.22", "02.06.22", "29.06.22")) %>%

 mutate(Site = fct_relevel(Site, "L1", "L5", "I1", "O1", "OF2")) %>%
 ggplot( aes(x=wl, y=att, group=date, color = date)) +
 geom_line() +
```

```
 facet_wrap(~ Site) +
 ylab("Attenuation") +
 xlab("Wavelength (nm)") +
 scale_color_manual(values = my_colour_palette)+
 My_theme + theme(axis.text.x = element_text(angle=90))

ggsave(filename = "att.pdf", width = 7.29, height = 4.75)
```

Gas chromatography

```
carbon <- read_xlsx("Gassanalyser_Tonje_s.xlsx")
library(marelac)

t <- 4

T <- 273.15 + t # K
R <- as.numeric(Constants$gasCt1[1]) # L*atm/K/mol

ph <- carbon$CO2 / 1000000 # (Atm) - assuming unit is ppm partial pressure in headspace

Vw <- 30 / 1000 # Water volume (L)
Vh <- 20 / 1000 # Headspace volume (L)

# Ideal gas law: p V = n R T -> n = p V / RT
nh <- (ph * Vh) / (R * T) # Moles CO2 in the headspace

# gas_solubility gives mmol/m3/bar = µM / bar
gs <- gas_solubility(t = t, S = carbon$Salinity, species = "CO2")  # S= salinity adapted from CTD-data
```

```
nw <- (ph * gs) * Vw # Moles CO2 in the water after equilibration

C0 <- (nh + nw) / Vw # Initial DIC concentration (µM) before acidification

carbon$C0 <- C0

saveRDS(carbon, "carbon.rds")
```

Prediction of DIC concentration

```
C0.min <- aggregate(C0 ~ Station + Date, data=df_light, FUN=min)
sal.mean <- aggregate(Salinity ~ Station + Date, data=df_light, FUN=mean)

df_1 <- merge(C0.min, sal.mean)

m_C0 <- lm(C0 ~ Salinity, data = df_1)
```

Predictions of minimum attenuation coefficient and wavelength at minimum

```
att.min <- aggregate(att ~ station + date, data=dfc, FUN=min)
wl.min <- aggregate(att ~ station + date, data=dfc, FUN=function(x) { wl[which.min(x)] })
sal.mean <- aggregate(salinity ~ station + date, data=dfc, FUN=mean)

wl.min$wl <- wl.min$att

wl.min <- subset(wl.min, select = - att)
```

```
df_1 <- merge(att.min, wl.min)
df_1 <- merge(df_1, sal.mean)


#Linear models for predictions
m_att <- lm(att ~ salinity, data = df_1)
m_wl <- lm(wl ~ salinity, data = df_1)

pred_att <- predict(m_att, newdata = list(salinity = c(0,33)), interval = "confidence")
pred_wl <- predict(m_wl, newdata = list(salinity = c(0,33)), interval = "confidence")
pred_C0 <- predict(m_C0, newdata = list(salinity = c(0,33)), interval = "confidence")

columns = c("Variable", "PSU", "fit", "lwr", "upr")

pred_df <- data.frame(matrix(nrow = 6, ncol = length(columns)))

pred_df$Variable <- c("Attenuation", "Attenuation", "Wavelength", "Wavelength", "DIC", "DIC")

pred_df$PSU <- c("0", "33", "0", "33", "0", "33")

pred_df$fit <- c(0.70783984, -0.07175787, 582.4851, 557.8619, 458.7964, 2065.5555)

pred_df$lwr <- c(0.5966106,-0.2110134, 577.5668, 551.7043, 352.0288, 1931.8859 )

pred_df$upr <- c(0.8190691, 0.06749763, 587.4035, 564.0195, 565.564, 2199.225)

pred_df <- pred_df[6:10]
```

```
pred_df_att <- subset(pred_df, Variable == "Attenuation")
pred_df_wl <- subset(pred_df, Variable == "Wavelength")
pred_df_C <- subset(pred_df, Variable == "DIC")

#95% confidence intervals for attenuation predictions
p1 = ggplot(pred_df_att, aes(x= PSU, y = fit, color = PSU )) +
 geom_point(size = 3) +
 geom_errorbar(aes(ymin = lwr, ymax = upr)) +
 ylab("Attenuation") +
 scale_color_manual(values = c("navy", "deepskyblue2")) +
 My_theme + theme(strip.text.x = element_text(size = 13))

#95% confidence intervals for wavelength predictions
p2 = ggplot(pred_df_wl, aes(x= PSU, y = fit, color = PSU )) +
 geom_point(size = 3) +
 geom_errorbar(aes(ymin = lwr, ymax = upr)) +
 ylab("Wavelength (nm)") +
 scale_color_manual(values = c("navy", "deepskyblue2")) +
 My_theme + theme(strip.text.x = element_text(size = 13))

#95% confidence intervals for DIC concentration predictions
p3 = ggplot(pred_df_C, aes(x= PSU, y = fit, color = PSU )) +
 geom_point(size = 3) +
 geom_errorbar(aes(ymin = lwr, ymax = upr)) +
 ylab("DIC (umol/L)") +
 scale_color_manual(values = c("navy", "deepskyblue2")) +
 My_theme + theme(strip.text.x = element_text(size = 13))
```

Plotting predictions for attenuation minimum, wavelength at minimum and minimum DIC

```
plot_grid(p1, p2, p3, labels = c("A", "B","C"))
ggsave(filename = "pred.pdf", width = 7.29, height = 4.75)
```

Integrating sphere spectrophotometry

```
L1_1 <- read.table("L1 C1 F1.txt", header = TRUE, sep = ",")
as.data.frame(L1_1)
L1_1$ID = "L1_1"
L1_1$Station= "L1"
L1_1$Abs. = L1_1$Abs. - 0.059


L1_1_bleach <- read.table("L1 C1 F1 bleach.txt", header = TRUE, sep = ",")
as.data.frame(L1_1_bleach)
L1_1_bleach$ID = "L1_1_bleach"
L1_1_bleach$Station= "L1"
L1_1_bleach$Abs. = L1_1_bleach$Abs. - 0.024

L1_2 <- read.table("L1 C1 F2.txt", header = TRUE, sep = ",")
as.data.frame(L1_2)
L1_2$ID = "L1_2"
L1_2$Station= "L1"
L1_2$Abs. = L1_2$Abs. - 0.057

L1_2_bleach <- read.table("L1 C1 F2 bleach.txt", header = TRUE, sep = ",")
as.data.frame(L1_2_bleach)
L1_2_bleach$ID = "L1_2_bleach"
L1_2_bleach$Station= "L1"
```

```
L1_2_bleach$Abs. = L1_2_bleach$Abs. - 0.037


L1_3 <- read.table("L1 C1 F3.txt", header = TRUE, sep = ",")
as.data.frame(L1_3)
L1_3$ID = "L1_3"
L1_3$Station= "L1"
L1_3$Abs. = L1_3$Abs. - 0.060

L1_3_bleach <- read.table("L1 C1 F3 bleach.txt", header = TRUE, sep = ",")
as.data.frame(L1_3_bleach)
L1_3_bleach$ID = "L1_3_bleach"
L1_3_bleach$Station= "L1"
L1_3_bleach$Abs. = L1_3_bleach$Abs. - 0.024



L5_1 <- read.table("L5 C1 F1.txt", header = TRUE, sep = ",")
as.data.frame(L5_1)
L5_1$ID = "L5_1"
L5_1$Station= "L5"
L5_1$Abs. = L5_1$Abs. - 0.005

L5_1_bleach <- read.table("L5 C1 F1 bleach.txt", header = TRUE, sep = ",")
as.data.frame(L5_1_bleach)
L5_1_bleach$ID = "L5_1_bleach"
L5_1_bleach$Station= "L5"
L5_1_bleach$Abs. = L5_1_bleach$Abs.- (-0.017)
```

```
L5_2 <- read.table("L5 C1 F2.txt", header = TRUE, sep = ",")
as.data.frame(L5_2)
L5_2$ID = "L5_2"
L5_2$Station= "L5"
L5_2$Abs. = L5_2$Abs. -(-0.034)

L5_2_bleach <- read.table("L5 C1 F2 bleach.txt", header = TRUE, sep = ",")
as.data.frame(L5_2_bleach)
L5_2_bleach$ID = "L5_2_bleach"
L5_2_bleach$Station= "L5"
L5_2_bleach$Abs. = L5_2_bleach$Abs. - (-0.036)


L5_3 <- read.table("L5 C1 F3.txt", header = TRUE, sep = ",")
as.data.frame(L5_3)
L5_3$ID = "L5_3"
L5_3$Station= "L5"
L5_3$Abs. = L5_3$Abs. - (-0.040)

L5_3_bleach <- read.table("L5 C1 F3 bleach.txt", header = TRUE, sep = ",")
as.data.frame(L5_3_bleach)
L5_3_bleach$ID = "L5_3_bleach"
L5_3_bleach$Station= "L5"
L5_3_bleach$Abs. = L5_3_bleach$Abs. - (-0.070)


I1_1 <- read.table("I1 C1 F1.txt", header = TRUE, sep = ",")
as.data.frame(I1_1)
I1_1$ID = "I1_1"
```

```
I1_1$Station= "I1"
I1_1$Abs. = I1_1$Abs. - (-0.023)



I1_1_bleach <- read.table("I1 C1 F1 bleach.txt", header = TRUE, sep = ",")
as.data.frame(I1_1)
I1_1_bleach$ID = "I1_1_bleach"
I1_1_bleach$Station= "I1"
I1_1_bleach$Abs. = I1_1_bleach$Abs. - (-0.053)


I1_2 <- read.table("I1 C1 F2.txt", header = TRUE, sep = ",")
as.data.frame(I1_2)
I1_2$ID = "I1_2"
I1_2$Station= "I1"
I1_2$Abs. = I1_2$Abs. - (-0.016)

I1_2_bleach <- read.table("I1 C1 F2 bleach.txt", header = TRUE, sep = ",")
as.data.frame(I1_2_bleach)
I1_2_bleach$ID = "I1_2_bleach"
I1_2_bleach$Station= "I1"
I1_2_bleach$Abs. = I1_2_bleach$Abs. - (-0.047)


I1_3 <- read.table("I1 C1 F3.txt", header = TRUE, sep = ",")
as.data.frame(I1_3)
I1_3$ID = "I1_3"
I1_3$Station= "I1"
```

```
I1_3$Abs. = I1_3$Abs. - (-0.019)


I1_3_bleach <- read.table("I1 C1 F3 bleach.txt", header = TRUE, sep = ",")
as.data.frame(I1_3_bleach)
I1_3_bleach$ID = "I1_3_bleach"
I1_3_bleach$Station= "I1"
I1_3_bleach$Abs. = I1_3_bleach$Abs. - (-0.058)


O1_1 <- read.table("O1 F1 C1.txt", header = TRUE, sep = ",")
as.data.frame(O1_1)
O1_1$ID = "O1_1"
O1_1$Station= "O1"
O1_1$Abs. = O1_1$Abs. - (-0.010)

O1_1_bleach <- read.table("O1 F1 C1 bleach.txt", header = TRUE, sep = ",")
as.data.frame(O1_1)
O1_1_bleach$ID = "O1_1_bleach"
O1_1_bleach$Station= "O1"
O1_1_bleach$Abs. = O1_1_bleach$Abs. - (-0.051)


O1_2 <- read.table("O1 F2 C1.txt", header = TRUE, sep = ",")
as.data.frame(O1_2)
O1_2$ID = "O1_2"
O1_2$Station= "O1"
O1_2$Abs. = O1_2$Abs. - (-0.067)
```

```
O1_2_bleach <- read.table("O1 F2 C1 bleach.txt", header = TRUE, sep = ",")
as.data.frame(O1_2_bleach)
O1_2_bleach$ID = "O1_2_bleach"
O1_2_bleach$Station= "O1"
O1_2_bleach$Abs. = O1_2_bleach$Abs. - (-0.072)

O1_3 <- read.table("O1 F3 C1.txt", header = TRUE, sep = ",")
as.data.frame(O1_3)
O1_3$ID = "O1_3"
O1_3$Station= "O1"
O1_3$Abs. = O1_3$Abs. - (-0.044)
O1_3_bleach <- read.table("O1 F3 C1 bleach.txt", header = TRUE, sep = ",")
as.data.frame(O1_3_bleach)
O1_3_bleach$ID = "O1_3_bleach"
O1_3_bleach$Station= "O1"
O1_3_bleach$Abs.= O1_3_bleach$Abs. - (-0.084)


OF2_1 <- read.table("OF2 F1 C1.txt", header = TRUE, sep = "," )
as.data.frame(OF2_1)
OF2_1$ID = "OF2_1"
OF2_1$Station= "OF2"
OF2_1$Abs. = OF2_1$Abs. - 0.096



OF2_1_bleach <- read.table("OF2 F1 C1 bleach.txt", header = TRUE, sep = "," )
as.data.frame(OF2_1_bleach)
```

```
OF2_1_bleach$ID = "OF2_1_bleach"
OF2_1_bleach$Station= "OF2"
OF2_1_bleach$Abs. = OF2_1_bleach$Abs. - 0.069


OF2_2 <- read.table("OF2 F2 C1.txt", header = TRUE, sep = "," )
as.data.frame(OF2_2)
OF2_2$ID = "OF2_2"
OF2_2$Station= "OF2"
OF2_2$Abs.= OF2_2$Abs.- 0.058


OF2_2_bleach <- read.table("OF2 F2 C1 bleach.txt", header = TRUE, sep = "," )
as.data.frame(OF2_2_bleach)
OF2_2_bleach$ID = "OF2_2_bleach"
OF2_2_bleach$Station= "OF2"
OF2_2_bleach$Abs. = OF2_2_bleach$Abs. - 0.056

OF2_3 <- read.table("OF2 F3 C1.txt", header = TRUE, sep = "," )
as.data.frame(OF2_3)
OF2_3$ID = "OF2_3"
OF2_3$Station= "OF2"
OF2_3$Abs. = OF2_3$Abs. - 0.068


OF2_3_bleach <- read.table("OF2 F3 C1 bleach.txt", header = TRUE, sep = "," )
as.data.frame(OF2_3_bleach)
OF2_3_bleach$ID = "OF2_3_bleach"
OF2_3_bleach$Station= "OF2"
```

```
OF2_3_bleach$Abs. = OF2_3_bleach$Abs. - 0.030


pigment_df <- rbind(L1_1, L1_2, L1_3, L5_1, L5_2, L5_3, I1_1, I1_2, I1_3, O1_1, O1_2, O1_3,
OF2_1, OF2_2, OF2_3)

bleached_pigment_df <- rbind(L1_1_bleach, L1_2_bleach, L1_3_bleach, L5_1_bleach,
L5_2_bleach, L5_3_bleach, I1_1_bleach, I1_2_bleach, I1_3_bleach, O1_1_bleach, O1_2_bleach,
O1_3_bleach, OF2_1_bleach, OF2_2_bleach, OF2_3_bleach)

pigment_df <- subset(pigment_df, Wavelength.nm. > 399)
pigment_df <- subset(pigment_df, Wavelength.nm. < 701)

bleached_pigment_df <- subset(bleached_pigment_df, Wavelength.nm. > 399)
bleached_pigment_df <- subset(bleached_pigment_df, Wavelength.nm. < 701)

pigment_df$Abs. <- pigment_df$Abs. - bleached_pigment_df$Abs.

pigment_df <- aggregate(Abs.~ Wavelength.nm. + Station, data = pigment_df, FUN = mean)
bleached_pigment_df <- aggregate(Abs.~ Wavelength.nm. + Station, data = bleached_pigment_df,
FUN = mean)
```

CDOM absorbance from UV-vis spectrophotometry

```
O1_cdom <- read.table("C1O1,3-4m.txt", header = TRUE, sep = ",")
as.data.frame(O1_cdom)
O1_cdom$Station= "O1"
O1_cdom$Abs. = O1_cdom$Abs. - 0.001

L1_cdom <- read.table("C1L1,3-4m.txt", header = TRUE, sep = ",")
```

```
as.data.frame(L1_cdom)
L1_cdom$Station= "L1"
L1_cdom$Abs. = L1_cdom$Abs. - 0.005

I1_cdom <- read.table("C1I1,3-4m.txt", header = TRUE, sep = ",")
as.data.frame(I1_cdom)
I1_cdom$Station= "I1"
I1_cdom$Abs. = I1_cdom$Abs. - 0.002

L5_cdom <- read.table("C1L5,3-4m.txt", header = TRUE, sep = ",")
as.data.frame(L5_cdom)
L5_cdom$Station= "L5"
L5_cdom$Abs. = L5_cdom$Abs. - 0.000

OF2_cdom <- read.table("C1OF2,3-4m.txt", header = TRUE, sep = ",")
as.data.frame(OF2_cdom)
OF2_cdom$Station= "OF2"
OF2_cdom$Abs. = OF2_cdom$Abs. - 0.000

cdom <- rbind(O1_cdom, L1_cdom, L5_cdom, I1_cdom, OF2_cdom)
cdom <- subset(cdom, Wavelength.nm. > 399)
cdom <- subset(cdom, Wavelength.nm. < 701)
```

Water absorbance coefficient from Morel & Prieur (1977)

```
water <- read_xlsx("water abs coeff.xlsx")
water <- subset(water, Wavelength.nm. > 399 )

ggplot(water, aes(x=Wavelength.nm., y =Abs_coeff)) +
 geom_line() +
```

```
 xlab("Wavelength (nm)") +
 ylab("Absorbance coefficient per meter") +
 My_theme

ggsave(filename = "waterabs.pdf", width = 7.29, height = 4.75 )
```

Pigment, detritus and CDOM absorbance coefficients

```
V <- 250/1000000 # m^3
A <- 363.05/1000000  #m^2

path <- V/A

pigment_df$abs_coeff_a <- log(10)*pigment_df$Abs./path

cdom$abs_coeff_dom <- log(10)*cdom$Abs./0.05

bleached_pigment_df$abs_coeff_d <- log(10)*bleached_pigment_df$Abs./path
```

PAR from STRÅNG

```
ex1 <- read_xlsx("par-strang1213.xlsx")
ex1$time.str <- with(ex1, paste0(V1, "-", V2, "-", V3, " ", V4, ":00:00"))
ex1$time <- as.POSIXct(strptime(ex1$time.str, "%Y-%m-%d %H:%M:%S"))

(sum.par <- 60 * 60 * sum(ex1$V5[19:43]) / 1000000) # J/m2/d fra watt (J/s) /m2
(par.mol <- 4.57 * sum.par) # Thimijan & Heins (1983) #mol kvanta per m2 per dag

#ca 30 mol quanta per square meter per day.
```

```
ggplot(data = ex1, aes(y=V5, x =time))+
 geom_line(color = "blue")+
 ylab("PAR (W/m^2)")+
 xlab("Date - Time ")+
 geom_vline(xintercept = ex1$time[19])+
 geom_vline(xintercept = ex1$time[43])+
 My_theme

ggsave(filename = "par1.pdf", width = 7.29, height = 4.75)
```

PAM fluorometry

```
h <- dir(pattern=".txt")
h <- h[grepl("LC1",h)]

hh <- strsplit(h, " ")

station <- sapply(hh, function(x) { x[1] })

date <- substr(sapply(hh, function(x) { x[2] }), 1, 8)
date <- as.Date(date, format="%d%m%Y")

QY <- matrix(NA, ncol=7, nrow=length(h))
colnames(QY) <- paste0("L", 0:6)

for (i in (1:length(h))) {
 df <- read.csv(h[i], sep = "\n")
 df <- strsplit(df[grep("QY", df[,1]), 1], "\t")
 QY[i, ] <- as.numeric(sapply(df, function(x) { x[2] }))
}
```

```
df <- data.frame(station, date, stack(as.data.frame(QY)))
EL <- data.frame(ind=paste0("L", 0:6), E=c(0, 10, 20, 50, 100, 300, 500))

df <- merge(df, EL)
names(df) <- c("ind", "station", "date", "QY","E")

df %>%
 mutate(station = fct_relevel(station,
              "L1", "L5", "I1",
              "O1", "OF2")) %>%
 ggplot( aes(x=E, y=QY, shape=station, color = station)) +
 geom_point(size = 3) +
 scale_y_log10() +
 xlab("E (µmol quanta/m2/s)") +
 My_theme
ggsave(filename = "QY1.pdf", width = 7.29, height = 4.75)


bleached_pigment_df$Abs_d = bleached_pigment_df$Abs.
bleached_pigment_df = subset(bleached_pigment_df, select = - Abs.)


pigment_df$Abs_a = pigment_df$Abs.
pigment_df = subset(pigment_df, select = - Abs.)

cdom$Abs_dom = cdom$Abs.
cdom = subset(cdom, select = - Abs.)
```

```
df_all <- merge(bleached_pigment_df, pigment_df)

df_all <- merge(df_all, cdom)

df_all$Abs_H2O <- approx(water$Wavelength.nm., water$Abs_coeff,
xout=df_all$Wavelength.nm.)$y

df_all$Date <- "12.05.22"
```

Cumulative absorbance, OF2

```
OF2 <- subset(df_all, station == "OF2")

OF2 <- data.frame(OF2, stack(data.frame(OF2$Abs_H2O, OF2$abs_coeff_dom, OF2$abs_coeff_d,
OF2$abs_coeff_a)))

p1 = ggplot(OF2, aes(x=Wavelength.nm., y=values, fill=ind)) +
 geom_area() +
 ylab("Absorbance (m-1)") +
 xlab("Wavelength (nm)") +
 ylim(0,6) +
 ggtitle("OF2 12/5-22") +
 scale_fill_manual(name = "Type",values = c("deepskyblue2", "darkgoldenrod3", "bisque4",
"chartreuse3"), labels = c("H2O", "CDOM", "Detritus", "Pigment"), guide = "legend")+
 My_theme
```

Cumulative absorbance, O1

```
O1 <- subset(df_all, station == "O1")
```

```
O1 <- data.frame(O1, stack(data.frame(O1$Abs_H2O, O1$abs_coeff_dom, O1$abs_coeff_d,
O1$abs_coeff_a))

p2 = ggplot(O1, aes(x=Wavelength.nm., y=values, fill=ind)) +
 geom_area() +
 ylab("Absorbance (m-1)") +
 xlab("Wavelength (nm)") +
 ylim(0,6) +
 ggtitle("O1 12/5-22") +
 scale_fill_manual(name = "Type",values = c("deepskyblue2", "darkgoldenrod3", "bisque4",
"chartreuse3"), labels = c("H2O", "CDOM", "Detritus", "Pigment"), guide = "legend")+
 My_theme
```

Cumulative absorbance, I1

```
I1 <- subset(df_all, station == "I1")

I1 <- data.frame(I1, stack(data.frame(I1$Abs_H2O, I1$abs_coeff_dom, I1$abs_coeff_d,
I1$abs_coeff_a)))

p3 = ggplot(I1, aes(x=Wavelength.nm., y=values, fill=ind)) +
 geom_area() +
 ylab("Absorbance (m-1)") +
 xlab("Wavelength (nm)") +
 ylim(0,6) +
 ggtitle("I1 12/5-22") +
 scale_fill_manual(name = "Type",values = c("deepskyblue2", "darkgoldenrod3", "bisque4",
"chartreuse3"), labels = c("H2O", "CDOM", "Detritus", "Pigment"), guide = "legend")+
 My_theme
```

Cumulative absorbance, L5

```
L5 <- subset(df_all, station == "L5")

L5 <- data.frame(L5, stack(data.frame(L5$Abs_H2O, L5$abs_coeff_dom, L5$abs_coeff_d,
L5$abs_coeff_a)))

p4 = ggplot(L5, aes(x=Wavelength.nm., y=values, fill=ind)) +
 geom_area() +
 ylab("Absorbance (m-1)") +
 xlab("Wavelength (nm)") +
 ylim(0,6) +
 ggtitle("L5 12/5-22") +
 scale_fill_manual(name = "Type",values = c("deepskyblue2", "darkgoldenrod3", "bisque4",
"chartreuse3"), labels = c("H2O", "CDOM", "Detritus", "Pigment"), guide = "legend")+
 My_theme
```

Cumulative absorbance, L1

```
L1 <- subset(df_all, station == "L1")

L1 <- data.frame(L1, stack(data.frame(L1$Abs_H2O, L1$abs_coeff_dom, L1$abs_coeff_d,
L1$abs_coeff_a)))



p5 = ggplot(L1, aes(x=Wavelength.nm., y=values, fill=ind)) +
 geom_area() +
 ylab("Absorbance (m-1)") +
```

```
 xlab("Wavelength (nm)") +
 ylim(0,6) +
 ggtitle("L1 12/5-22") +
 scale_fill_manual(name = "Type",values = c("deepskyblue2", "darkgoldenrod3", "bisque4",
"chartreuse3"), labels = c("H2O", "CDOM", "Detritus", "Pigment"), guide = "legend")+
 My_theme


plot_grid(p5, p1, labels = c('A', 'B'), label_size = 14)

ggsave(filename = "pigment11.pdf", width = 7.29, height = 4.75)

plot_grid(p2, p3, p4, labels = c( 'C','D', 'E'), label_size = 14)

ggsave(filename = "pigment1.pdf", width = 7.29, height = 4.75)
```

Spectrally averaged pigment, CDOM, detritus and water absorbance

```
abs_coeff_d_df <- subset(df_all, select = - c(abs_coeff_a, Abs_H2O, Abs_dom, Abs_a,
abs_coeff_dom, Abs_d))

abs_coeff_d_df$Value <-abs_coeff_d_df$abs_coeff_d

abs_coeff_d_df$Type <- "Abs_coeff_d"

abs_coeff_d_df <- subset(abs_coeff_d_df, select = - abs_coeff_d)
```

```
abs_coeff_a_df <- subset(df_all, select = - c(abs_coeff_d, Abs_H2O, Abs_dom, Abs_a,
abs_coeff_dom, Abs_d))

abs_coeff_a_df$Value <-abs_coeff_a_df$abs_coeff_a

abs_coeff_a_df$Type <- "Abs_coeff_a"

abs_coeff_a_df <- subset(abs_coeff_a_df, select = - abs_coeff_a)


abs_coeff_dom_df <- subset(df_all, select = - c(abs_coeff_a, Abs_H2O, Abs_dom, Abs_a,
abs_coeff_d, Abs_d))

abs_coeff_dom_df$Value <-abs_coeff_dom_df$abs_coeff_dom

abs_coeff_dom_df$Type <- "Abs_coeff_dom"

abs_coeff_dom_df <- subset(abs_coeff_dom_df, select = - abs_coeff_dom)


abs_coeff_H2O_df <- subset(df_all, select = - c(abs_coeff_a, abs_coeff_d, Abs_dom, Abs_a,
abs_coeff_dom, Abs_d))

abs_coeff_H2O_df$Value <-abs_coeff_H2O_df$Abs_H2O

abs_coeff_H2O_df$Type <- "Abs_coeff_H2O"

abs_coeff_H2O_df <- subset(abs_coeff_H2O_df, select = - Abs_H2O)
```

```
df_abs <- rbind(abs_coeff_H2O_df, abs_coeff_a_df, abs_coeff_d_df, abs_coeff_dom_df)

df_abs$Abs_mean <- df_abs$Value/300

saveRDS(df_abs, "df_abs1")
```

Total spectrally averaged absorbance across stations and dates

```
df_abs1 <- readRDS("df_abs1")

df_abs2 <- readRDS("df_abs2")

df_abs3 <- readRDS("df_abs3")

df_abs <- rbind(df_abs1, df_abs2, df_abs3)

saveRDS(df_abs, "df_abs")

abs <- df_abs %>%
 mutate(Station = fct_relevel(Station,
              "L1", "L5", "I1",
              "O1", "OF2")) %>%
 mutate(Date = fct_relevel(Date, "12.05.22", "02.06.22", "29.06.22")) %>%
 ggplot( aes(fill=Type, y=Abs_mean, x=Date)) +
 facet_grid(~ Station)+
 geom_bar(position="stack", stat="identity") +
```

```
 scale_fill_manual(name = "Type",values = c("deepskyblue2","chartreuse3", "bisque4",
"darkgoldenrod3"), labels = c( "H2O", "Pigment", "Detritus", "CDOM")) +
 My_theme + theme(strip.text.x = element_text(size = 13))+
 theme(axis.text.x = element_text(angle=90))+
 labs(y = bquote('Absorbance'~(m^-1)), x = "Date")
abs

ggsave(filename = "abstot.pdf", width = 7.29, height = 4.75)
```

Bio optical rates of carbon uptake, cruise 1

```
ctd <- readRDS("ctd.rds")

ctd_shallow <- subset(ctd, Depth == "Shallow" & Date == "12.05.2022")

OF2_pp <- subset(df_abs, Station == "OF2")
OF2_Pycnocline <- ctd_shallow$Pycnocline[5]
OF2_Salinity <- ctd_shallow$salinity[5]
OF2_tot.abs <- sum(OF2_pp$Abs_mean)

OF2_QY <- subset(df, station == "OF2")

OF2_QY_mean <- mean(OF2_QY$QY)

OF2_a <- subset(df_abs, Station == "OF2" & Type == "Abs_coeff_a")
OF2_cdom <- subset(df_abs, Station == "OF2" & Type == "Abs_coeff_dom")


O1_pp <- subset(df_abs, Station == "O1")
```

```
O1_Pycnocline <- ctd_shallow$Pycnocline[4]
O1_Salinity <- ctd_shallow$salinity[4]
O1_tot.abs <- sum(O1_pp$Abs_mean)

O1_QY <- subset(df, station == "O1")

O1_QY_mean <- mean(O1_QY$QY)

O1_a <- subset(df_abs, Station == "O1" & Type == "Abs_coeff_a")
O1_cdom <- subset(df_abs, Station == "O1" & Type == "Abs_coeff_dom")
I1_pp <- subset(df_abs, Station == "I1")
I1_Pycnocline <- ctd_shallow$Pycnocline[3]
I1_Salinity <- ctd_shallow$salinity[3]
I1_tot.abs <- sum(I1_pp$Abs_mean)

I1_QY <- subset(df, station == "I1")

I1_QY_mean <- mean(I1_QY$QY)

I1_a <- subset(df_abs, Station == "I1" & Type == "Abs_coeff_a")
I1_cdom <- subset(df_abs, Station == "I1" & Type == "Abs_coeff_dom")


L5_pp <- subset(df_abs, Station == "L5")
L5_Pycnocline <- ctd_shallow$Pycnocline[2]
L5_Salinity <- ctd_shallow$salinity[2]
L5_tot.abs <- sum(L5_pp$Abs_mean)

L5_QY <- subset(df, station == "L5")
```

```
L5_QY_mean <- mean(L5_QY$QY)

L5_a <- subset(df_abs, Station == "L5" & Type == "Abs_coeff_a")
L5_cdom <- subset(df_abs, Station == "L5" & Type == "Abs_coeff_dom")



L1_pp <- subset(df_abs, Station == "L1")
L1_Pycnocline <- ctd_shallow$Pycnocline[1]
L1_Salinity <- ctd_shallow$salinity[1]
L1_tot.abs <- sum(L1_pp$Abs_mean)

L1_QY <- subset(df, station == "L1")

L1_QY_mean <- mean(L1_QY$QY)

L1_a <- subset(df_abs, Station == "L1" & Type == "Abs_coeff_a")
L1_cdom <- subset(df_abs, Station == "L1" & Type == "Abs_coeff_dom")



E_0 <- 30 #mol/m^2/d

E_OF2_pyc <- E_0 * exp( - OF2_tot.abs * OF2_Pycnocline)

delta_E_OF2 = E_0 - E_OF2_pyc

delta_Ea_OF2 = (sum(OF2_a$Abs_mean)/OF2_tot.abs)*delta_E_OF2
```

```
OF2_pp <- 0.08*delta_Ea_OF2*OF2_QY_mean

OF2_pp_mg <- OF2_pp *12000


columns <- c("Station", "Date","Pycnocline", "Salinity", "E_0","E_pyc", "delta_E", "delta_Ea",
"Abs_a", "Abs_cdom", "Tot_abs", "pp", "pp_mg")
new_df_OF2 <- data.frame(matrix(nrow = 1, ncol = length(columns)))

new_df_OF2$Station <- "OF2"
new_df_OF2$Date <- "12.05.22"
new_df_OF2$Pycnocline <- OF2_Pycnocline
new_df_OF2$Salinity <- OF2_Salinity
new_df_OF2$E_0 <- 30
new_df_OF2$E_pyc <- E_OF2_pyc
new_df_OF2$delta_E <- delta_E_OF2
new_df_OF2$delta_Ea <- delta_Ea_OF2
new_df_OF2$Abs_a <- sum(OF2_a$Abs_mean)
new_df_OF2$Abs_cdom <- sum(OF2_cdom$Abs_mean)
new_df_OF2$Tot_abs <- OF2_tot.abs
new_df_OF2$pp <- OF2_pp
new_df_OF2$pp_mg <- OF2_pp_mg


new_df_OF2 <- new_df_OF2[14:26]
```

```
E_O1_pyc <- E_0 * exp( - O1_tot.abs * O1_Pycnocline)

delta_E_O1 = E_0 - E_O1_pyc

delta_Ea_O1 = (sum(O1_a$Abs_mean)/O1_tot.abs)*delta_E_O1

O1_pp <- 0.08*delta_Ea_O1*O1_QY_mean

O1_pp_mg <- O1_pp *12000


columns <- c("Station", "Date","Pycnocline", "Salinity", "E_0","E_pyc", "delta_E", "delta_Ea",
"Abs_a", "Abs_cdom", "Tot_abs", "pp", "pp_mg")
new_df_O1 <- data.frame(matrix(nrow = 1, ncol = length(columns)))

new_df_O1$Station <- "O1"
new_df_O1$Date <- "12.05.22"
new_df_O1$Pycnocline <- O1_Pycnocline
new_df_O1$Salinity <- O1_Salinity
new_df_O1$E_0 <- 30
new_df_O1$E_pyc <- E_O1_pyc
new_df_O1$delta_E <- delta_E_O1
new_df_O1$delta_Ea <- delta_Ea_O1
new_df_O1$Abs_a <- sum(O1_a$Abs_mean)
new_df_O1$Abs_cdom <- sum(O1_cdom$Abs_mean)
new_df_O1$Tot_abs <- O1_tot.abs
new_df_O1$pp <- O1_pp
new_df_O1$pp_mg <- O1_pp_mg
```

```
new_df_O1 <- new_df_O1[14:26]


E_I1_pyc <- E_0 * exp( - I1_tot.abs * I1_Pycnocline)

delta_E_I1 = E_0 - E_I1_pyc

delta_Ea_I1 = (sum(I1_a$Abs_mean)/I1_tot.abs)*delta_E_I1

I1_pp <- 0.08*delta_Ea_I1*I1_QY_mean

I1_pp_mg <- I1_pp *12000

columns <- c("Station", "Date","Pycnocline", "Salinity", "E_0","E_pyc", "delta_E", "delta_Ea",
"Abs_a", "Abs_cdom", "Tot_abs", "pp", "pp_mg")
new_df_I1 <- data.frame(matrix(nrow = 1, ncol = length(columns)))

new_df_I1$Station <- "I1"
new_df_I1$Date <- "12.05.22"
new_df_I1$Pycnocline <- I1_Pycnocline
new_df_I1$Salinity <- I1_Salinity
new_df_I1$E_0 <- 30
new_df_I1$E_pyc <- E_I1_pyc
new_df_I1$delta_E <- delta_E_I1
new_df_I1$delta_Ea <- delta_Ea_I1
new_df_I1$Abs_a <- sum(I1_a$Abs_mean)
new_df_I1$Abs_cdom <- sum(I1_cdom$Abs_mean)
new_df_I1$Tot_abs <- I1_tot.abs
```

```
new_df_I1$pp <- I1_pp
new_df_I1$pp_mg <- I1_pp_mg


new_df_I1 <- new_df_I1[14:26]


E_L5_pyc <- E_0 * exp( - L5_tot.abs * L5_Pycnocline)

delta_E_L5 = E_0 - E_L5_pyc

delta_Ea_L5 = (sum(L5_a$Abs_mean)/L5_tot.abs)*delta_E_L5


L5_pp <- 0.08*delta_Ea_L5*L5_QY_mean

L5_pp_mg <- L5_pp *12000


columns <- c("Station", "Date","Pycnocline", "Salinity", "E_0","E_pyc", "delta_E", "delta_Ea",
"Abs_a", "Abs_cdom", "Tot_abs", "pp", "pp_mg")
new_df_L5 <- data.frame(matrix(nrow = 1, ncol = length(columns)))

new_df_L5$Station <- "L5"
new_df_L5$Date <- "12.05.22"
new_df_L5$Pycnocline <- L5_Pycnocline
new_df_L5$Salinity <- L5_Salinity
new_df_L5$E_0 <- 30
new_df_L5$E_pyc <- E_L5_pyc
```

```
new_df_L5$delta_E <- delta_E_L5
new_df_L5$delta_Ea <- delta_Ea_L5
new_df_L5$Abs_a <- sum(L5_a$Abs_mean)
new_df_L5$Abs_cdom <- sum(L5_cdom$Abs_mean)
new_df_L5$Tot_abs <- L5_tot.abs
new_df_L5$pp <- L5_pp
new_df_L5$pp_mg <- L5_pp_mg


new_df_L5 <- new_df_L5[14:26]


E_L1_pyc <- E_0 * exp( - L1_tot.abs * L1_Pycnocline)

delta_E_L1 = E_0 - E_L1_pyc

delta_Ea_L1 = (sum(L1_a$Abs_mean)/L1_tot.abs)*delta_E_L1


L1_pp <- 0.08*delta_Ea_L1*L1_QY_mean

L1_pp_mg <- L1_pp *12000


columns <- c("Station", "Date","Pycnocline", "Salinity", "E_0","E_pyc", "delta_E", "delta_Ea",
"Abs_a", "Abs_cdom", "Tot_abs", "pp", "pp_mg")
new_df_L1 <- data.frame(matrix(nrow = 1, ncol = length(columns)))

new_df_L1$Station <- "L1"
```

```
new_df_L1$Date <- "12.05.22"
new_df_L1$Pycnocline <- L1_Pycnocline
new_df_L1$Salinity <- L1_Salinity
new_df_L1$E_0 <- 30
new_df_L1$E_pyc <- E_L1_pyc
new_df_L1$delta_E <- delta_E_L1
new_df_L1$delta_Ea <- delta_Ea_L1
new_df_L1$Abs_a <- sum(L1_a$Abs_mean)
new_df_L1$Abs_cdom <- sum(L1_cdom$Abs_mean)
new_df_L1$Tot_abs <- L1_tot.abs
new_df_L1$pp <- L1_pp
new_df_L1$pp_mg <- L1_pp_mg


new_df_L1 <- new_df_L1[14:26]


new_df <- rbind(new_df_L1, new_df_L5)

new_df <- rbind(new_df, new_df_I1)

new_df <- rbind(new_df, new_df_O1)

new_df <- rbind(new_df, new_df_OF2)


saveRDS(new_df, "pp_sal.rds")
```

```
pp1_sal <- readRDS("pp_sal.rds")
pp2_sal <- readRDS("pp2_sal.rds")
pp3_sal <- readRDS("pp3_dom.rds")

pp_sal <- rbind(pp1_sal, pp2_sal, pp3_sal)

saveRDS(pp_sal, "pp_sal_bo.rds")



pp_sal %>%
 mutate(Station = fct_relevel(Station,
              "L1", "L5", "I1",
              "O1", "OF2")) %>%
 mutate(Date = fct_relevel(Date, "12.05.22", "02.06.22", "29.06.22")) %>%
 ggplot( aes(x= Salinity, y = pp_mg, colour = Date, shape = Station)) +
 geom_point(size = 3) +
 ylab("Carbon uptake mg C/ m2/ day") +
 xlab("Salinity (PSU)") +
 ylim(0,3000) +
 scale_color_manual(values = my_colour_palette)+
 My_theme
ggsave(filename = "biooptical.pdf", width = 7.29, height = 4.75)
```

VGPM

```
pp_vgpm <- subset(pigment_df, Wavelength.nm. > 630)
```

```
pp_vgpm_OF2 <- subset(pp_vgpm, Station == "OF2")

pp_vgpm_O1 <- subset(pp_vgpm, Station == "O1")

pp_vgpm_I1 <- subset(pp_vgpm, Station == "I1")

pp_vgpm_L5 <- subset(pp_vgpm, Station == "L5")

pp_vgpm_L1 <- subset(pp_vgpm, Station == "L1")
```

#Day length function from BIOS4400 - Pelagic ecology, adapted from Brock (1981)

```
my_function <- function(latitude){
 Lat <- latitude # defining the latitude (degrees)

 lat <- 2 * pi * Lat / 360 # Latitude in radians
 t <- 1:365 # Day of year

 #declination, angle of the sun above the equator (measured in radians))
 dec <- 2 * pi * (23.45 / 360) * sin(2 * pi * (284 + t) / 365)

 #cos(ω) as a function of declination (δ), latitude (φ)
 cos.w <- -tan(dec) * tan(lat)

 #restrict −1<cos(ω)<1
 cos.w[cos.w > 1] <- 1
 cos.w[cos.w < -1] <- -1

 #calculate the angle (in radians) between south and the rising, or setting, sun.
```

```
 w <- acos(cos.w)

 # recalculate the hour angle of sunrise into daylength in hours
 dl <- 2 * w / (2 * pi * (15 / 360))

 # Trigonometric function because the distance from the Sun to Earth varies throughout the year
(because of Earth´s elliptical shaped orbit)
 Rx <- 1 / sqrt( 1 + 0.033 * cos(2 * pi * t / 365))

 #find the zenith angle or the solar elevation angle at noon by observing that ω=0 at noon (->
cos(ω) = 1)
 # Find the solar elevation angle
 cos.a <- sin(dec) * sin(lat) + cos(dec) * cos(lat)
 cos.a[cos.a < 0] <- 0

 SolarK <- 1373 # Solar constant (W / m2)
 AtmAtt <- 0.5 # Atmospheric attenuation
 ParFrac <- 0.42 # Fraction PAR (400-700 nm) by energy

 PAR.noon <- AtmAtt * ParFrac * SolarK * cos.a / (Rx * Rx)

 daylength <-return(dl)

 plot(t, dl, type="l", lwd=2, col=2,
    xlab="Day of year", ylab="Daylength (hours)")

}
```

```
daylength <- my_function(59) #latitude at Drøbak

a <- 0.011 #m^2/mg Chla from Mitchell & Kiefer (1988), at 670 nm

par <- 0.66125 * (E_0/(E_0 + 4.1)) #Behrenfeld & Falkowski (1997)

dl <- daylength[132] #h

pb_opt <- function(sst) {
 return(1.2956 + 2.749e-1*sst + 6.17e-2*sst^2 - 2.05e-2*sst^3 +
     2.462e-3*sst^4 - 1.348e-4*sst^5 + 3.4132e-6*sst^6 - 3.27e-8*sst^7)
}

OF2_peak_pos <- which.max(pp_vgpm_OF2$abs_coeff_a)

OF2_peak <- pp_vgpm_OF2$abs_coeff_a[41]

OF2_peak_wl <- pp_vgpm_OF2$Wavelength.nm.[41] #671 nm

OF2_trios <- subset(trios, Station == "OF2" & Date == "12.05.22")

OF2_lwr_ep_zone <- approx(OF2_trios$pwr.rel, OF2_trios$depth, 0.01)$y

a_OF2 <- OF2_peak/a
```

```
sst_OF2 <- ctd_shallow$temperature[5]


PB_OF2 <- pb_opt(sst_OF2)

VGPM_OF2 <- a_OF2 * PB_OF2 * dl * par * OF2_lwr_ep_zone


columns_vgpm <- c("Station", "Date", "Salinity", "Euphotic", "Temperature", "E_0","E_0_func",
"Chla", "Abs_dom", "Pb_opt", "daylength", "VGPM")
vgpm_df_OF2 <- data.frame(matrix(nrow = 1, ncol = length(columns_vgpm)))

vgpm_df_OF2$Station <- "OF2"
vgpm_df_OF2$Date <- "12.05.22"
vgpm_df_OF2$Salinity <- OF2_Salinity
vgpm_df_OF2$Euphotic <- OF2_lwr_ep_zone
vgpm_df_OF2$Temperature <- sst_OF2
vgpm_df_OF2$E_0 <- 30
vgpm_df_OF2$E_0_func <- par
vgpm_df_OF2$Chla <- a_OF2
vgpm_df_OF2$Abs_cdom <- sum(OF2_cdom$Abs_mean)
vgpm_df_OF2$Pb_opt <- PB_OF2
vgpm_df_OF2$daylength <- dl
vgpm_df_OF2$VGPM <- VGPM_OF2

vgpm_df_OF2 <- vgpm_df_OF2[13:24]
```

```
O1_peak_pos <- which.max(pp_vgpm_O1$abs_coeff_a)

O1_peak <- pp_vgpm_O1$abs_coeff_a[45]

O1_peak_wl <- pp_vgpm_O1$Wavelength.nm.[45] #675 nm

O1_trios <- subset(trios, Station == "O1" & Date == "12.05.22")

O1_lwr_ep_zone <- approx(O1_trios$pwr.rel, O1_trios$depth, 0.01)$y

a_O1 <- O1_peak/a


sst_O1 <- ctd_shallow$temperature[4]


PB_O1 <- pb_opt(sst_O1)

VGPM_O1 <- a_O1 * PB_O1 * dl * par * O1_lwr_ep_zone


columns_vgpm <- c("Station", "Date", "Salinity", "Euphotic", "Temperature", "E_0","E_0_func",
"Chla", "Abs_cdom", "Pb_opt", "daylength", "VGPM")
vgpm_df_O1 <- data.frame(matrix(nrow = 1, ncol = length(columns_vgpm)))

vgpm_df_O1$Station <- "O1"
vgpm_df_O1$Date <- "12.05.22"
```

```
vgpm_df_O1$Salinity <- O1_Salinity
vgpm_df_O1$Euphotic <- O1_lwr_ep_zone
vgpm_df_O1$Temperature <- sst_O1
vgpm_df_O1$E_0 <- 30
vgpm_df_O1$E_0_func <- par
vgpm_df_O1$Chla <- a_O1
vgpm_df_O1$Abs_cdom <- sum(O1_cdom$Abs_mean)
vgpm_df_O1$Pb_opt <- PB_O1
vgpm_df_O1$daylength <- dl
vgpm_df_O1$VGPM <- VGPM_O1

vgpm_df_O1 <- vgpm_df_O1[13:24]



I1_peak_pos <- which.max(pp_vgpm_I1$abs_coeff_a)

I1_peak <- pp_vgpm_I1$abs_coeff_a[45]

I1_peak_wl <- pp_vgpm_I1$Wavelength.nm.[45] #675 nm



I1_trios <- subset(trios, Station == "I1" & Date == "12.05.22")

I1_lwr_ep_zone <- approx(I1_trios$pwr.rel, I1_trios$depth, 0.01)$y

a_I1 <- I1_peak/a

sst_I1 <- ctd_shallow$temperature[3]
```

```
PB_I1 <- pb_opt(sst_I1)

VGPM_I1 <- a_I1 * PB_I1 * dl * par * I1_lwr_ep_zone


columns_vgpm <- c("Station", "Date", "Salinity", "Euphotic", "Temperature", "E_0","E_0_func",
"Chla", "Abs_cdom", "Pb_opt", "daylength", "VGPM")
vgpm_df_I1 <- data.frame(matrix(nrow = 1, ncol = length(columns_vgpm)))

vgpm_df_I1$Station <- "I1"
vgpm_df_I1$Date <- "12.05.22"
vgpm_df_I1$Salinity <- I1_Salinity
vgpm_df_I1$Euphotic <- I1_lwr_ep_zone
vgpm_df_I1$Temperature <- sst_I1
vgpm_df_I1$E_0 <- 30
vgpm_df_I1$E_0_func <- par
vgpm_df_I1$Chla <- a_I1
vgpm_df_I1$Abs_cdom <- sum(I1_cdom$Abs_mean)
vgpm_df_I1$Pb_opt <- PB_I1
vgpm_df_I1$daylength <- dl
vgpm_df_I1$VGPM <- VGPM_I1

vgpm_df_I1 <- vgpm_df_I1[13:24]
L5_peak_pos <- which.max(pp_vgpm_L5$abs_coeff_a)

L5_peak <- pp_vgpm_L5$abs_coeff_a[47]

L5_peak_wl <- pp_vgpm_L5$Wavelength.nm.[47] #677 nm
```

```
L5_trios <- subset(trios, Station == "L5" & Date == "12.05.22")

L5_lwr_ep_zone <- approx(L5_trios$pwr.rel, L5_trios$depth, 0.01)$y

a_L5 <- L5_peak/a


sst_L5 <- ctd_shallow$temperature[2]


PB_L5 <- pb_opt(sst_L5)

VGPM_L5 <- a_L5 * PB_L5 * dl * par * L5_lwr_ep_zone


columns_vgpm <- c("Station", "Date", "Salinity", "Euphotic", "Temperature", "E_0","E_0_func",
"Chla", "Abs_cdom", "Pb_opt", "daylength", "VGPM")
vgpm_df_L5 <- data.frame(matrix(nrow = 1, ncol = length(columns_vgpm)))

vgpm_df_L5$Station <- "L5"
vgpm_df_L5$Date <- "12.05.22"
vgpm_df_L5$Salinity <- L5_Salinity
vgpm_df_L5$Euphotic <- L5_lwr_ep_zone
vgpm_df_L5$Temperature <- sst_L5
vgpm_df_L5$E_0 <- 30
vgpm_df_L5$E_0_func <- par
vgpm_df_L5$Chla <- a_L5
```

```
vgpm_df_L5$Abs_cdom <- sum(L5_cdom$Abs_mean)
vgpm_df_L5$Pb_opt <- PB_L5
vgpm_df_L5$daylength <- dl
vgpm_df_L5$VGPM <- VGPM_L5

vgpm_df_L5 <- vgpm_df_L5[13:24]



L1_peak_pos <- which.max(pp_vgpm_L1$abs_coeff_a)

L1_peak <- pp_vgpm_L1$abs_coeff_a[38]

L1_peak_wl <- pp_vgpm_L1$Wavelength.nm.[38] #668 nm

L1_trios <- subset(trios, Station == "L1" & Date == "12.05.22")

L1_lwr_ep_zone <- approx(L1_trios$pwr.rel, L1_trios$depth, 0.01)$y


a_L1 <- L1_peak/a

sst_L1 <- ctd_shallow$temperature[1]


PB_L1 <- pb_opt(sst_L1)

VGPM_L1 <- a_L1 * PB_L1 * dl * par * L1_lwr_ep_zone
```

```
columns_vgpm <- c("Station", "Date", "Salinity", "Euphotic", "Temperature", "E_0","E_0_func",
"Chla", "Abs_cdom", "Pb_opt", "daylength", "VGPM")
vgpm_df_L1 <- data.frame(matrix(nrow = 1, ncol = length(columns_vgpm)))

vgpm_df_L1$Station <- "L1"
vgpm_df_L1$Date <- "12.05.22"
vgpm_df_L1$Salinity <- L1_Salinity
vgpm_df_L1$Euphotic <- L1_lwr_ep_zone
vgpm_df_L1$Temperature <- sst_L1
vgpm_df_L1$E_0 <- 30
vgpm_df_L1$E_0_func <- par
vgpm_df_L1$Chla <- a_L1
vgpm_df_L1$Abs_cdom <- sum(L1_cdom$Abs_mean)
vgpm_df_L1$Pb_opt <- PB_L1
vgpm_df_L1$daylength <- dl
vgpm_df_L1$VGPM <- VGPM_L1

vgpm_df_L1 <- vgpm_df_L1[13:24]



vgpm_df <- rbind(vgpm_df_L1, vgpm_df_L5, vgpm_df_I1, vgpm_df_O1, vgpm_df_OF2)

saveRDS(vgpm_df, "vgpm_df_eu_sal.rds")



vgpm_1_sal <- readRDS("vgpm_df_eu_sal.rds")

vgpm_2_sal <- readRDS("vgpm_df2_eu_sal.rds")
```

```
vgpm_3_sal <- readRDS("vgpm_df3_eu_sal.rds")

vgpm_sal <- rbind(vgpm_1_sal, vgpm_2_sal, vgpm_3_sal)



saveRDS(vgpm_sal, "vgpm_sal.rds")

vgpm_sal %>%
 mutate(Station = fct_relevel(Station,
              "L1", "L5", "I1",
              "O1", "OF2")) %>%
 mutate(Date = fct_relevel(Date, "12.05.22", "02.06.22", "29.06.22")) %>%
 ggplot( aes(x= Station, y = VGPM, colour = Date)) +
 geom_point() +
 ggtitle("Rates of carbon uptake across stations and dates") +
 ylab("Carbon uptake mg C/ m2/ day") +
 ylim(0, 6000) +
 scale_color_manual(values = my_colour_palette)
```

^{13}C-PP

```
# 13C:12C in IAEA Pee Dee Belemnite reference = 0.0112372
# Definition of d13C = 1000 * ((R / R.PDB) - 1) where R is the 13C:12C ratio
# --> R = (1 + d13C / 1000) * R.PDB
# Utility functions for converting between isotope deltas, ratios and concentrations

delta2R <- function(delta, R.PDB=0.01123720) {
 return((1 + (delta / 1000)) * R.PDB)
}
```

```
R2delta <- function(R, R.PDB=0.01123720) {
 return(1000 * ((R / R.PDB) - 1))
}

R2conc <- function(R, Ctot) {
 return(list(
  C13 = (R / (1 + R)) * Ctot,
  C12 = (1 / (1 + R)) * Ctot
 ))
}

conc2R <- function(C13, C12) {
 return(C13 / C12)
}


# Rau et al. (1996) Table 1
# https://www.int-res.com/articles/meps/133/m133p275.pdf

d13C.DIC <-  1.7
d13C.POC <- -22.2



# https://www.sigmaaldrich.com/NO/en/product/aldrich/372382
# 98% NaH13CO3 molecular weight 85.00

# Lopez-Sandoval et al. (2019)
```

```
# https://aslopubs.onlinelibrary.wiley.com/doi/full/10.1002/lom3.10305
# added 5 mL 13C.stock (2.18 g NaH13CO3 / L) per liter sample

DIC.stock <- 1000 * (2.18 / 85) # 25.6 mmol/L
DIC.add <- 1000 * (5 / 1000) * DIC.stock # 128.2 umol/L

df <- readRDS("C_df.rds")



df$DIC <- df$C0 #DIC in umol/L
C.DIC <- R2conc(delta2R(d13C.DIC), df$DIC)

# Calculating the isotope ratio in DIC
# after the isotope spike at the start of the incubation

df$DI13C <- 0.98 * DIC.add + C.DIC[["C13"]]
df$DI12C <- 0.02 * DIC.add + C.DIC[["C12"]]

df$d13C.DIC <- R2delta(df$DI13C / df$DI12C)

# Calculating the isotope ratio in POC after incubation

df$POC <- df$C_ug / 12 # POC as umol/L
C.POC <- R2conc(delta2R(df$d13C), df$POC)

df$PO13C <- C.POC[["C13"]]
df$PO12C <- C.POC[["C12"]]
```

 # POC production as µmol/L over the incubation

```
df$delta_POC <- with(df, (PO13C / DI13C) * DI12C)
```

#Calculating rate

```
df$PP <- with(df, (d13C / d13C.DIC) * POC)

df$SIPM <- with(df, (PP*12) * Euphotic * E_0_func)
```

#Light and dark bottles

```
df_light <- subset(df, Incubation == "light")
df_dark <- subset(df, Incubation == "dark")

d.POC.C.L <- df$delta_POC[1:15]
d.POC.C.D <- df$delta_POC[16:30]

df_light$d.POC.C <- d.POC.C.L - d.POC.C.D
df_light$delta_C_ug <- df_light$C_ug - df_dark$C_ug

d.PP.L <- df$PP[1:15]
d.PP.D <- df$PP[16:30]

df_light$d.PP.C <- d.PP.L - d.PP.D
```

```
df_light$SIPM.delta <- with(df_light, (d.PP.C*12) * Euphotic * E_0_func)


saveRDS(df_light, "df_light_si.rds")
```

Comparison

```
bo_sal <- readRDS("pp_sal_bo.rds")
vgpm_sal <- readRDS("vgpm_sal.rds")
df_light <- readRDS("df_light_si.rds")


all <- merge(bo_sal,vgpm_sal)
all <- merge(all, df_light)

saveRDS(all, "all.rds")

all <- rename(all,
      PP_BO = "pp_mg",
      PP_vgpm = "VGPM",
      PP_13C = "SIPM.delta",
      CDOM = "Abs_cdom")



library(GGally)

p <- ggpairs(all, columns = c("Salinity", "CDOM", "PP_BO", "PP_13C", "PP_vgpm"))
```

```
p + theme(axis.text.x = element_text(angle=90))
```

^{13}C-PP against salinity

```
all %>%
 mutate(Station = fct_relevel(Station,
                "L1", "L5", "I1",
                "O1", "OF2")) %>%
 mutate(Date = fct_relevel(Date, "12.05.22", "02.06.22", "29.06.22")) %>%
 ggplot( aes(x=Salinity, y = PP_13C, colour = Date, shape = Station)) +
 geom_point(size = 3) +
 ylim(0,400) +
 xlim(0, 25)+
 xlab("Salinity (PSU)")+
 ylab("Carbon uptake (mg C/m2/d)")+
 scale_colour_manual(values = my_colour_palette ) +
 My_theme

ggsave(filename = "PP13C.pdf", width = 7.29, height = 4.75)
```

Volumetric production

```
all$PP_vol <- 12*all$d.PP.C

p3 = ggplot(all, aes(x= Chla, y = PP_vol)) +
 geom_point(size = 3) +
 geom_smooth(method = "lm",se =FALSE)+
 ylab("13C-PP (ug/L)")+
 xlab("Chlorophyll a (ug/L)") +
 ylim(0,70)+
```

```
 xlim(0,12.5)+
 My_theme

summary(lm(all$PP_vol ~ all$Chla))
#4.029   1.483



SST <- 0:30

df_pb_sst <- data.frame(x= SST, y= pb_opt(SST))
```

Chlorophyll specific production (mg C / mg Chla)

```
all$PP_Chla <- (12*all$d.PP.C)/all$Chla



#Chlorophyll specific production vs temperature
p4 = ggplot(all, aes(x= Temperature, y = PP_Chla)) +
 geom_point(size = 3) +
 geom_line(data= df_pb_sst, aes(x = x, y= y) ) +
 ylab("Primary production (mg C/mg Chla)")+
 xlab("Temperature ( C)") +
 ylim(0,10)+
 xlim(0,30) +
 My_theme
```

```
#Chlorophyll specific production vs salinity
p5 = ggplot(all, aes(x= Salinity, y = PP_Chla)) +
 geom_point(size = 3) +
 geom_smooth(method = "lm",se =FALSE)+
 ylab("Primary production (mg C/mg Chla)")+
 xlab("Salinity (PSU)") +
 ylim(0,10)+
 xlim(0,30) +
 My_theme
summary(lm(all$PP_Chla ~ all$Salinity))
#0.15523  0.04555


#Chlorophyll specific production vs CDOM
p6 = ggplot(all, aes(x= CDOM, y = PP_Chla)) +
 geom_point(size = 3) +
 geom_smooth(method = "lm",se =FALSE)+
 ylab("Primary production (mg C/mg Chla)")+
 xlab("CDOM (m-1)") +
 ylim(0,10)+
 xlim(0,1.5) +
 My_theme

summary(lm(all$PP_Chla ~ all$CDOM))
#-2.2336   1.2577
```

```
plot_grid(p3,p4,p5, p6, labels = c("A", "B", "C", "D"))

ggsave(filename = "4siste.pdf", width = 7.29, height = 4.75)
```

CDOM vs salinity

```
p7 = ggplot(all, aes(x= Salinity, y = CDOM)) +
 geom_point(size = 3) +
 geom_smooth(method = "lm",se =FALSE)+
 ylab("CDOM (m-1)")+
 xlab("Salinity (PSU)") +
 ylim(0,1.5)+
 xlim(0,30) +
 My_theme
ggsave(filename = "CDOMsal.pdf", width = 7.29, height = 4.75)

summary(lm(all$CDOM ~ all$Salinity))
#-0.031962  0.008734
```